NTNU – Trondheim
Norwegian University of
Science and Technology

Adaptation of anaerobic ammonium oxidizing (anammox) bacteria to salinity in a continuous reactor.

Are Johan Rønning

Chemical Engineering and Biotechnology
Submission date: June 2013
Supervisor: Kjetill Østgaard, IBT

Norwegian University of Science and Technology
Department of Biotechnology

Preface

I am sending my gratitude to my supervisor Prof. Kjetill Østgaard for guidance and for finding the time for weekly meetings. I would like to thank my co-supervisor *Ph.D.* candidate Blanca Magdalena Gonzalez Silva for the guidance, meetings and for all the help and assistance she has provided me in the lab. I would also like to thank Ingrid Bakke for introducing me to DGGE analysis and to statistical methods. I am also sending my gratitude to Randi Utgård for her tips, technical assistance and for bringing me coffee, and also Øyvind Johansen for his technical assistance. I would like to thank my fellow master student Kjell Rune Jonassen for all his help and assistance in the lab and for his cooperation in general. Finally, I want to thank my girlfriend and my family for their good support during my 5 years as a student.

Abstract

The **an**aerobic **amm**onium **ox**idation (anammox) process is the most recent discovery in the nitrogen cycle on Earth. The anammox process is a microbial process where ammonium (NH_4^+) is anaerobically oxidized to gaseous nitrogen. The electron acceptor of the process is nitrite (NO_2^-), with a theoretical molar consumption ratio of NH_4^+/NO_2^- of 1:1.32. This biological conversion is attractive as it presents the opportunity for a nitrogen removal process that improves the overall energy and material balance in full-scale treatment systems. Marine aquaculture effluents are rich in nitrogenous compounds, *e.g.* proteins and ammonium, thus being a candidate for applying the anammox process.

The report presented is a master thesis project which is a part of a pilot *Ph.D.* project at the Department of Biotechnology at the Norwegian University of Science and Technology (NTNU). Two of the major goals in this pilot are to develop start-up strategies for the application of the anammox process for marine aquaculture effluents, and to monitor the dynamics of the microbial community during the adaptation to marine conditions.

The major goal of this study was to adapt anammox bacteria to salinity (NaCl) in a continuous up flow reactor. The secondary goal was to do initial analyses of the microbial community's dynamics during the adaptation. The reactor was inoculated with activated sludge from Norsk Institutt for Vannforskning. The continuous reactor was operated for 147 days, and the reactor was monitored by measuring the concentrations of $N-NO_2^-$, $N-NH_4^+$ and $N-NO_3^-$ in the inlet and the effluent of the reactor. The adaptation to salinity (NaCl) was started at day 47 by adding NaCl to the medium fed to the reactor. The community composition in two samples of the activated sludge in the reactor were analyzed by the use of the Polymerase Chain Reaction (PCR) with universal bacterial primers, denaturing gradient gel electrophoresis (DGGE) and statistical methods in computational programs (Gel2k and PAST). The samples were sampled at day 44 (0 g NaCl/L) and 114 (3.0 g NaCl/L) of continuous operation. The major result of the experiment was acclimation to 3 g NaCl/L by the microbial community in the reactor. The molecular analyses indicated that the adaptation was caused by acclimation of the original community, because the microbial composition in the samples were similar.

Further work should be performed to reach the long-term goals of the pilot project, both in terms of reaching higher levels of adaptation and to do more thoroughly analyses of the community dynamics as a response to salt adaptation. The biomass in the reactor could be split in two parallel reactors. One of them could be the reference with only NaCl as the selective factor, and the other with a mixture of NaCl and KCl to study if K^+ has an antagonistic effect. Another option is to add parts of sea water to the mineral medium, because marine conditions is the real target of the project. The molecular experiments should be optimized by the use of specific anammox primers, and other methods such as fluorescent *in situ* hybridization (FISH) should also be considered.

Sammendrag

Bakterier som bærer navnet anammox-bakterier (*eng*: **an**aerobic **amm**onium **ox**idizing) oksiderer ammonium (NH_4^+) til nitrogengass (N_2) under anaerobe forhold. Elektronakseptoren i denne mikrobielle prosessen er nitritt (NO_2^-), hvor det teoretiske molare forholdet mellom NH_4^+/NO_2^- er 1:1,32. Denne mikrobielle omdannelsen fremstår som veldig attraktiv fordi den kan bidra til å forbedre de totale material- og energibalansene i fullskala renseanlegg for nitrogenrike avfalls- og prosessvann. Avfalls- og prosessvann fra akvakulturanlegg innholder mye nitrogen i form av proteiner og ammonium. Anammoxprosessen er derfor egnet som renseprosess for disse anleggene.

Masteroppgaven som blir presentert er en del av et større *Ph.D.* pilotprosjekt ved Institutt for bioteknologi på Norges teknisk-naturvitenskapelige universitet (NTNU). Hovedmålene i dette pilotprosjektet er å utvikle oppstartsstrategier for å anvende anammoxprosessen på avløps- og prosessvann fra akvakulturen. I tillegg skal endringen(e) til det mikrobielle samfunnet følges mens det tilpasses marine forhold.

Hovedmålet i mastergraden som blir presentert var å adaptere anammoxbakterier til salinitet (NaCl) i en kontinuerlig oppstrømsreaktor. Det sekundære målet var å gjøre innledende analyser av det mikrobielle samfunnets dynamikk som følge av saltadapteringen. Reaktoren ble innokulert med aktivt slam fra Norsk Institutt for Vannforskning. Reaktoren ble drevet i 147 dager, og reaktoren ble overvåket ved å måle konsentrasjonene av $N-NO_2^-$, $N-NH_4^+$ og $N-NO_3^-$ i innløpet og utløpet til reaktoren. Adapteringen til NaCl ble startet på dag 47 ved å tilsette NaCl til mediumet som ble pumpet inn i reaktoren. To prøver av det mikrobielle samfunnet ble analysert ved bruk av PCR og universelle bakterielle primere, denaturerende gradient gelelektroforese (DGGE), samt statistiske programvarer (Gel2k og PAST). Slamprøvene ble tatt ut fra reaktoren på dag 44 (0 g NaCl/L) og dag 114 (3,0 g NaCl/L) etter innokulering. Hovedresultatene av forsøkene var at det bakterielle samfunnet i reaktoren ble adaptert til 3 g NaCl/L, og de molekylære analysene indikerte at det opprinnelige mikrobielle samfunnet ble akklimatisert til saltet fordi sammensetningen av det mikrobielle samfunnet var relativt likt i de to slamprøvene.

Videre arbeid kreves for å nå de langsiktige målene til pilotprosjektet. Forslag til videre arbeid er å dele biomassen i reaktoren i to parallelle reaktorer, hvor den ene blir drevet som en referanse med NaCl som seleksjonsfaktor. Den andre reaktoren kan tilsettes en blanding av NaCl og KCl for å studere om K^+ har en antagonistisk effekt på det mikrobielle samfunnet. Et annet forslag er å tilsette deler av sjøvann til mediumet som pumpes inn i reaktoren, siden adaptering til marine forhold er det reelle målet. De molekylære eksperimentene og metodene bør også optimaliseres ved bruk av anammoxspesifikke primere. Andre metoder som fluorescens *in situ* hybridisering (FISH) bør også vurderes.

Contents

List of Figures

List of Tables

Chapter 1

Introduction

1.1 The anaerobic ammonium oxidation process

The existence of the anaerobic ammonium oxidation (anammox) process was first proposed by the Austrian physicist Broda in 1977 (Broda, 1977). The conventional knowledge at the time was that ammonium was chemically inert, and because of that anaerobic oxidation of ammonium would not be feasible (Kuenen, 2008). It took almost 20 years before the process was proven in 1995 in the Netherlands by Van de Graaf et al. (1995). Today the process is applied in several waste water treatment plants *e.g.* in the Netherlands (Ward et al., 2011), and the process is applicable for waste waters such as municipal sewage and waste waters from agriculture and aquaculture (Strous et al., 1999a).

The position of the anammox process in the nitrogen cycle on Earth is presented in Figure 1.1, and the process appears to be ubiquitous in anoxic places where fixed nitrogen is found (Kartal et al., 2012). The anammox bacteria are present in various freshwater and marine ecosystems, in which they are a major or even the only converter of fixed nitrogen (Jetten et al., 2005). The microbial process accounts for 40 % of the nitrogen turn over in the marine environment (Kuenen et al., 2011), and globally it is causing approximately 50 % of the nitrogen gas released into the atmosphere (Kartal et al., 2012).

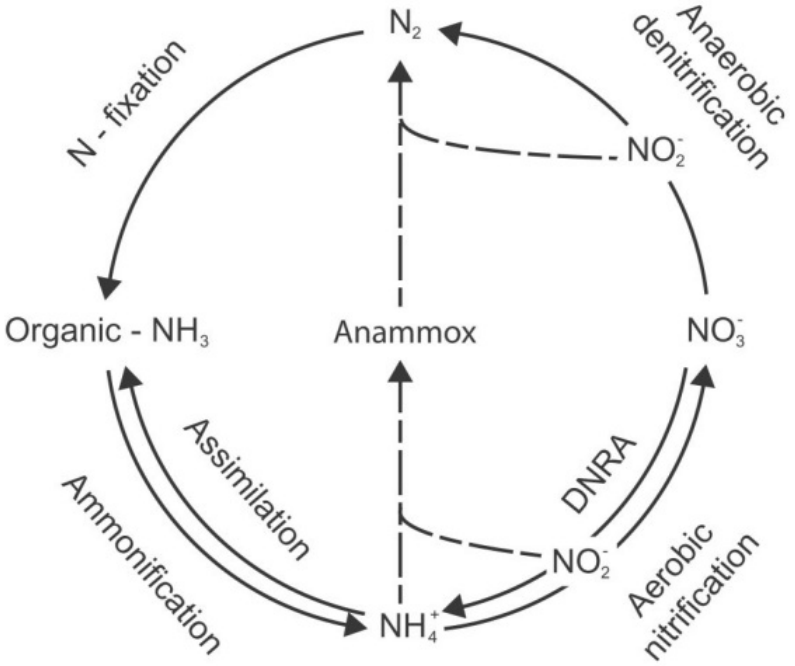

Figure 1.1: Simplified schematic presentation of the nitrogen cycle on Earth including the most important steps. The anammox process can be seen in the middle of the figure. The figure is adapted from Trimmer et al. (2003).

1.1.1 Phylogeny

The bacteria performing the anammox process was first noted as a planctomyces-like bacteria within the phylum *Planctomycetes* (Jetten et al., 2003). Today the anammox bacteria are noted as an separate monophyletic cluster branching off deep within the *Planctomycetes* phylum (Date et al., 2009), consisting of 5 different families presented in Figure 1.2. The five different families are named *Brocadia*, *Jettenia*, *Scalindua*, *Kuenenia* and *Anammoxoglobus*, and all of them have status as *Candidatus* because no one has been able to enrich the bacteria in a pure culture (Li and Gu, 2011). According to Terada et al. (2011) no one has been able to successfully isolate the anammox bacteria (January 2011) either. Regarding application of anammox bacteria to waste water treatment the two families *Brocadia* and *Kuenenia* are the most relevant (Lotti et al., 2012).

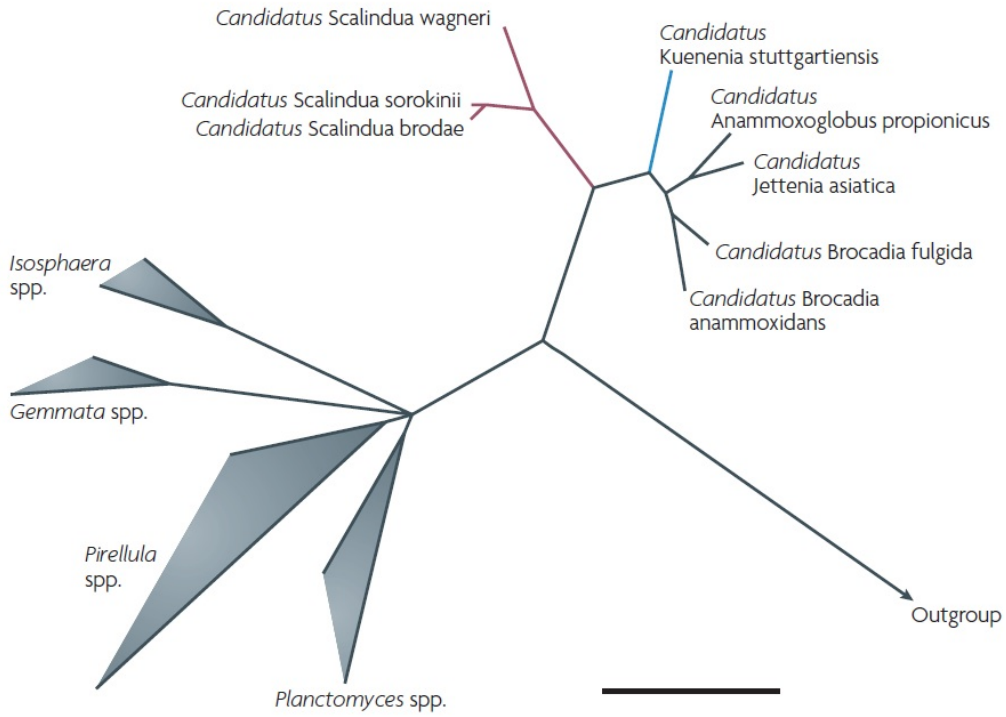

Figure 1.2: Phylogenetic tree of the phylum *Planctomycetes* based on the 16S rRNA gene of the five anammox families within the anaerobic ammonium oxidizing bacteria genera. The genera *Planctomyces*, *Pirellula*, *Gemmata* and *Isophaera* are also included in the figure. The bar at the right bottom of the figure represents 10% sequence divergence, and the sequence divergence from other Bacteria (named Outgroup) is high. The figure is adapted from Kuenen (2008).

1.1.2 Metabolic mechanisms and cell structure

The total anammox reaction is presented in Equation 1.1, where ammonium (NH_4^+) is oxidized to gaseous nitrogen (N_2) under anoxic conditions by the use of nitrite (NO_2^-) as the electron acceptor (Sun et al., 2011). According to Kumar and Lin (2010) 90 % of the nitrogen (NH_4^+ and NO_2^-) is converted to gaseous nitrogen, and the last 10 % is converted to nitrate (NO_3^-). This microbiological conversion is very attractive as it presents the opportunity for a nitrogen removal process that improves the overall energy and material balance (Imajo et al., 2004). The conventional opportunities will be presented further in Section 1.4. As Equation 1.1 shows the carbon source is bicarbonate, which means that

the anammox bacteria are able to fixate CO_2, making the anammox organisms chemo lithoautotrophs (Kartal et al., 2012).

$$NH_4^+ + 1.32NO_2^- + 0.066\mathrm{HCO}_3^- + 0.13\mathrm{H}^+ \rightarrow \\ 1.02N_2 + 0.256NO_3^- + 0.066CH_2O_{0.5}N_{0.15} + 2.03H_2O \quad (1.1)$$

Equation 1.1 might be divided into two partial reactions, where Equation 1.2 is the energy generating process and Equation 1.3 is the biomass generating process (Kartal et al., 2012). According to Sliekers et al. (2003) the energy generating process can proceed without production of nitrate and cell material as well.

$$NH_4^+ + NO_2^- \rightarrow N_2 + 2H_2O \qquad \Delta G_0^{'} = -357kJ/mol \quad (1.2)$$

$$0.26NO_2^- + 0.066\mathrm{HCO}_3^- \rightarrow 0.256NO_3^- + 0.066CH_2O_{0.5}N_{0.15} \quad (1.3)$$

The energy generating mechanism in the anammox bacteria is given in Equation 1.4-1.6 (Kartal et al., 2011), which are all red-ox reactions that can be summarized by Equation 1.2 as the overall reaction.

$$NO_2^- + 2H^+ + e^- \rightarrow NO + H_2O \qquad E_0' = +0.38V \quad (1.4)$$

$$NO + NH_4^+ + 2H^+ + 3e^- \rightarrow N_2H_4 + H_2O \qquad E_0' = +0.06V \quad (1.5)$$

$$N_2H_4 \rightarrow N_2 + 4H^+ + 4e^- \qquad E_0' = -0.75V \quad (1.6)$$

The anammox bacteria use a complex reaction mechanism involving both nitric oxide (NO) and hydrazine (N_2H_4) as intermediates. There are four main enzymes involved in the mechanism; *hydrazine synthase*, *hydrazine dehydrogenase*, *nitrite reductase* and *nitrate reductase* (Kartal et al., 2011), as presented in Figure 1.3.

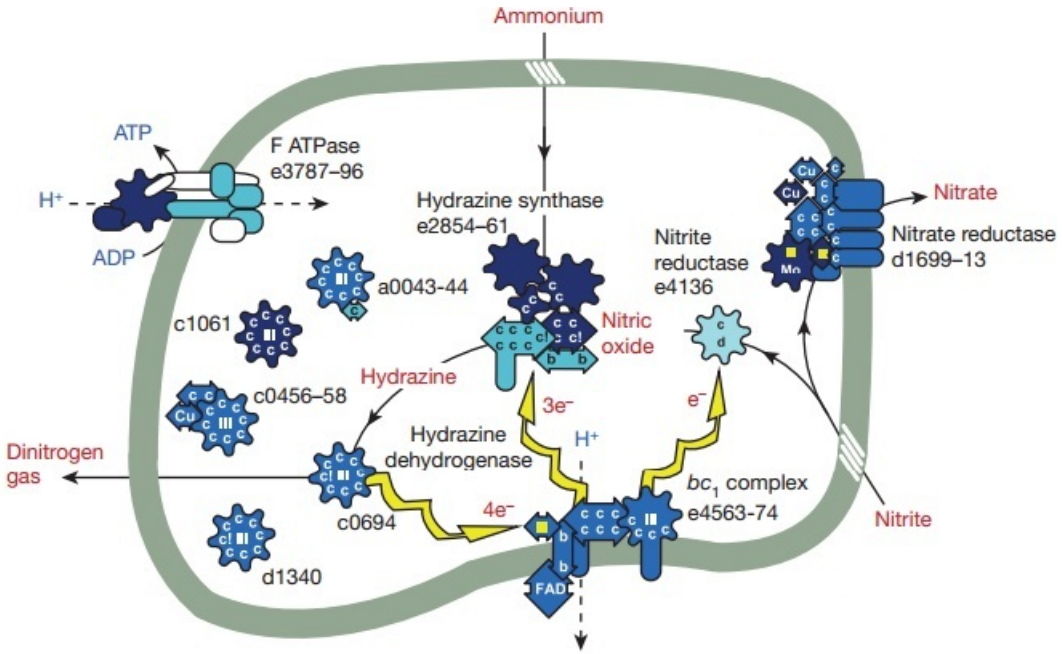

Figure 1.3: Schematic presentation of the enzymatic mechanism of the anammox process in the anammox organism *Kuenenia stuttgartiensis*. More details about the mechanism are presented in the text. The figure is adapted from Kartal et al. (2011).

The N−N bond in N_2 is formed by the hydrazine synthase enzyme, which according to Kartal et al. (2012) is one of the two known enzymes able to forge the N−N bond. The nitrite reductase enzyme is reducing nitrite to nitric oxide (NO), which is converted to the extremely energy-rich and toxic intermediate hydrazine together with ammonium by the hydrazine synthase enzyme (Kartal et al., 2010). The hydrazine dehydrogenase enzyme is removing the hydrogen protons from hydrazine, creating nitrogen gas (Schalk et al., 1998). This conversion generates electrons to the acetyl-CoA pathway for bicarbonate fixation (Strous et al., 2006). The nitrate reductase is oxidizing nitrite to nitrate, which is part of the bicarbonate fixation into cell biomass, as given in Equation 1.3. The anammox microorganisms have a unique prokaryotic organelle, called the anammoxosome, which exclusively contains hydrazine oxidoreductase as the major protein to combine nitrite and ammonium in a one-to-one fashion (Jetten et al., 2005). This unique organelle is surrounded by ladderane lipids and is placed in the middle of the cell where it accounts for 30 % of the cell volume (Jetten et al., 2005). The shape of the

anammox cell is coccoid or irregular jagged (Nozhevnikova et al., 2012). A schematic presentation of the anammox cell structure is presented in Figure 1.4.

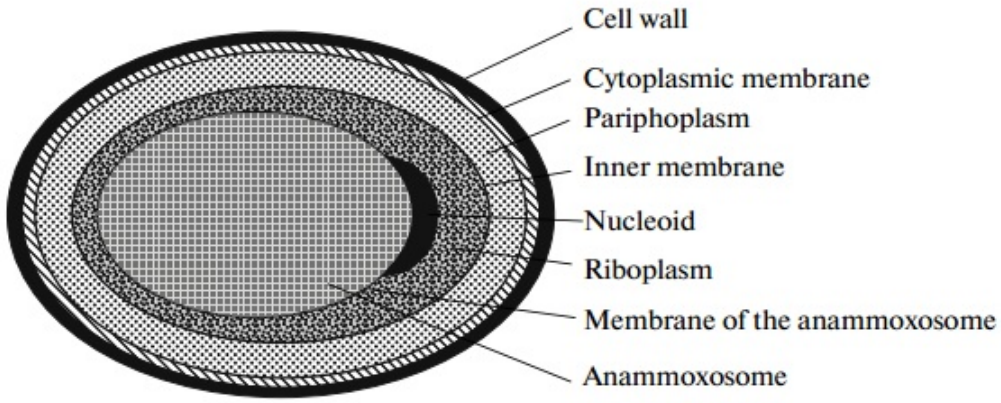

Figure 1.4: Schematic presentation of the anammox cell structure. The figure is adapted from Nozhevnikova et al. (2012).

1.1.3 Growth physiology

The anammox bacteria are slow growers and have a doubling time in the range of 7-11 days (Strous et al. (1999b), Jetten et al. (2001)). The long doubling time of the anammox bacteria is believed to be due to the organisms gearing down their metabolic activity because of the low concentrations of ammonium and nitrite in their natural habitat (Ward et al., 2011). Other important physiological characteristics such as pH and temperature for optimal growth are in the range of 6.5-9.0 and 20-45 °C, respectively (Kartal et al., 2012). The anammox bacteria were first believed to be obligate anaerobe (Strous et al., 1997), but more recent studies show that some anammox species are able to tolerant dissolved oxygen to be present (Kartal et al. (2012), Li et al. (2012)). The effects of dissolved oxygen will be further presented in Section 1.2.3.

1.1.4 Metabolic versatility

The anammox mechanism presented in the previous paragraphs is according to Kartal et al. (2012) thought to be the most common anammox process. As the anammox process has been studied deeper and wider, there are evidences of anammox bacteria being able to convert nitrate (NO_3^-) to both nitrite and ammonium. This conversion is believed to follow the dissimilatory nitrate reduction pathway (Kartal et al., 2007), and especially the specie *Kuenenia stuttgartiensis* seems to able to shift its metabolism. The generation of ammonium and nitrite from nitrate causes a drop in the activity down to 10 % of the "normal" anammox activity presented in Figure 1.3 (Kartal et al., 2007). This use of nitrate as a substrate might disguise the anammox bacteria as denitrifiers.

The alternative anammox process described above is presented in Figure 1.5 (pathway B). For this specific metabolism, there are many options of electron donors, both organic and inorganic compounds (Kartal et al., 2012). The anammox bacteria seem to be able to generate ammonium and nitrite from nitrate even if both of the primary substrates are available for the bacteria (Kartal et al., 2007). One suggested explanation why the anammox bacteria might shift their metabolism is because of the high concentrations of nitrate compared to nitrite and ammonium in anoxic sediments (Kartal et al., 2007). The enzymatic steps in the dissimilatory nitrate reduction pathway in anammox bacteria are not fully understood at this point (Kartal et al., 2012).

There are also reported studies that some anammox species are able to metabolize organic and inorganic substrates, in addition to, or instead of ammonium and nitrite (Strous et al. (2006), Kartal et al. (2007)). A full schematic presentation of the metabolic versatility of the anammox bacteria is given in Figure 1.5, and Table 1.1 gives further details of each metabolic pathway.

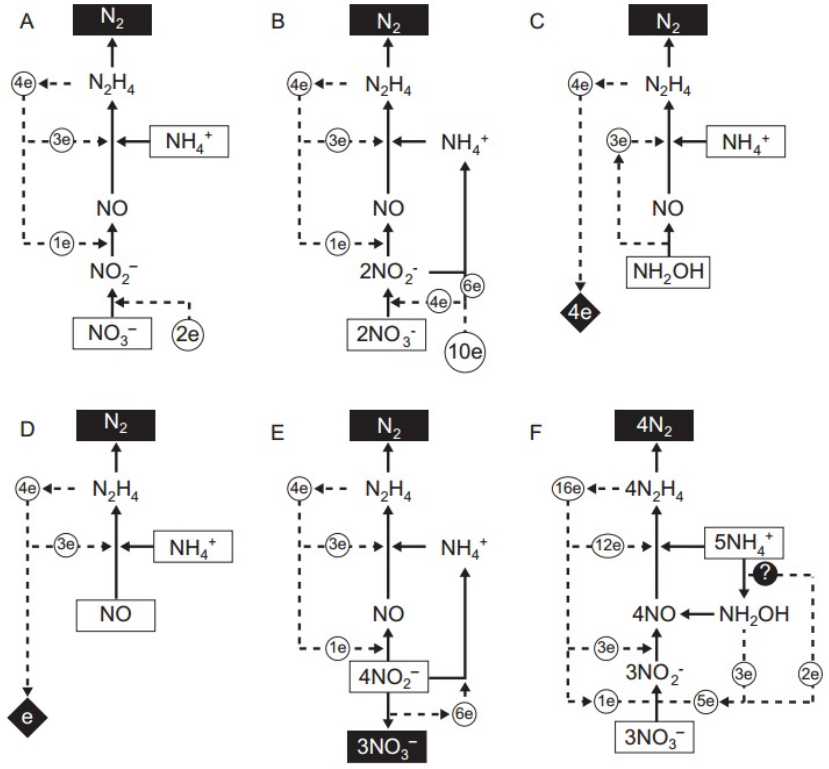

Figure 1.5: Schematic presentation of the metabolic versatility of anammox bacteria. The different metabolic pathways are presented more detailed in Table 1.1. Substrate and electron flows are represented by solid and dashed lines, respectively. Substrates are boxed in white and products in black. The figure is adapted from Kartal et al. (2012).

Table 1.1: Description of the metabolic pathways in Figure 1.5.

Metabolic pathway	Description
A	Ammonium and nitrate metabolism supported by an external electron donor
B	"Disguised denitrification" by the reduction of nitrate to N_2 supported by an external electron donor
C	Stimulation of the anammox process by hydroxylamine
D	Stimulation of the anammox process by nitric oxide
E	Nitrite disproportionation
F	Anammox process from ammonium and nitrate alone

1.2 Drawbacks of the anammox process

The major negative issues of the anammox process are the sensitivity to compounds which might inhibit the process severely (Kumar and Lin, 2010). The major compounds which potentially might inhibit the process are O_2, organic matter as well as NH_4^+ and NO_2^-, the process' substrates (Jin et al., 2012). The minimum optimal temperature for the anammox process is 20 °C, making the anammox process an unsuitable option for waste waters or process waters below this temperature (Jin et al., 2012). Even though continuous reactor experiments conducted with anammox bacteria at temperatures below 20 °C have been reported (Isaka et al. (2008), Ma et al. (2013)), the anammox activity was lost below 6 °C (Isaka et al., 2008). The anammox bacteria have a low growth rate as well, as already presented in Section 1.1.3. The last main drawback is that there is no pure culture of the different enriched anammox species (Kartal et al., 2012), which together with the slow growth cause a long start-up period in a full-scale application of the process. The positive aspect of the slow growth is the low amount of excess sludge that is produced in the anammox process unit, which also contributes to lower the operational costs (Dapena-Mora et al., 2004).

1.2.1 Ammonium

Even though ammonium is the electron donor in the anammox process the compound might be an inhibitor to the process (Jin et al., 2012). It is the free ammonia (NH_3) which is the real inhibitor, at concentrations of 770 mg $N{-}NH_3$/L or higher (Aktan et al., 2012). Other reported values in the literature contradict this value, and concentrations as low as 38 mg $N{-}NH_3$/L and 20-25 mg $N{-}NH_3$/L have been reported as inhibiting in short- and long-term tests, respectively. The lowest value reported of ammonium according to Jin et al. (2012) is 1.7 mg $N{-}NH_3$/L as toxic to an anammox start-up process. The concentration of free ammonia is a function of both temperature and pH, and it is increasing with an increase of both of the parameters (Aktan et al., 2012). The huge range in the reported values of toxicity and inhibition effects of ammonium/ammonia causes a difficulty in generalizing the effects, and thus to avoid them in a laboratory experiment or in a full-scale treatment plant. The only thing that is cer-

tain is that the operating conditions (pH, temperature, system design, *etc*.), the physical structure of the sludge and the microbial community play important roles (Kumar and Lin, 2010).

1.2.2 Nitrite

Nitrite is as previously stated the electron acceptor in the anammox process, as presented in Equation 1.1. This molecule is one of the most critical aspects in the stability of the anammox process (Lotti et al., 2012), because of the equilibrium with the toxic and non-charged molecule nitrous acid (HNO_2) (Fernández et al., 2012). As with ammonium, the literature shows a huge diversity in the reported values in which the levels of nitrite are inhibitory or toxic to the process. Concentrations as low as 5-40 mg $N{-}NO_2^-$/L have been reported as strongly inhibiting (Dapena-Mora et al., 2007), and a level of 100 mg $N{-}NO_2^-$/L has been reported as complete, irreversible inhibiting (Jin et al., 2012). But there are also values in the literature which claim that anammox bacteria are able to maintain their activity up to concentrations as high as 300 mg $N{-}NO_2^-$/L (Lotti et al., 2012).

Even though there is a huge range in the reported values of nitrite inhibition, there is an overall agreement that nitrite is a more important inhibitor compared to ammonium for the anammox process (Dapena-Mora et al., 2007). As the inhibitory levels of nitrite and ammonium are hard to predict, the specific microbial population must be thoroughly tested in the laboratory before it is suitable for industrial applications. The most crucial parameters regarding nitrite inhibition are the exposure concentration combined with the exposure time (Dapena-Mora et al. (2007), Lotti et al. (2012)). The latter is also important regarding the inhibition of ammonium (Jin et al., 2012).

1.2.3 Oxygen

The anammox process is sensitive to oxygen (dissolved oxygen = DO). Concentrations of dissolved oxygen as low as 2 μM ($\approx$ 0.064 mg O_2/L) have been reported to inhibit the process (Jung et al., 2007) and dissolved oxygen higher than 72 μM ($\approx$ 2.3 mg

O_2/L) have been reported to be toxic to the process (Ward et al., 2011). One of the first conclusions regarding oxygen inhibition of anammox was reported by Strous et al. (1997) stating that oxygen is reversibly inhibiting at any detectable levels. The literature is not consistent regarding this topic, and the inhibition levels of dissolved oxygen are dependent on the biomass system, *e.g.* granular sludge is more tolerant to oxygen than non-granular sludge because of anaerobic micro zones in the inner parts of the granules (Ward et al., 2011). Oxygen might also cause other microorganisms to out-compete the anammox bacteria, because nitrifiers have a higher growth rate than anammox (0.6-1.0 day^{-1}, (Ward et al., 2011)). These microorganisms might remove the ammonium, as presented in Section 1.3 (Jetten et al., 2001). Low concentrations of dissolved oxygen might trigger partial nitrification to occur simultaneously to an anammox process in a microbial community where both of the organisms are present. Blackburne et al. (2008) reported that the ammonium oxidizing bacteria (AOB) have lower oxygen affinity (0.03 mg O_2/L) compared to the nitrite oxidizing bacteria (NOB) (0.43 mg O_2/L). This will cause accumulation of nitrite, and only the reaction given in Equation 1.7 will take place.

One of the latest presented specific values regarding oxygen tolerance of anammox in the literature is of the specie *Kuenenia stuttgartiensis*, with tolerant levels of dissolved oxygen ranging from 0-200 μM (0-6.4 mg O_2/L) (Kartal et al., 2012), which is 100 times higher than the concentrations reported by Jung et al. (2007) and almost 3 times higher than the toxic concentrations reported by Ward et al. (2011). There are also reported levels of dissolved oxygen in medium fed to anammox bacteria of 2-5 mg O_2/L with no inhibitory effect (Li et al., 2012).

1.2.4 Organic matter

Organic matter is another important inhibitor to the anammox process. The denitrification process, presented in Section 1.3, might out-compete the anammox bacteria by the use of nitrite as the electron acceptor. This will result in removal of the nitrite, and the anammox bacteria will not be able to oxidize ammonium because of lack of the electron acceptor. There are anammox bacteria able to use organic matter as substrate (Jin et al., 2012), thus showing the metabolic diversity presented in Section 1.1.4. These

potential metabolisms cause the desired nitrogen removal to decrease, which indicates that organic matter should be removed in a pre-treatment unit when an anammox treatment step is applied (Ward et al., 2011). There are also organic compounds in which anammox bacteria are able to compete and coexist with denitrifiers, such as short fatty acids (*e.g.* formate and acetate) (Dapena-Mora et al., 2007). But there are few conventional applications suitable for this matter, because it requires these fatty acids to be the only organic matter present, which is unlikely in a complex treatment plant (Ward et al., 2011).

1.3 Conventional biological nitrogen removal

The main reasons to choose a biological process for the removal of nitrogen are the economical and energy aspects, because the biological process has a lower price compared to the physical-chemical methods (Dapena-Mora et al., 2004). In addition, biological treatment is more sustainable regarding environmental aspects (De Graaff et al., 2011). The traditional way to remove nitrogen biologically is by nitrification followed by denitrification (Nozhevnikova et al., 2012). In nitrification, ammonium is oxidized to nitrite, followed by oxidation of nitrite to nitrate. Oxygen (O_2) is the electron acceptor in both steps. The nitrification reactions are given in Equation 1.7 and 1.8 (Ruiz et al., 2003).

$$NH_4^+ + 1.5O_2 \rightarrow NO_2^- + H_2O + 2H^+ \tag{1.7}$$

$$NO_2^- + 0.5O_2 \rightarrow NO_3^- \tag{1.8}$$

The nitrogen removal is completed by anoxic denitrification. This microbial process uses organic matter as the carbon and energy source, producing gaseous nitrogen by the use of nitrite or nitrate as the electron acceptor (Madigan et al., 2009). Heterotrophic denitrification might convert a huge diversity of organic matter, and the general denitrification reaction and mechanism of the conversion of nitrate are given in Equation 1.9 and 1.10, respectively (van Rijn et al., 2006). There is also autotrophic dentrification, in which inorganic compounds are used as the electron donor (Ward et al., 2011).

$$org.matter + NO_3^- + H^+ \rightarrow HCO_3^- + N_2 + H_2O \tag{1.9}$$

$$NO_3^- \rightarrow NO_2^- \rightarrow NO \rightarrow N_2O \rightarrow N_2 \tag{1.10}$$

There are two main options regarding design of the treatment system when applying the nitrification-denitrification process; post- or pre-denitrification (Kumar and Lin, 2010). The major advantage of pre-denitrification compared to post-denitrification with respect to the nitrification step in the treatment system is that no addition of external carbon source is required. The system is also more robust to alkalinity and no post-treatment is needed. The major advantages of post-denitrification are higher efficiency, less space requirements and a more adaptable system to dilute waste waters (Ward et al., 2011).

1.4 The anammox process compared to conventional biological N-removal

Equation 1.7 and 1.8 in Section 1.3 show that 2 moles of oxygen are required in total to oxidize 1 mole of ammonium to nitrate in the nitrification process. If the anammox process is connected with partial nitrification to generate nitrite, less oxygen is required. This process will only include the first step given in Equation 1.7. In addition, if the anammox process is connected to partial nitrification, about half of the ammonium will be converted by the anammox process in a post-treatment unit. This will also decrease the total amount of oxygen required (Ward et al., 2011). Since the amount of needed oxygen for microbial nitrogen removal is less when partial nitrification and anammox are connected, the energy demand is decreased by 60 % compared to complete nitrification. This reduction of aeration reduces the operation costs in a full-scale treatment plant (Ward et al., 2011). In addition, less area requirements are needed according to Dapena-Mora et al. (2010).

Another crucial point in the comparison of the anammox process and a conventional nitrification-denitrification process is the needed addition of external organic matter to complete the denitrification process (Aktan et al., 2012), as given in Equation 1.9. In the anammox process this addition is not necessary, which also reduces the operational costs, as well as the emissions of CO_2 to the environment. Even though the addition of external organic matter might be avoided by treatment system design, the nitrification-denitrification process still has emissions of CO_2 (Jetten et al., 2001). If the denitrification step is replaced with the anammox process in a full-scale treatment system, Jetten et al. (2005) claim that the operational costs might be reduced by 90 %.

A case study done by Van Dongen et al. (2001) concluded that the anammox process has the lowest cost/kg N removed from waste waters. A theoretical study shows that a municipal sewage treatment plant where the anammox process is combined with partial nitrification will have a net positive energy consumption (Kuenen et al., 2011). In that specific system there was a digester unit for the excess biomass, resulting in production of biogas (methane). This shows the possibility of new, innovative and sustainable waste water treatment plants (Kartal et al., 2010).

1.5 Adaptation of anammox bacteria to salinity

The master project presented in this thesis is a part of a *PhD* project looking upon the possibilities of applying the anammox process to aquaculture effluents. In order to succeed, salt tolerance of the microbial population is one of the key factors. During the last decade several experiments on testing the inhibitory effects of salinity on the anammox process have been reported, *e.g.* Kartal et al. (2006), Dapena-Mora et al. (2010) and Ma et al. (2012). The first reported experiment on adaptation of freshwater anammox bacteria to salinity was conducted by Kartal et al. (2006). They performed an experiment over a period of 400 days, and their major results are presented in Figure 1.6. The figure presents the salt concentration and the nitrogen loading in their experiment. Both the salt concentration and the nitrogen loading were increased step-wise when nitrogen removal was close to complete removal. The figure shows that the freshwater anammox population was able to adapt to NaCl concentration of 30 g/L. A salinity level of 45 g/L was proved to be reversible inhibitory to the population, but the population recovered its anammox activity at 30 g/L of NaCl.

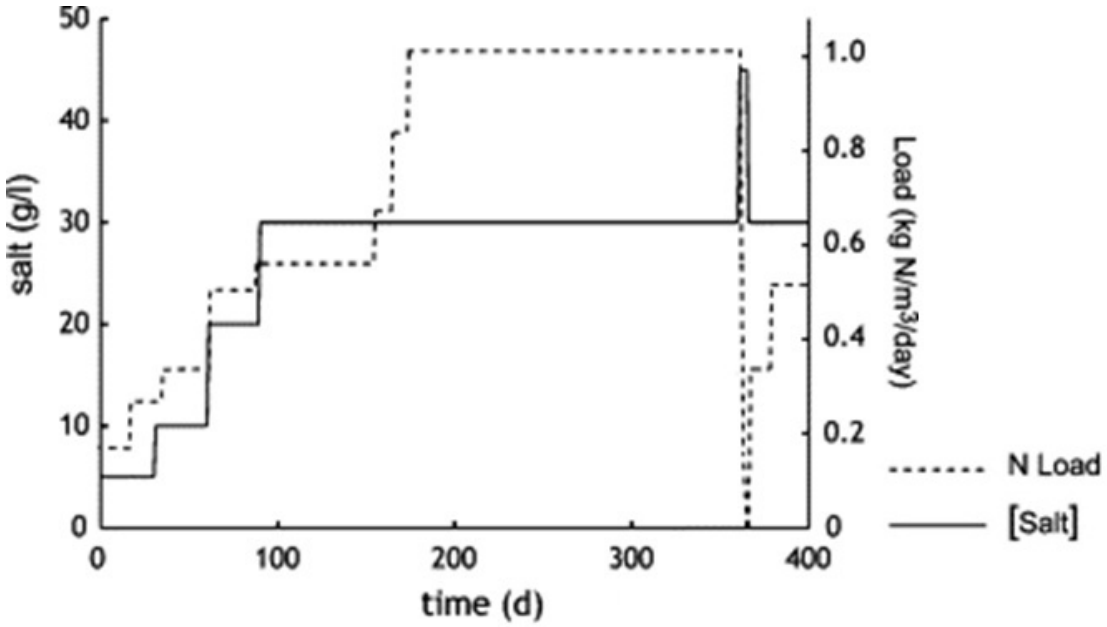

Figure 1.6: Results from a previous experiment adapting a freshwater anammox population to salinity. The figure is adapted from Kartal et al. (2006).

An other reported experiment evaluating the inhibitory effects of salinity on the anammox process was performed by Dapena-Mora et al. (2007). They showed that concentrations of NaCl up to 150 mM (≈8.8 g/L) do not affect the anammox activity. At concentrations higher than 230 mM (≈13.5 g/L) the anammox activity was decreased to less than 50 % of the normal activity. These presented results are similar to the results reported by Ma et al. (2012), which showed that anammox bacteria were able to maintain or even increase their activity in NaCl concentrations up to 10 g/L when anammox bacteria were shock loaded with salinity. Even at 30 g/L, the anammox bacteria were able to keep 50 % of their activity. The suggested threshold of salinity by Ma et al. (2012) was 30 g/L of NaCl, which is the same as presented in Figure 1.6 by Kartal et al. (2006).

Other reported results presented by Liu et al. (2009) and Yang et al. (2011) also support the suggested threshold by Kartal et al. (2006) and Ma et al. (2012) of 30 g/L. Yet an other reported adaptation level is of 7 g/L by Yi et al. (2011), which is lower than the conclusion made by Dapena-Mora et al. (2007). These differences in the reported concentrations anammox bacteria are able to adapt to indicate that parameters such as the kind of enriched anammox bacteria present and the degree of enrichment (the amount of anammox bacteria in the community) in the reactor are important (Dapena-Mora et al., 2010). Table 1.2 presents a summary of reported results related to adaptation of freshwater anammox bacteria to salinity.

Table 1.2: Summary of reported results related to adapting freshwater anammox bacteria to salinity.

Adaptation level, NaCl (g/L)	Operational mode	Reference
30	Sequencing batch reactor	Kartal et al. (2006)
9	Batch	Dapena-Mora et al. (2007)
30	Continuous	Liu et al. (2009)
15	Continuous	Dapena-Mora et al. (2010)
30	Continuous	Yang et al. (2011)
7	Sequencing batch reactor	Yi et al. (2011)
30	Continuous	Ma et al. (2012)

The major strategy on adaptation of anammox bacteria to salinity have been to step-wise increase the concentration of NaCl in the medium fed to the biomass, as presented in Figure 1.6. There have been differences in the articles of how the biomass responded to the salinity. Both Dapena-Mora et al. (2010) and Yang et al. (2011) experienced inhibition at 20 g NaCl/L, in which they both decreased the salinity and the nitrogen loading in the system to recover the activity. An other strategy presented by Liu et al. (2009) was to only decrease the salinity when inhibition of the biomass was observed, and then increase it later on when the activity was recovered.

The two major conclusions of the adaptation to salinity with anammox bacteria are that there have been a population shift in the reactor or an acclimation of the existing population (Kartal et al. (2006), Dapena-Mora et al. (2010)). In some of the articles presented in Table 1.2 the focus has been to characterize the dominating species in the microbial community after the adaptation by the use of cloning libraries or fluorescence *in situ* hybridization (FISH). But there has been little or no focus on the dynamics of the microbial community during the adaptation to the salt.

Kartal et al. (2006) showed that the freshwater anammox species *Candidatus "Kuenenia stuttgartiensis"* was the most dominating species in the anammox population after the adaption to salt in the experiment presented in Figure 1.6. Their initial anammox population consisted of 50 % of the freshwater species and 50 % of an anammox species mostly found in marine environments (*Candidatus "Scalindua wagneri"*). This was surprisingly, because the marine anammox species was believed to be more competitive under the saline conditions. Liu et al. (2009) characterized their microbial community after salt adaptation, but they did not have any reference sample of the initial community to compare to. Therefore, they could not say anything regarding the dynamics of the community as a response to the salt, but they assumed that the adaptation was caused by a population shift in the reactor. Yang et al. (2011) reported that the number of clones of the most dominating anammox species decreased after their microbial community was adapted to salt. Other unidentified clones seemed to increase in number as a response to the salt.

1.5.1 General effects of salinity to bacteria

Bacteria that are present in environments with no or low levels of salinity will have a net diffusion of water into the cell. This is due to the osmotic pressure caused by high concentrations of solute inside the cytoplasm of the cells (Madigan et al., 2009). A higher concentration of inorganic compounds in the environment will increase the osmotic pressure, resulting in a reverse diffusion of the intracellular water out of the cell. This makes the water balance of the cells negative, which become dehydrated. Dehydrated cells will lose their activity, and eventually die or become unable to grow (Lay et al., 2010). The main microbial strategy for counteracting the negative water balance is to increase the concentrations of their internal solutes. This is done by pumping inorganic ions into the cell or to synthesize or concentrate an organic solute. These inorganic ions or organic solutes must be non inhibitory to biochemical process within the cells.

One important ionic pump in bacteria which might be affected when exposed to different salinity conditions, is the Na^+/K^+-pump (Na^+/K^+-ATPase). This pump accounts for 20 % of the cell energy consumption in many bacterial cells (Hall and Guyton, 2006). This pump is also responsible for regulation of the cell volume Lewin (2007). Failure of the Na^+/K^+-pump can result in swelling of the cell, which could cause lysis of the cell. The Na^+/K^+-pump operates very slow compared to the ionic flux through cell membranes which is close to the diffusion rate of ions in water (Lewin, 2007). The failure of this pump might be avoided by adding Potassium (K^+) to the system, as Potassium has been shown to be an antagonist for Sodium in other anaerobic bacteria, such as methanogenes (Østgaard, 1995).

Other factors that are changed when salinity (NaCl) is introduced to a system, is that the ionic strength of the water changes (Moe and Smidsrød, 2008), as well as the water activity (a_w) and the ionic balance (Madigan et al., 2009). An other important fact regarding salinity and waste water treatment is that the water density increases as a function of concentration of salt (Doran, 1995). This increase of water density might cause a higher potential of wash out of biomass with low settling abilities in a continuous system (Kartal et al., 2006).

1.6 Molecular methods

To be able to do initial analysis of the dynamics of the microbial community during the adaptation to salinity, molecular methods such as Polymerase Chain Reaction and Denaturing Gradient Gel Electrophoresis have been used in this master project.

1.6.1 Polymerase Chain Reaction

Polymerase chain reaction (PCR) is a rapid method of DNA cloning, which makes the user able to copy a specific DNA sequence even at very small quantities of the DNA of interest (Klug et al., 2009). An other major advantage of this method is that no host cells are needed to copy the DNA. Even though PCR is considered a valuable technique to clone DNA, some information about the nucleotide sequence must be known in order to be able to clone the specific DNA sequence of interest. The information of the sequence makes the user able to find or synthesize suitable primers; one complementary to the 5' end and one complementary to the 3' end of the target DNA. The major limitations of PCR in addition to the necessity of sequence information are that the PCR samples are easily contaminated and the PCR experiments must always be performed in parallel with carefully designed and appropriate controls (Klug et al., 2009). The primers that are used must result in amplicons of proper lengths that are suitable for further analysis, such as denaturing gradient gel electrophoresis (presented in the next section). Further, the amplified region should be informative in phylogenetic or diversity analysis (Bakke et al., 2011).

The PCR process contains three major steps (Hyde, 2009), as presented in Figure 1.7. First, the DNA of interest must be denatured into single strands, as usual by heat at 90-95 °C. Second, the temperature is lowered (50-70 °C) to allow the primers to anneal to their complementary target sequences. The last step includes increasing of the temperature (70-75 °C) so that the DNA strand can be synthesized by DNA polymerase. After three cycles of these three steps the first desired product that begins and ends with the oligonucleotide sequences on both strands are generated (Hyde, 2009).

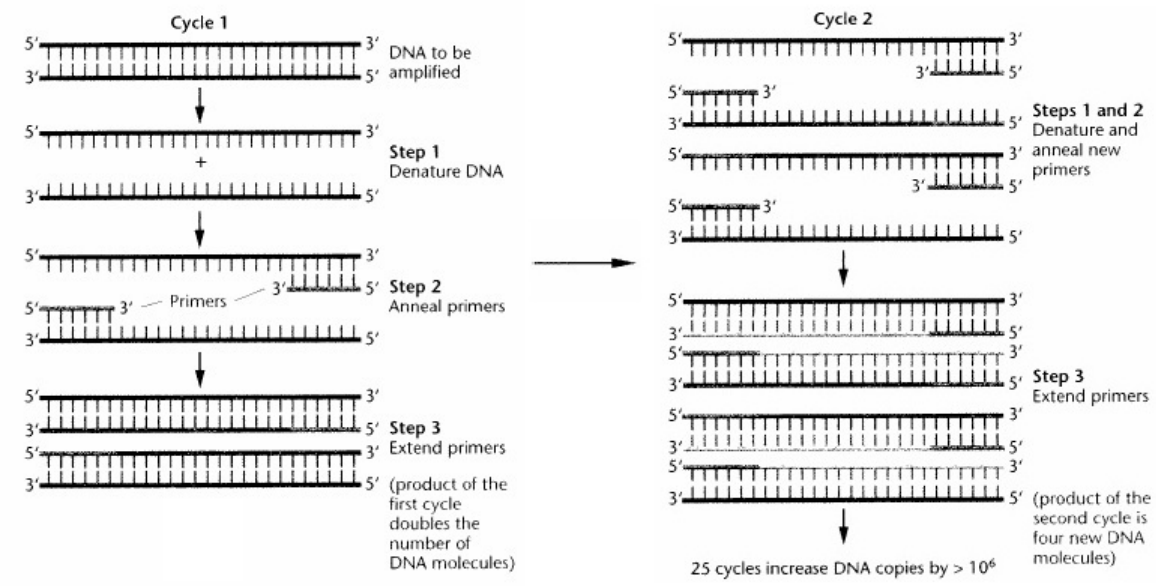

Figure 1.7: Schematic presentation of the Polymerase Chain Reaction (PCR) process. When the three steps in the PCR process are repeated in cycles, a huge number of PCR products are generated in a short time. The figure is adapted from Klug et al. (2009).

1.6.2 Denaturing Gradient Gel Electrophoresis

Denaturing gradient gel electrophoresis (DGGE) is a molecular genetic method based on the melting characteristics of a mixture of DNA fragments of the same length, but with different sequences (Muyzer and Smalla, 1998). The mixture of DNA fragments are influenced by an electric field, causing the DNA fragments to migrate in a gel (Klug et al., 2009). Prior to the use of DGGE, the PCR process described in the previous section should be applied in order to get as much DNA of interest as possible. A GC-clamp should be attached to one of the primers in the PCR prior tot the DGGE, because a GC-clamp attached to the 5' end to one of the primers has been shown to increase the resolution of the DGGE fragments (Muyzer et al., 1993). DGGE makes the user able to analyze many samples taken at different time intervals during a study simultaneously. The method also detects the occurrence of sets of phylogenetically related populations as a consistent pattern of community structure (Ferris et al., 1996). These two aspects make the technique a powerful tool for monitoring community behavior after environmental changes (Muyzer and Smalla, 1998).

As an example, two identical DNA fragments except for a single nucleotide position will have similar but not identical melting properties. As a result, they will be denatured under slightly different conditions (Hames, 1998). If these two fragments are subjected to electrophoresis through a gradient of increasing denaturing concentrations, they will become denatured at slightly different positions along their path through the gel. The migration rate of the fragments depends on their denaturation state, causing the two fragments to exhibit different patterns of migration rate as they begin to denature. The net result of this is that they will travel to different positions along the gradient gel after electrophoresis for the same amount of time (Hames, 1998).

1.6.3 Methodological drawbacks

The combination of PCR and DGGE is a powerful tool to analyze microbial communities by the use of complex DNA mixtures, but the methods have drawbacks. The PCR have limitations in the annealing step presented in Figure 1.7 and during the amplification in general. The primers might be mismatched in the annealing step. This might be caused by differences in accessibility of the primer site, primer universality or presence of inhibitors (Inglis et al., 2012). Amplification biases might be caused by the formation of heteroduplexes, chimeras, sequence mismatches or single-stranded DNA (Kanagawa, 2003).

The DGGE technique has limitations as well. When complex communities are studied, multiple taxa can occupy the same position in the gel, providing an under-estimation of the diversity in the sample (Muyzer and Smalla, 1998). Multiple bands in the gel might also correspond to a single taxon since a specie can contain several 16S rRNA genes. This will results in an over-estimation of abundance and/or diversity (Acinas et al., 2004). Only small regions of the full 16S rRNA gene are used in the methods. This might cause difficulties in obtaining proper results at the species level from the DNA sequence information obtained from DGGE bands, unless a near-perfect match exists within a database (Inglis et al., 2012).

1.7 Scope

The master thesis presented in this report is a part of a pilot project at the Department of Biotechnology at NTNU. The main goal of the thesis was to adapt anammox bacteria to salinity (NaCl) in a continuous reactor system by increasing the concentration of NaCl step-wise. The experimental setup and the establishment of a continuous reactor system were tested in a project work in order to gain experience with the bacterial community and the system in general (Rønning, 2012). The secondary goal of the thesis was to do initial analysis of the dynamics of the bacterial community in the reactor during the adaptation.

Chapter 2

Materials and methods

2.1 Anammox cultivation system

2.1.1 Source of anammox bacteria and inoculation of the reactor

An up flow reactor was inoculated with activated sludge obtained form an already running anammox reactor at Norsk Institutt for Vannforskning (NIVA). The concentrations of total suspended solids (TSS) and volatile suspended solids (VSS) in the activated sludge were 9.69 g/L and 4.59 g/L, respectively (Vogelsang, 2012). The total inoculation volume was 100 mL, where the total sedimented biomass had a volume of 12 mL.

2.1.2 Cultivation medium

The mineral medium fed to the continuous reactor had the composition presented in Table 2.1-2.3, and was similar to the mineral medium reported by Kartal et al. (2006), Sun et al. (2011) and Ma et al. (2012). Table 2.1 presents the macro nutrients, and Table 2.2 and Table 2.3 present the micro nutrients. The compounds were dissolved in ultra pure milliQ water, made with a MILLI-Q® Water System. The pH in the medium was measured with a pH-meter of the type MeterLab™ Standard pH Meter PHM210 and

adjusted to 7.5 $\pm$ 0.1 by the use of 3M NaOH or 3M HCl. After adjustment of pH the medium was flushed with argon gas (Ar) for 20 minutes in order to keep anoxic conditions in the medium and in the head space of the medium container. The concentration of dissolved oxygen (DO) in the medium was measured with a FDO® 925 oxygen electrode (WTW), and was measured to be in the range between 0.01-0.5 mg DO/L. New medium was made every 2^{nd}-5^{th} day.

Table 2.1: Mineral medium composition with chemical compounds and their respective concentrations.

Compound	Concentration (g/L)
$CaCl_2 \cdot 2H_2O$	0.30
$MgSO_4 \cdot 7H_2O$	0.20
KH_2PO_4	0.025
$NaHCO_3$	1.0
NH_4HCO_3	Varying
$NaNO_2$	Varying
Trace solution 1*	1 mL
Trace solution 2**	1 mL

* See Table 2.2

** See Table 2.3

Table 2.2: Composition of trace solution 1. The trace solution was identical to Imajo et al. (2004), Date et al. (2009) and Sun et al. (2011).

Compound	Concentration (g/L)
$FeSO_4 \cdot 7H_2O$	5.0
$EDTA$	5.0

Table 2.3: Composition of trace solution 2. The trace solution was identical to Kartal et al. (2006), Ma et al. (2012) and Vogelsang (2012).

Compound	Concentration (g/L)
$EDTA$	15
$ZnSO_4 \cdot 7H_2O$	0.43
$CoCl_2 \cdot 6H_2O$	0.24
$MnCl_2 \cdot 4H_2O$	0.629
$CuSO_4 \cdot 5H_2O$	0.25
$Na_2MoO_4 \cdot 2H_2O$	0.22
$NiCl_2 \cdot 6H_2O$	0.19
$Na_2SeO_4 \cdot 10H_2O$	0.21
H_3BO_3	0.014
$NaWO_4 \cdot 2H_2O$	0.05

2.1.3 Reactor set-up and regulation

The reactor was an up flow reactor made of glass with a hydraulic volume of 360 mL. The reactor system was chosen because this reactor design has been suggested to be the most suitable for the application of an anammox treatment system (Imajo et al., 2004). The application of an up flow reactor is suggested to be the best because of the ability to keep a selective environment for the biomass to granulate (Abma et al., 2007). The granulating process is essential to succeed when using anammox bacteria, because granular sludge makes it possible to maintain a large amount of active biomass in a reactor (Imajo et al., 2004). In addition to the reactor, there was also a sedimentation trap to collect any biomass that might have been washed out from the reactor.

The reactor had an outer jacket for temperature control. The heating water was heated and circulated with a Polystat® bath (Cole Parmer) at a temperature of 30 °C. The reactor was covered with a black fabric in order to avoid phototrophic growth inside the reactor. The medium was fed from underneath the reactor with an adjustable Masterflex® pump with an Easy-load® (Model 7518-00, Cole Parmer) pump head and Masterflex ® PharMed® (06508-14) tubes. A 3.8 L Tedlar® gas bag (Sigma-Aldrich) was connected

to the medium container at day 98 to refill the head space in the container with Argon gas as the volume of the medium inside decreased. Figure 2.1 shows a picture of the continuous up flow reactor system as it was operated from day 134 and Figure 2.2 shows a schematic presentation of the continuous reactor system.

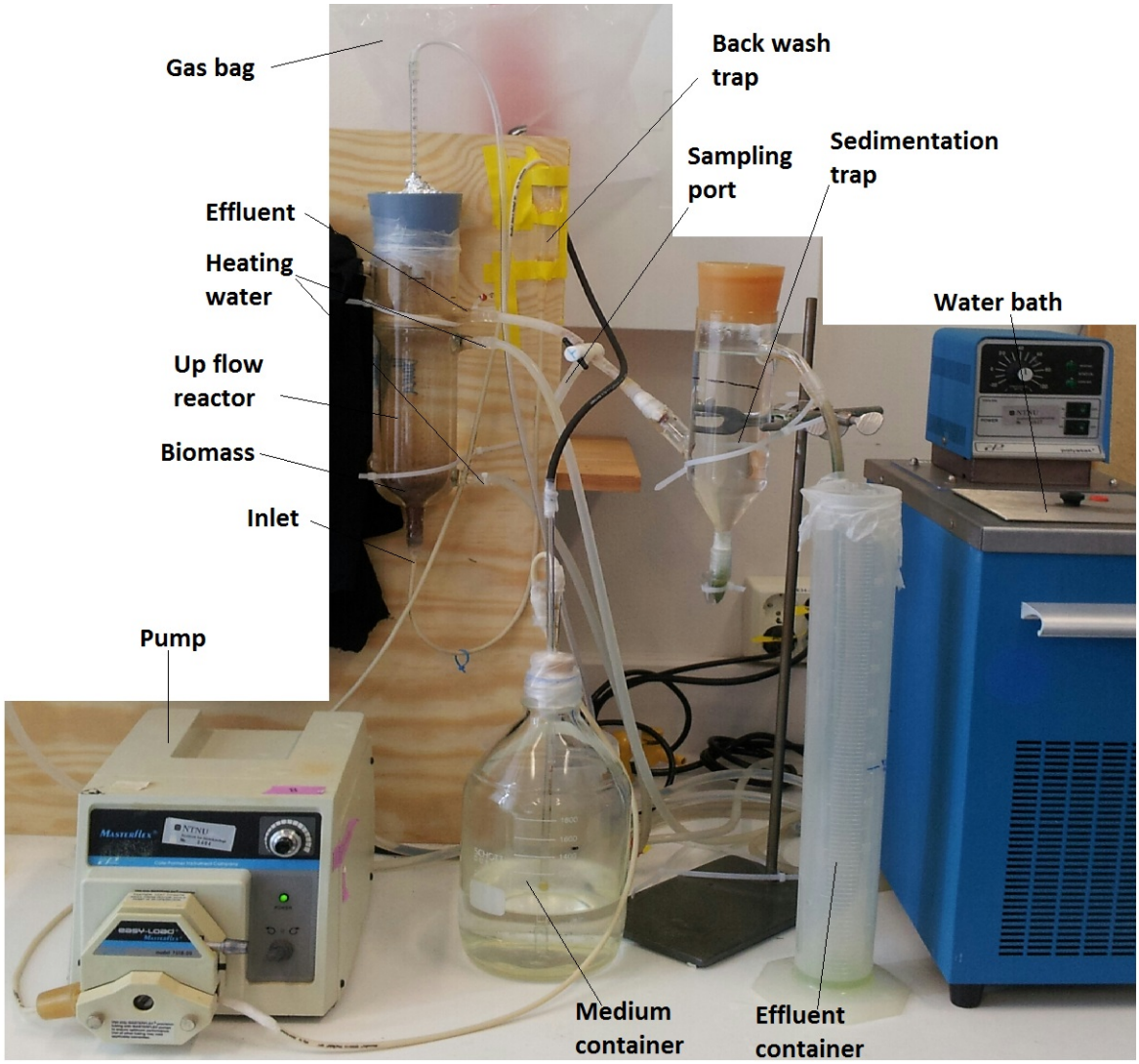

Figure 2.1: A picture of the continuous up flow reactor system. The major units in the system are presented in the picture.

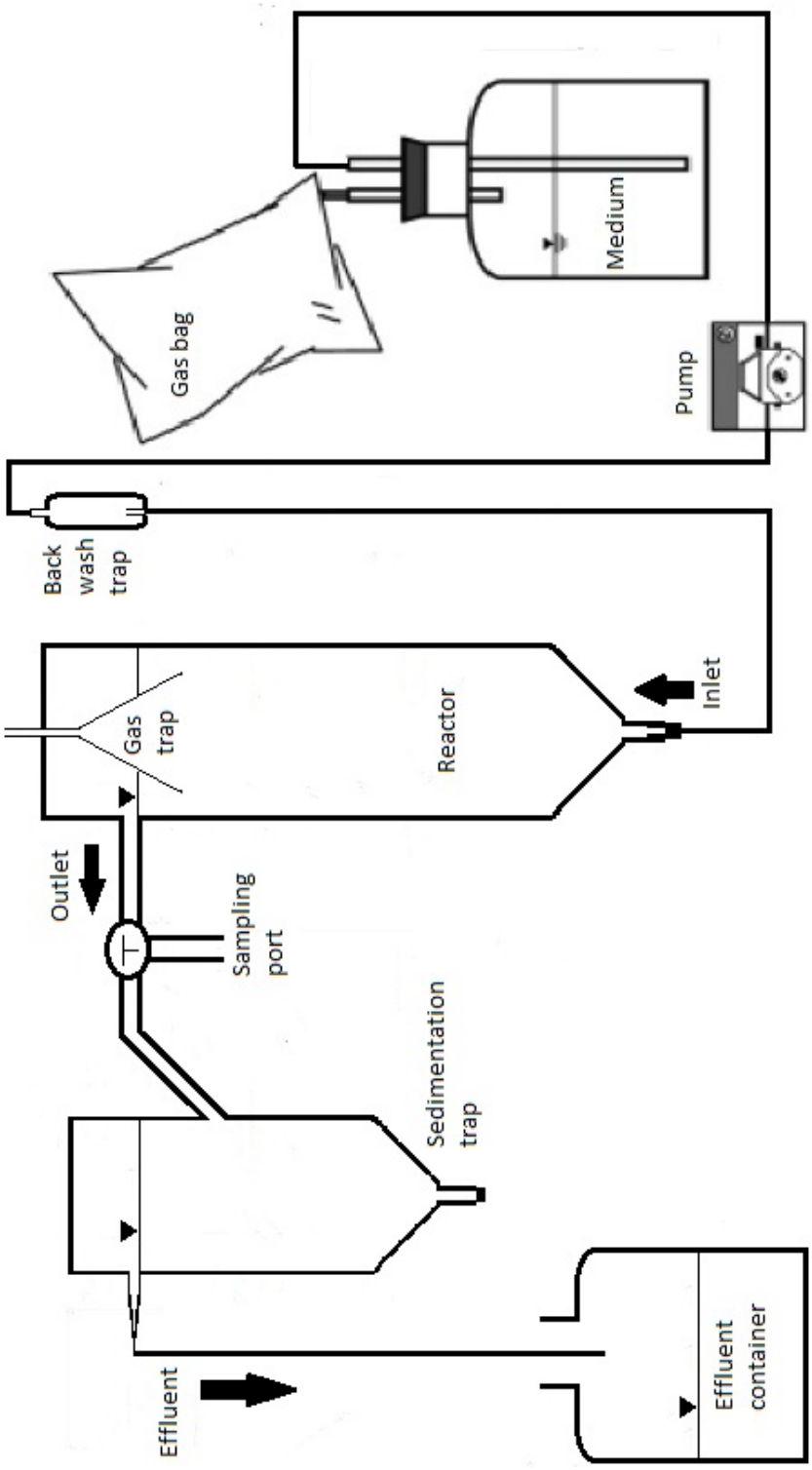

Figure 2.2: Schematic presentation of the continuous up flow reactor system. The figure is partly adapted from Kindaichi et al. (2011).

2.1.4 Operational timeline

Figure 2.3 presents the operational changes that were made during the experiment. The changes were *e.g.* change of HRT, concentration of NaCl in the medium and other external changes. Table 2.4 presents more information about each operational event given in the timeline. The sampling of the activated sludge from the reactor are highlighted in bold. The reactor was operated by *Ph.D.* candidate Blanca Magdalena Gonzalez Silva in the periods day 63-76 and day 132-147. The experimental and operational procedures were conducted in the same way as the rest.

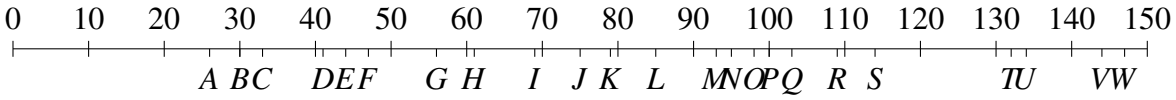

Figure 2.3: The figure presents the operational timeline of the whole experiment. More details about the events are presented in Table 2.4

Table 2.4: The table gives information about the operational changes presented in Figure 2.3.

Day	Event	Description
26	A	Changed ratio mg $N-NO_2^-$/mg $N-NH_4^+$ in the medium from approximately 1.0 to approximately 1.3.
30	B	Decreased the HRT from 30 hours to 27 hours.
33	C	Decreased HRT from 27 hours to 21 hours.
41	D	Decreased HRT from 21 hours to 18 hours.
44	**E**	**Sampling of biomass for DGGE analysis.**
47	F	Start of adaptation to salinity, 3,0 g NaCl/L in the medium.
56	G	Decreased salinity to 1.5 g NaCl/L in the medium.
61	H	Decreased salinity to 0 g NaCl/L in the medium.
69	I	Increased salinity to 0.8 g NaCL/L in the medium.
75	J	Increased salinity to 1.7 g NaCL/L in the medium.
79	K	Decreased salinity to 1.0 g NaCL/L in the medium.
85	L	Decreased salinity to 0 g NaCl/L in the medium.
93	M	Changed the medium container.

Continued on next page

Table 2.4 – *Continued from previous page*

Day	Event	Description
95	N	Increased salinity to 1.0 g NaCL/L in the medium.
98	O	Inserted a gas bag to the medium container.
100	P	Increased salinity to 1.5 g NaCl/L in the medium.
103	Q	Increased salinity to 2.0 g NaCl/L in the medium.
109	R	Increased salinity to 3.0 g NaCl/L in the medium.
114	**S**	**Sampling of biomass for DGGE analysis.**
132	T	Decreased salinity to 1.5 g NaCL/L in the medium.
134	U	Changed tubes to avoid penetration of oxygen.
144	V	Increased salinity to 3.0 g NaCl/L in the medium.
147	W	End of the experiment presented in this report.

2.2 Analytical procedures for monitoring the anammox activity

To monitor the anammox activity in continuous reactor, the concentrations (mg/L) of ammonium, nitrite and nitrate were measured and expressed as $N{-}NH_4^+$, $N{-}NO_2^-$ and $N{-}NO_3^-$, respectively. The concentrations were measured every - 3^{rd} day, and the samples were obtained by a sample port after the outlet of the reactor (see Figure 2.2). The samples ($\sim$ 3 mL) were filtered through a 0.45 μm or 0.2 μm non-pyrogenic sterile-R filter (Sarstedt). The concentrations of $N{-}NH_4^+$, $N{-}NO_2^-$ and $N{-}NO_3^-$ were measured photometrically by the use of Dr. Lange cuvette tests (Hach Lange) LCK 303, LCK 341 and LCK 339, respectively. The procedures were carried out according to the manufacturer's instructions. The spectrophotometer used was of the type Dr. Lange Lasa100 spectrophotometer. When the medium was prepared, the same tests (only LCK 303 and LCK 341 since no NO_3^- was added) were used to measure the inlet concentrations of each compound. When high concentrations of nitrite was observed in the effluent, the concentrations of nitrate was adjusted by the use of the *ax*-term given by the equation in Figure C.1 in Appendix C. This was done because of influence of nitrite on the measurements of nitrate.

The removal of ammonium expressed as ARR, nitrite expressed as NRR and the total nitrogen removal expressed as TNRR in the reactor, were determined by the use of Equation 2.1-2.3, respectively. The total nitrogen loading rate (TNLR) was also calculated as given in Equation 2.4. The production rate of nitrate (NPR) was monitored as presented in Equation 2.5. The hydraulic retention time (HRT) used in the equations is defined by Drapcho et al. (2008) as the hydraulic volume of the reactor (360 mL) divided on the volumetric flow rate (mL/h) of the medium. Flow measurements were conducted by the use of a timer and a measuring cylinder.

$$ARR\ (mg\,N{-}NH_4^+/L\,d) = \frac{(N{-}NH_4^+)_{in}(\frac{mg}{L}) - (N{-}NH_4^+)_{out}(\frac{mg}{L})}{HRT(h)} \cdot \frac{24h}{day} \tag{2.1}$$

$$NRR\ (mg\,N{-}NO_2^-/L\,d) = \frac{(N{-}NO_2^-)_{in}(\frac{mg}{L}) - (N{-}NO_2^-)_{out}(\frac{mg}{L})}{HRT(h)} \cdot \frac{24h}{day} \tag{2.2}$$

$$TNRR\ (mg\,\mathrm{N}/L\,d) = ARR + NRR \tag{2.3}$$

$$TNLR\ (mg\,\mathrm{N}/L\,d) = \frac{(\mathrm{N{-}NO_2^-})_{in}(\frac{mg}{L}) + (\mathrm{N{-}NH_4^+})_{in}(\frac{mg}{L})}{HRT(h)} \cdot \frac{24h}{day} \tag{2.4}$$

$$NPR\ (mg\,\mathrm{N}/L\,d) = \frac{(\mathrm{N{-}NO_3^-})_{out}(\frac{mg}{L})}{HRT(h)} \cdot \frac{24h}{day} \tag{2.5}$$

One of the key parameters to monitor the anammox activity in the reactor is the consumption ratio of nitrite with respect to ammonium, as presented in Equation 2.6 (Jetten et al. (2005), Kartal et al. (2006), Dapena-Mora et al. (2007)). This was done to check whether the consumption of both nitrite and ammonium were close to the theoretical ratio given in Equation 1.1.

$$Consumption\ ratio\ (mg\ \mathrm{N{-}NO_2^-}_{consumed}/mg\ \mathrm{N{-}NH_4^+}_{consumed}) = \frac{NRR}{ARR} \tag{2.6}$$

The two last parameters that were monitored in the reactor were the production ratio of nitrate with respect to the consumption of ammonium, as well as the loss of nitrogen in the reactor with respect to the nitrogen that was consumed. This was done to check whether the production of nitrate (NO_3^-) and nitrogen gas (N_2) were close to the theoretical ratios given in Equation 1.1. The production ratio of nitrate/ammonium is given by Equation 2.7 and the loss of nitrogen is given by Equation 2.8.

$$Production\ ratio\ (mg\ \mathrm{N{-}NO_3^-}_{produced}/mg\ \mathrm{N{-}NH_4^+}_{consumed} = \frac{NPR}{ARR} \tag{2.7}$$

$$Loss\ of\ N\ (mg\ N/mg\ N) = \frac{(\mathrm{N{-}NO_2^-} + \mathrm{N{-}NH_4^+})_{in} - (\mathrm{N{-}NO_2^-} + \mathrm{N{-}NH_4^+} + \mathrm{N{-}NO_3^-})_{out}}{(\mathrm{N{-}NO_2^-} + \mathrm{N{-}NH_4^+})_{in} - (\mathrm{N{-}NO_2^-} + \mathrm{N{-}NH_4^+})_{out}} \tag{2.8}$$

2.3 Analysis of microbial community composition

2.3.1 Sampling of biomass from the reactor

In order to be able to do analysis of the microbial community in the reactor along with the adaptation to salinity, samples of the sludge in the reactor were sampled by opening the reactor and removing 1 mL of sample (containing 600-700 μL of sludge) by the use of a pipette and Peleus ball. The samples were stored at -20 °C. After the sampling, the head space in the reactor was flushed with Argon gas for 5 minutes to keep anoxic conditions in the reactor.

2.3.2 Extraction of DNA

The extraction of the DNA from the samples taken from the reactor was done as described in the Instruction Manual to the PowerSoil® DNA Isolation Kit (Cat. No.: 12888-100) delivered by MO BIO Laboratories. The extracted DNA was stored at -80 °C. The concentrations of the extracted DNA were measured by using a NanoDrop® ND-1000 spectrophotometer.

2.3.3 Polymerase Chain Reaction for gel analysis

The PCR reagents and buffers that were used to amplify the extracted DNA are presented in Table 2.5. The different PCR samples were prepared by making a master mix consisting of the components given in Table 2.5, which again was split into separate eppindorf tubes. The DNA templates were added to the master mix solution in each tube and the PCR mixtures were amplified by the use of a Arktik Thermal Cycler (Thermo Scientific).

Table 2.5: The table presents the different PCR reagents and buffers, including their amount and concentrations. The total reaction volume was 25 μL.

Reagent	Volume (μL)	Final concentration
10x reaction buffer	2.50	1x
dNTP (10 mM)	0.50	200 μM
$MgCl_2$ (25 mM)	0.50	2 mM (10x buffer also contained $MgCl_2$)
BSA (10 mg/mL)	0.75	
Primer 338F-GC (10 μM)	0.75	0.3 μM
Primer 518R (10 μM)	0.75	0.3 μM
Taq DNA Polymerase	0.125	
DNA template	1.00	
Filtered H_2O	18.125	

The primers used were the universal primers 338F-GC (GC-clamp in italics) (sequence 5'-*cgcccgccgcgcgcggcgggcggggcgggggcacgggggg* actcctacgggaggcagcag-3') and 518R (sequence 5'-aattaccgcggctgctgg-3'). These primers are targeting the v3 region of the bacterial 16S rRNA gene, giving amplified sequences of approximately 240 base pairs. This primer pair is widely used for generating PCR products for DGGE analysis (Bakke et al., 2011). The thermocycling parameters are presented in Table 2.6 (Bakke et al., 2011). Step 2-4 were repeated in cycles 35 times prior to step 5. The PCR products were evaluated by the use of an agarose gel, presented in the next section.

Table 2.6: The table presents the temperature regimes in the PCR of the extracted DNA. Step 2-4 were repeated in cycles 35 times before step 5 started.

Step number	Step explanation	Temperature (°C)	Time
1	Initial denaturation	95	3 min
2	Denaturation	95	30 sec
3	Annealing	53	30 sec
4	Elongation	72	60 sec
5	Final elongation	72	30 min
6	Stop	10	$\propto$

2.3.4 Verification of PCR products

The PCR products were verified by the use of an agarose gel electrophoresis in an Owl EasyCast Mini Gel System (Thermo Scientific). The agarose gels were prepared by mixing 4 g SeaKem® LE agarose (Lonza) in 400 mL of 1xTAE buffer (5.04 g tris-base, 2 mL 0.5 M EDTA and 1.14 mL glacial acetic acid/L). The mixture was heated to reflux and then slowly cooled to 65 °C. 20 μL of GelRed™ Nucleic Acid Gel Stain (QIAGEN) was added to the mixture.

A mixture containing 5 μL of the PCR products and 1 μL of 6x loading dye (Fermentas) was added to each well in the gels, and the gels were run for 45-60 minutes. A ladder (GeneRuler™ 1 kb Plus, Fermentas) was used to verify the length of the PCR products. The gels were transferred to a G:BOX UV visualizer (Syngene) after the electrophoresis, and photos of the gels were taken using the associating GeneSnap software.

2.3.5 Denaturing gradient gel electrophoresis

The PCR products of the extracted DNA from the reactor were run together with two other samples, a control and a reference/ladder through an acrylamide gel in the process of denaturing gradient gel electrophoresis. The PCR products had the same length and were separated based on the base composition. The protocol for the DGGE is presented in detail in Appendix E. The volume of each sample was 7.5 μL, which contained 5 μL PCR product and 3 μL of a loading buffer. The reference sample/ladder was amplified by the use of the primers presented in the Section 2.3.3, and consisted of nine PCR products from pure cultures.

The electrophoresis was performed with a INGEN PhorU system with a self cast 8 % acrylamide gel with a 35-50 % denaturing gradient. The gel was run at 100 V for approximately 20 hours. The gel was stained with SYBR Gold (Invitrogen) after the electrophoresis, and then incubated in darkness for 1 hour during the staining reaction. The gel was rinsed with MilliQ water before it was transferred to a G:BOX UV visualizer (Syngene). Then a photo was taken using the a GeneSnap software.

2.3.6 PCR of DNA from DGGE gel for sequencing

When the DGGE-gel was analyzed, samples of distinct DNA bands were excised by removing some of the gel by the use a pipette tip. UV light was used to visualize the bands in the gel. The small fractions of the gel were mixed with 20 μL MilliQ water, and this mix was used as template for the new PCR experiment. The PCR reagents and buffers were the same as presented in Table 2.5, except that the forward primer 338F-M13R (sequence 5'-caggaaacagctatgac cgcccgccgcgcgcggcgggcggggcgggggcacgggggg actcctacgggaggcagcag-3') which was used instead of 338F-GC. The thermocycling parameteres were as presented in Table 2.7 Step 2-4 were repeated in cycles 38 times before step 5 started.

Table 2.7: The table presents the temperature regimes in the PCR of the DNA bands from the DGGE gel. Step 2-4 were repeated in cycles 38 times before step 5 started.

Step number	Step explanation	Temperature (°C)	Time
1	Initial denaturation	95	3 min
2	Denaturation	95	30 sec
3	Annealing	53	30 sec
4	Elongation	72	60 sec
5	Final elongation	72	10 min
6	Stop	10	$\propto$

The PCR products were purified by the use of the QIAquick® PCR Purification Kit (Cat. No. 28106) delivered by QIAGEN, and the procedure was done according to the manual. The DNA concentration of the purified products were measured by using a NanoDrop® ND-1000 spectrophotometer.

2.3.7 Sequencing of DNA from the DGGE gel

To start initial tests to be able to identify species present in the reactor, the PCR products of the DNA sampled from the DGGE gel were sent to for sequencing. 5 μL of PCR

product was mixed with 5 μL of the primer 338F-M13R and they were all sent to GATC BIOTECH (Germany) for sequencing.

The results were returned by e-mail, and the results were analyzed by the use of the Classifier tool available at the online database Ribosomal Database Project (RDP), (Wang et al., 2007) (available at *http://rdp.cme.msu.edu*).

2.3.8 DGGE band pattern analysis

The band patterns in the DGGE gel were analyzed by the use of a program called Gel2k developed by Norland (2004). The program is used to identify the bands in the gel, generating histograms for each lane in gel based on the bands and quantifying the DGGE patterns based on the peak areas in the histograms. This quantification makes the user able to do further computational analysis with the results from the DGGE gel.

An other program called PAST, developed by Hammer et al. (2001), was used to calculate the Shannon diversity index (*H'*) and the Bray-Curtis similarity. The Shannon diversity index is a measurement of the specie diversity of a community in a specific sample, and the equation is given in Equation 2.9 (Peet, 1975). The *p*-value is the normalized fractional area of a band's histogram peak area. *S* is the number of bands in a specific lane, which corresponds to the Band richness (k). The Bray-Curtis similarity (ranging between 0 and 1) is indicating the similarity between to samples (Bray and Curtis, 1957).

$$H^{'} = -\sum_{i=1}^{s} p_i \, ln \, p_i \tag{2.9}$$

2.4 Experimental flow scheme

Figure 2.4 presents the total experimental flow scheme of the experiments presented in this report. Red rectangles represent the reactor, ellipses represent to molecular experiments, diamonds represent computational and statistical methods and the circle represents sequencing of DNA. Blue colors represent microbial analysis as a whole and green colors represent sampling of DNA. The thick lines represent the division between the main experiment (red colors) and the secondary experiments (blue colors). The dashed line is representing an experimental pathway that has not been emphasized in this report.

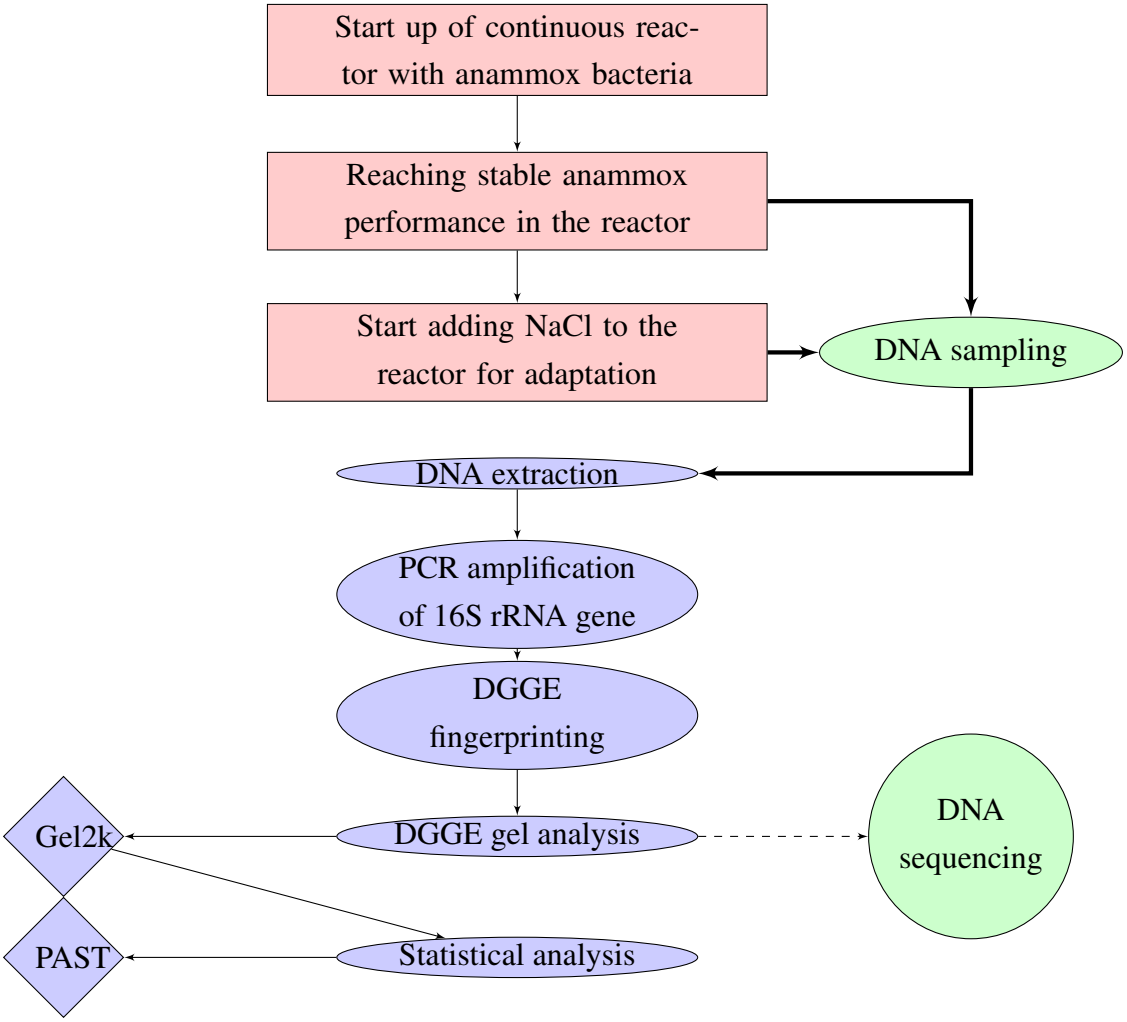

Figure 2.4: The figure presents the total experimental flow scheme of the experiments presented in this report. See the text above the figure for more details about the flow scheme.

Chapter 3

Results and discussion

The results are presented in three different sections. The operation of the continuous reactor is presented in Section 3.1, where the equations presented in Section 2.2 have been used to monitor the performance in the up flow reactor. Section 3.2 presents the general effects of salinity to the system, followed by the results and analyses of the community dynamics in Section 3.3.

3.1 Operation of the continuous reactor

3.1.1 Concentrations in and out of the reactor

Figure 3.1 presents the measured concentrations of $N{-}NO_2^-$, $N{-}NH_4^+$ and $N{-}NO_3^-$ in the effluent as well as the concentrations of $N{-}NO_2^-$ and $N{-}NH_4^+$ in the inlet. The figure also includes the hydraulic retention time (HRT) in the reactor. The raw data for the figure are presented in Table A.1 in Appendix A.

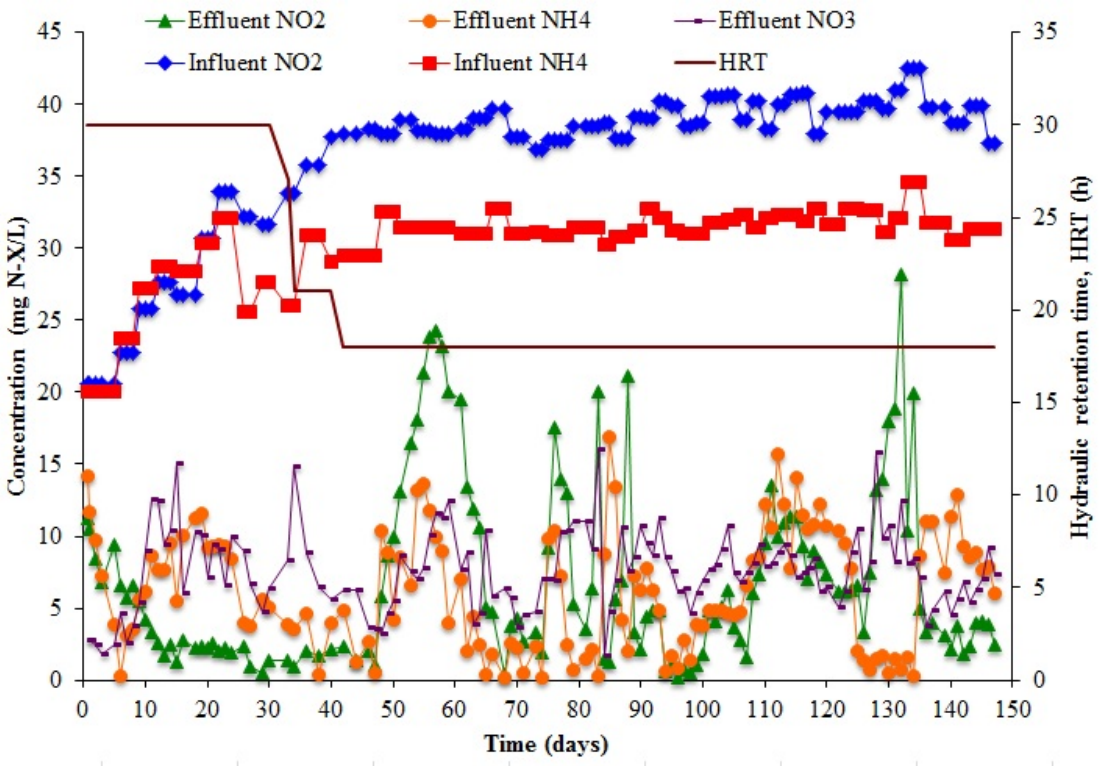

Figure 3.1: The figure presents the measured concentrations of $N-NO_2^-$, $N-NH_4^+$ and $N-NO_3^-$ in the effluent and the inlet of the reactor (all primary y-axis) and the hydraulic retention time (HRT) (secondary y-axis) as functions of time. The inlet concentrations of $N-NO_2^-$ and $N-NH_4^+$ are represented by blue diamonds and red squares, respectively. The effluent concentrations of $N-NO_2^-$, $N-NH_4^+$ and $N-NO_3^-$ are represented by green triangles, orange circles and purple lines, respectively. The HRT is represented by a brown line.

Figure 3.1 shows that the inlet concentrations of both nitrite and ammonium was 20 mg N/L in the beginning of the experiment. These concentrations were gradually increased together in a ratio of approximately 1:1. From day 26 the ratio was changed to approximately 1,32 to keep the feeding ratio similar to the theoretical consumption ratio, presented in Equation (1.1). The concentrations were increased further and kept relative constant from day 47 at 37-42 mg $N-NO_2^-$/L and 30-34 mg $N-NH_4^+$/L throughout the experiment. The HRT was 30 hours the first 30 days of the experiment before it was reduced to 27 hours, 22 hours and finally 18 hours. The HRT was kept stable at 18 hours from day 42 and during the rest of the continuous experiment. The HRT was reduced (by increasing the flow) to increase the activity (the removal of nitrogen) in the reactor.

The effluent concentrations of both nitrite and ammonium were generally low throughout the experiment. It can be seen in the figure that the effluent concentration of ammonium dropped when the inlet ratio of ammonium and nitrite was changed from 1:1 to 1.32:1 (from day 26). From day 47-58 there was an increase of both ammonium and especially nitrite in the effluent. This was caused by the addition of NaCl to the system, and will be further presented in Section 3.1.2. The concentrations decreased gradually again from day 58-69 when the salinity was removed from the system. This matter will also be further presented in Section 3.1.2. The different peaks of nitrite and ammonium in the period between day 75-88 and the increase of nitrite between day 127-134 will also be further discussed in Section 3.1.2 and 3.1.3. The measured effluent concentrations of nitrate were more or less fluctuating during the whole experiment, but stayed for the most of the time in the range of 5-11 mg N/L.

3.1.2 Total nitrogen removal in the reactor

One of the key parameters used in this report to monitor the anammox performance of the biomass in the reactor was to follow the total nitrogen removal rate (TNRR), as presented in Equation 2.3. Figure 3.2 presents the TNRR together with the total nitrogen loading rate (TNLR) and the concentration of NaCl (salinity) in the medium fed to the reactor. The TNLR is calculated as presented in Equation 2.4. The raw data for the figure are presented in Table A.2 in Appendix A. The periods presented in the figure include the following data points (days): Period I = 11-47, Period II = 48-88 and Period III = 89-147.

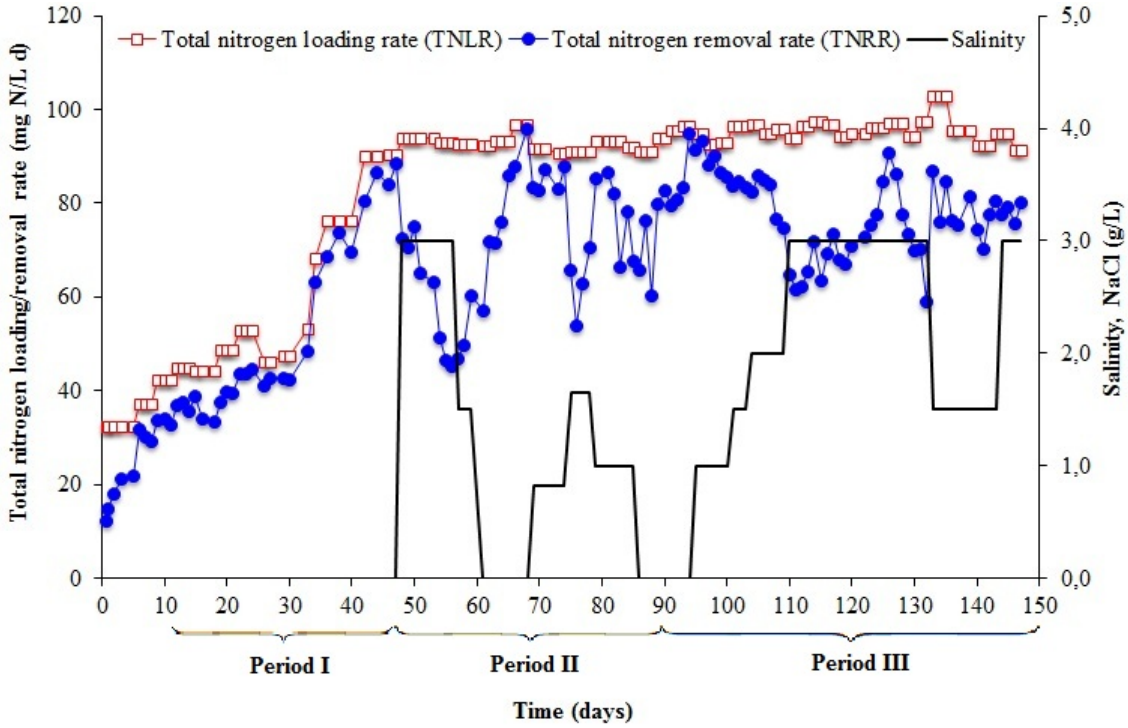

Figure 3.2: The figure presents the total nitrogen loading rate (TNLR), total nitrogen removal rate (TNRR) (both primary y-axis) and salinity in the medium (secondary y-axis) as functions of time, represented by red and unfilled squares, blue circles and a black line, respectively.

Figure 3.2 shows that the TNLR was gradually increased from day 0-47, and then kept relative constant (90-102 mg N/L d) throughout the experiment. The TNLR was increased by increasing the concentrations of $N-NO_2^-$ and $N-NH_4^+$ in the medium fed to the reactor or by decreasing the HRT as presented in Figure 3.1 (day 30-42). The drop in the TNLR at day 26 was caused by the change of the ratio $N-NO_2^-/N-NH_4^+$ in the medium from approximately 1:1 to approximately 1.32:1, as presented previously in Section 3.1.1. The concentrations of $N-NO_2^-$ and $N-NH_4^+$ were kept at approximately 40 mg $N-NO_2^-$/L and 30 mg $N-NH_4^+$/L to avoid the inhibitory effects of the substrate components presented in Section 1.2.

Figure 3.2 shows that the total nitrogen removal rate (TNRR) in the reactor followed the total nitrogen loading rate (TNLR) before the salinity was added (at day 47). This period is denoted as *Period I*, which include all the points before the adaptation to salinity

started, except for a start-up period the first 10-11 days. In Period I the microbial community in the reactor responded quickly to any increase in the TNLR. When the salinity (3 g NaCl/L) was introduced to the system (start of *Period II*) the TNRR immediately dropped and kept dropping until the salinity was reduced (to 1.5 g NaCl/L at day 57) and removed completely in the medium (at day 61). When the salinity was removed, the TNRR increased day by day until it was similar as the TNLR, indicating full removal of nitrogen. The TNRR slightly dropped when salinity (0.8 g NaCl/L at day 69) was introduced again, but it remained relative high and stable. When the salinity was increased further to 1.7 g NaCl/L at day 75, the TNRR dropped again, but it started to increase before the salinity was decreased to 1.0 g/L. This reduction in salinity at day 79 was caused by an error in calculations when the medium was prepared. In this case the bacteria seemed to recover the activity within a few days, before the TNRR fluctuated between day 82-89, indicating instability in the reactor. Even when the salinity was removed again from the system (at day 86) the TNRR still fluctuated, but it was stable again a few days after the salinity was removed. The salinity was removed from the system in order to see if the instability in the reactor was caused by the NaCl since the effluent concentrations of both ammonium and nitrite were fluctuating severely, as can be seen in Figure 3.1.

The period denoted as *Period III* started at day 89, when the reactor was stabilized in terms of the TNRR. When complete nitrogen removal was reached, the salinity was again added to the system, and slowly increased up to 3.0 g NaCl from day 109 to 132. The TNRR decreased step by step from 95 to 75 mg N/L d when the salinity was increased from 0-2 g NaCl/L. When the salinity was increased to 3.0 g/L the TNRR dropped even further to 62 mg N/L d. As the salinity was kept at 3.0 g NaCl/L the TNRR increased slowly again to 91 mg N/L d at day 126. From day 126 to 132 the TNRR decreased step-wise to 59 mg N/L. This matter will be further discussed in the next section, where the TNRR is being further analyzed by dividing it into the removal rates of the to major nitrogen components (ammonium and nitrite). When the salinity was reduced to 1.5 g NaCl/L the TNRR increased again to 80 mg N/L d, and it stabilized around 80 mg N/L d when the salinity was increased again to 3.0 NaCl/L.

3.1.3 Removal and production rates in the reactor

Figure 3.3 presents the removal rate of nitrite (NRR) and ammonium (ARR), the production rate of nitrate (NPR) in the reactor and the salinity in the medium fed to the reactor. The ARR, NRR and NPR are calculated as presented in Equation 2.1, 2.2 and 2.5 in Section 2.2, respectively. The raw data for the figure are presented in Table A.2 in Appendix A, which are calculated based on the concentrations presented in Figure 3.1. The periods presented in the figure are the same as in Figure 3.2.

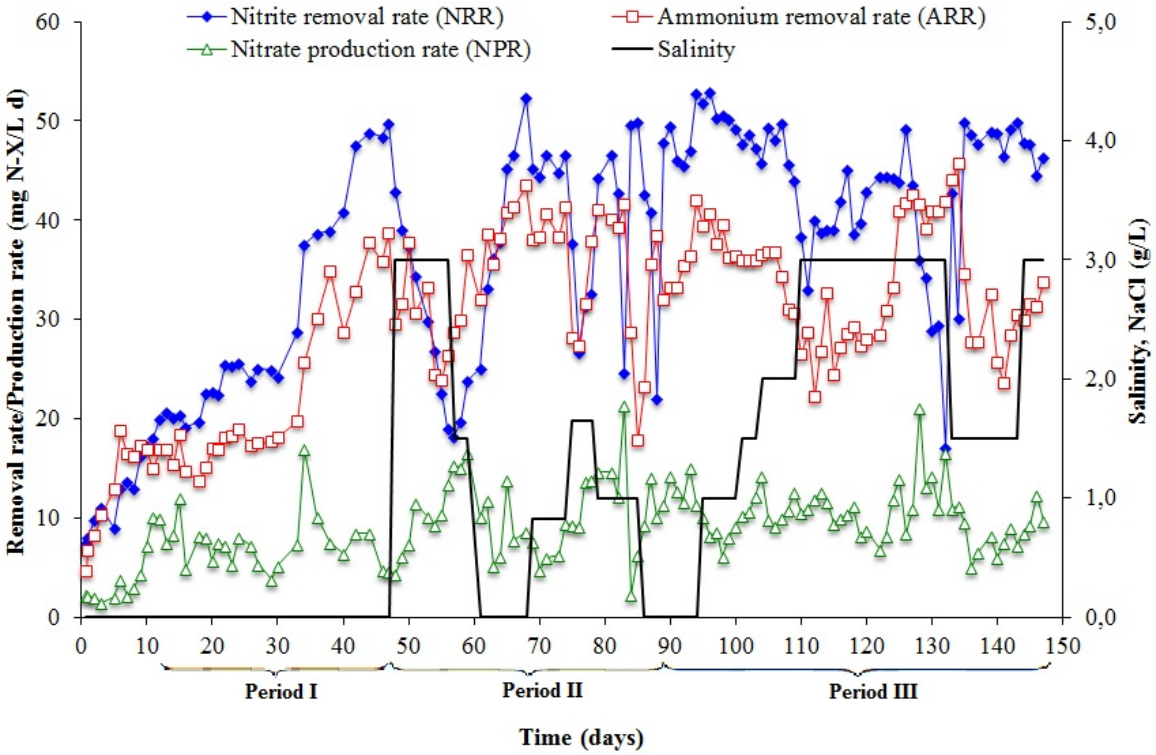

Figure 3.3: The figure presents the removal rates of NO_2^- and NH_4^+, the production rate of NO_3^- (all primary y-axis) and the salinity in the reactor (secondary y-axis) as functions of time. The different rates and the salinity are represented by blue diamonds, red and unfilled squares, green and unfilled triangles and a black line, respectively.

The figure shows that the NRR was higher than the ARR most of time during the experiment. This is in accordance with the fact that the concentrations of nitrite in the medium fed to the reactor were higher than the concentrations of ammonium, and the fact that the theoretical anammox consumption ratio of the components is 1,32. The figure also

shows that these two removal rates had the same pattern during most of the experiment. When comparing Figure 3.3 and Figure 3.2, the figures show that when the TNRR was stable, both NRR and ARR were stable or moving together. When there were severe fluctuations in the TNRR, such as between day 83-88 and between day 126-141, the NRR and ARR were fluctuating separately. These observations imply that the system was unstable. The inhibitory effects of the NaCl will be further discussed in Section 4.1.

The huge drop in the nitrite removal rate from day 126-132 is believed to be caused by oxygen contamination in the system. The dissolved oxygen inside the reactor was measured to be 0.39 and 0.45 mg O_2/L at day 130 and 132, respectively. The dissolved oxygen in the medium container was measured to be 0.8 mg and 1.0 mg O_2/L the same days. These concentrations could lead to partial nitrification (Ye et al., 2009), which would lead to production of nitrite as well as less nitrite would be consumed by the anammox bacteria. Because the concentration of nitrite increased from 3.3 to 28.2 mg $N-NO_2^-$/L in this period and there was complete removal of ammonium, this might have been the case. When the salinity was decreased (at day 132) and tubing in the medium container was changed (day 134) the nitrite removal rate increased again to almost complete removal of nitrite. Since two changes where done almost at the same time, the true effect of each of them is unknown. But the two changes resulted in an improvement of the system in terms of a relative stable performance of the reactor.

The production rate of nitrate (NPR) was fluctuating more or less through the whole experiment, which is also shown in Figure 3.1 as the effluent concentration of nitrate was fluctuating. It might seem to be a trend that the NPR was increasing step-wise when the salinity was added or increased in Period II and III and decreasing again when the salinity was removed or reduced. But there were still fluctuations within this possible trend, so it is hard to describe a general development of the nitrate production rate.

3.1.4 Consumption ratio of nitrite and ammonium and production ratio of nitrate

Figure 3.4 presents the consumption ratio of nitrite with respect to ammonium, the production ratio of nitrate with respect to the consumption of ammonium and the salinity in the reactor. The calculated values are based on Equation 2.6 and Equation 2.7 in Section 2.2, and the values are presented in Table A.2 in Appendix A.

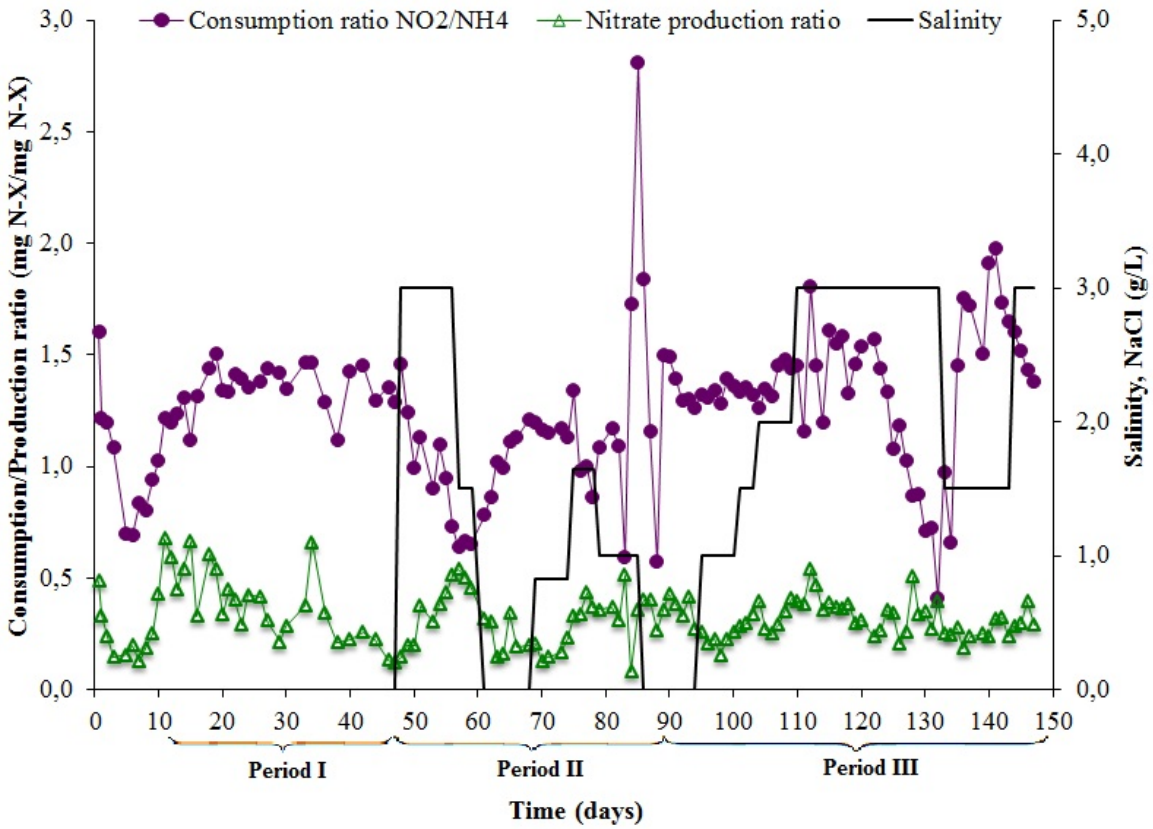

Figure 3.4: The figure presents the consumption ratio of mg $N-NO_2^-$/ mg $N-NH_4^+$, the production ratio of mg $N-NO_3^-$ produced/mg $N-NH_4^+$ consumed (both primary y-axis) and salinity (secondary y-axis) in the reactor as functions of time. The consumption ratio, the production ratio and the salinity are represented by purple circles, green and unfilled triangles and a black line, respectively.

Consumption ratio of nitrite and ammonium

The average consumption ratio of nitrite and ammonium the first period (day 11-47) was 1.3 $\pm$ 0.1, which is in accordance to the theoretical value of 1.32. Figure 3.4 shows that the consumption ratio was fluctuating, but it was relative stable over the given period. The small standard deviation in that period is also indicating a stable removal of nitrogen. In the start-up period the fluctuations were more severe, and the fact that the ratio the first 10-11 days was going down at first and then up again to around 1.20 is the main reason why the start up period has not been included in the calculations presented in this report.

When the salinity was added to the system for the first time (day 47) the consumption ratio changed along with the decrease in the TNRR from approximately 1.4 to approximately 0.6. When the salinity was decreased and totally removed the ratio increased day by day together with the increase in the TNRR (Figure 3.2). When the salinity again was added to the system (0.5 g NaCl/L at day 69), the consumption ratio was still stable, but dropped when the salinity was further increased to 1.0 g NaCl/L at day 75. The extreme fluctuations between day 83-88 from 0.6 to 2.8 is the reason why the salinity was removed from the system, to see if this was caused by inhibition of the NaCl or not. Since the performance was still fluctuating, external changes of the system were made (presented in Figure 2.3 on page 28). The average consumption ratio in the second period was 1.1 $\pm$ 0.4, which is deviating from the theoretical value of 1.32. The high standard deviation of 0.40 is also indicating an unstable performance in the reactor, compared to Period I where the standard deviation was 0.10.

In the third period, the consumption ratio was stable from day 89-109 when the concentration of NaCl was increased from 0 to 2.0 g NaCl/L. When the salinity was increased to 3.0 g NaCl/L the ratio was fluctuating more. Between day 126-135 the consumption ratio dropped day by day, caused by the increase in the effluent concentration of nitrite as presented in Figure 3.1. This drop is as discussed in Section 3.1.3 believed to be caused by partial nitrification due to oxygen contamination in the reactor. From day 132-141 the consumption ratio increased from 0.4 to 1.9, before it dropped day by day until the end of the experiment. The ratio kept dropping when the salinity was increased to 3.0 g NaCl/L at day 144, and stopped at 1.38. The figure (3.4) shows that the

consumption ratio was approaching the theoretical ratio of 1.32 at the end of the experiment. The drop in the ratio from day 141-147 was caused by the increased consumption of ammonium. This can be seen in Figure 3.3, as the ARR were increasing in within that period. The average consumption ratio for Period III was 1.4 ± 0.3.

Production ratio of nitrate

The production ratio of nitrate was fluctuating during the whole experiment in the same pattern as the nitrate production rate (NPR) presented in Figure 3.3, but with less severe fluctuations from day to day. This is natural since the ratio is a function of the nitrate production, which again is a function of the consumption of ammonium. It is hard to see any general trends regarding this parameter as a function of the salinity. In Period III the ratio was relative stable without any severe fluctuations from day to day even though the concentration of NaCl was increased. The values of the ratios in the three periods will be presented in Table 3.1.

3.1.5 Loss of nitrogen in the reactor

Figure 3.5 presents the total loss of nitrogen with respect to the consumption of the main substrates (nitrite and ammonium) and the salinity in the reactor. The values are calculated according to Equation (2.8) in Section 2.2, and they are presented in Table A.2 in Appendix A.

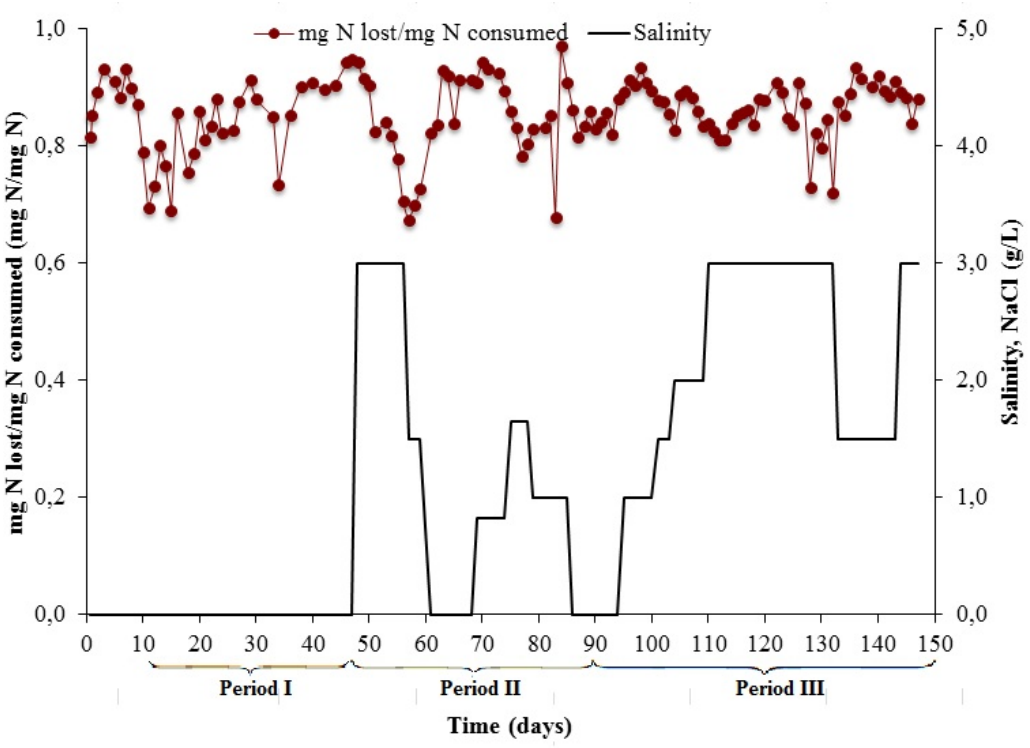

Figure 3.5: The figure presents the loss of nitrogen in mg N lost/mg N consumed (primary y-axis) and the salinity (secondary y-axis) in the reactor as functions of time, represented by brown circles and a black line, respectively.

As presented in Table 3.1 on page 50, the average loss of nitrogen$\pm\sigma$ during the three periods were; 0.83 $\pm$ 0.06 (Period I), 0.85 $\pm$ 0.08 (Period II) and 0.86 $\pm$ 0.04 (Period III). These values deviate from the theoretical value of the production of N_2 gas of 1.02 presented in Equation (1.1). This is natural, since the equation used for the calculations (Eq. 2.8) will always result in a number between 0 and 1 as long as there is production of nitrate in the system. Since there was no collection of the produced N_2 gas in the reactor, the validity of the loss of nitrogen in the system as representative for the gas production in the system is uncertain. Nitrogen is also one of the key substances for microbial growth which is likely to have occurred in the reactor. This might contribute to the loss of nitrogen as well. As there was no direct monitoring of the microbial growth in the system, the contribution of the growth to the loss of nitrogen in the system is unknown.

3.1.6 Summary of the consumption ratio, the production ratio of nitrate and the loss of nitrogen

In order to summarize the consumption ratio, loss of nitrogen and the production ratio of nitrate in the reactor for the different periods of the experiment, the average values $\pm$ standard deviation (σ) are presented in Table 3.1. The average values and the standard deviation are calculated by the use of integrated Microsoft Excel functions. The raw data used are presented in Table A.2 in Appendix A.

Table 3.1: Summary of the average consumption ratio, average production ratio and average loss of nitrogen in the reactor.

Parameter	Period I	Period II	Period III
Consumption ratio ($N-NO_2^-/N-NH_4^+$) $\pm \sigma$	1.3 $\pm$ 0.1	1.1 $\pm$ 0.4	1.4 $\pm$ 0.3
Production ratio ($N-NO_3^-/N-NH_4^+$) $\pm \sigma$	0.4 $\pm$ 0.2	0.3 $\pm$ 0.1	0.3 $\pm$ 0.1
Loss of nitrogen (mg N lost/mg N consumed) $\pm \sigma$	0.83 $\pm$ 0.06	0.85 $\pm$ 0.08	0.86 $\pm$ 0.04

When the consumption ratios for the three periods are compared to values presented in the literature, the reported values are ranging between 1.04 - 1.5 according to Aktan et al. (2012). The ratio will also change when anammox bacteria are exposed to stressed conditions, such as NaCl. The consumption ratio for the three periods were all within the previous reported values. The fact that the consumption ratio in both Period I and III were close to the theoretical ratio of 1.32 is a good indication that the anammox bacteria was the dominating population in the reactor. The lower consumption ratio and higher standard deviation in Period II indicates that the consumption ratio of nitrite and ammonium was less stable in this period, and that the microbial community was more stressed compared to Period I. The standard deviation of 0.3 in Period III also indicates the microbial community was more stressed in Period III compared to Period I.

All of the production ratios of nitrate during the three periods were higher than the

theoretical value of 0.26. In the literature there have been found values ranging from 0.02 (Suneethi and Joseph (2011), no standard deviation given) to 0.33 (Date et al. (2009), no standard deviation given). The value of 0.33 is in accordance with all the three different values presented in Table 3.1.

3.2 The effect of the salinity on the total nitrogen removal rate

Figure 3.6 presents the correlation between the salinity and the total nitrogen removal rate in the reactor, under the first order approximation of the data set. The figure includes the salinity and TNRR from day 42 to day 147. The raw data for the figure are presented in Table A.2 in Appendix A.1. The calculations of the correlation coefficient are presented in Appendix B.

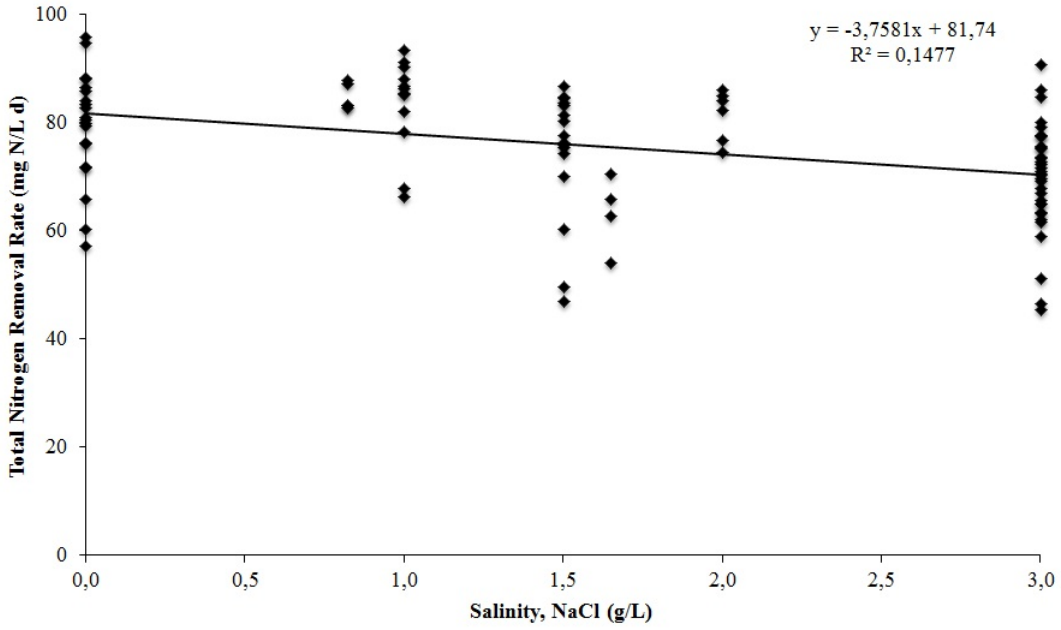

Figure 3.6: The figure presents the correlation between the salinity and the total nitrogen removal rate in the reactor. The figure includes points from day 42 to day 147.

The figure presents the square of the correlation coefficient, R^2. The value of R^2 = 0.148, which makes the correlation coefficient r = 0.38. This observed correlation is highly significant, because the p-value of this data set is less than 0.05 % (N = 97) (Taylor, 1997). The observation indicated that the general trend in this experiment is that the salinity is affecting the total nitrogen removal in the reactor, thus inhibiting the biomass in the reactor.

Figure 3.7 presents a modified version of Figure 3.6, where the transient periods in the

reactor are removed from the data set. The transient periods are chosen to be the two days after the salinity was changed, which is approximately 3×HRT. The figure includes the salinity and TNRR at day 42-47, 50-51, 53-56, 59, 63-66, 68, 71-74, 77-78, 81-85, 88-94, 97-100, 103, 106-109, 112-132, 135-144 and 146-147. The raw data for the figure are presented in Table A.2 in Appendix A.1. The calculations of the correlation coefficient are presented in Appendix B.

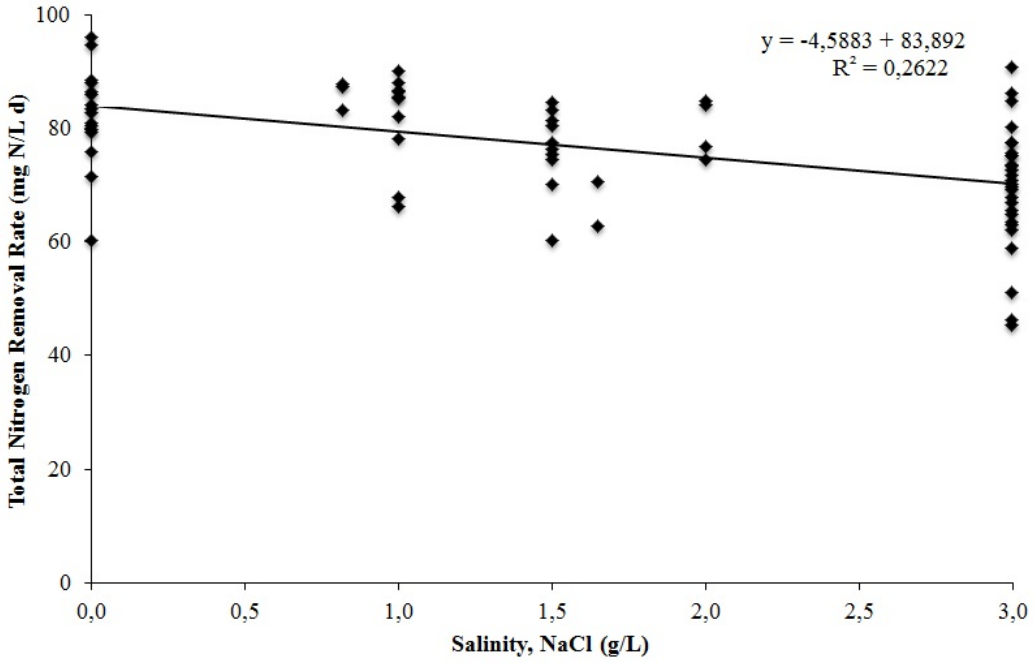

Figure 3.7: The figure presents the correlation between the salinity and the total nitrogen removal rate in the reactor. In this figure all points within the two days after the salinity was changed are left out, in order to avoid the transient periods in the reactor.

The figure presents the square of the correlation coefficient, R^2. The value of R^2 = 0.262, which makes the correlation coefficient r = 0.51. This observed correlation is also highly significant, because the p-value of this data set is also less than 0.05 % (N = 71) (Taylor, 1997). The correlation coefficient is higher when the data set has been adjusted, which shows that the general effect of salinity is even better described in Figure 3.7 compared to Figure 3.6. But both of the figures describes the general trend in the experiment in a highly significant way, so the generalization o the effect of salinity

on the microbial community in the reactor can be made with both of the figures.

These figures are generalizing the effect of the NaCl during the whole experiment, and it has been presented previously in Figure 3.2 that the response to the NaCl was different in Period II and III. The five highest point at 3.0 g NaCl/L (day 125-127 and 146-147) have a great influence on the correlation factor, which is 0.62 when these points are excluded. But as presented in Figure 3.2 there was always a drop in the TNRR when the salinity was increased, except for the last time at the end of the experiment. This indicate that the salinity had short-term inhibitory effect to the microbial community until the biomass seemed to be able to adapt to the salinity at the end. The period (day 126-132) might have been excluded from the data set, since the drop might have been caused by partial nitrification instead of inhibition of the salinity. When these point were excluded, the correlation coefficient in Figure 3.7 changed from 0.51 to 0.52. This shows that these points do not contribute severely to the correlation between the salinity and the total nitrogen removal rate.

3.3 DGGE analysis of the microbial community's dynamics

To analyze the microbial community's dynamics in the reactor, two sludge samples sampled at day 44 and 114 were analyzed. The v3 region of the 16S rRNA was amplified, and the PCR products were analyzed on a DGGE gel (Figure 3.8). It is assumed that the bands migrating to the same denaturing position in the gel represents the same species.

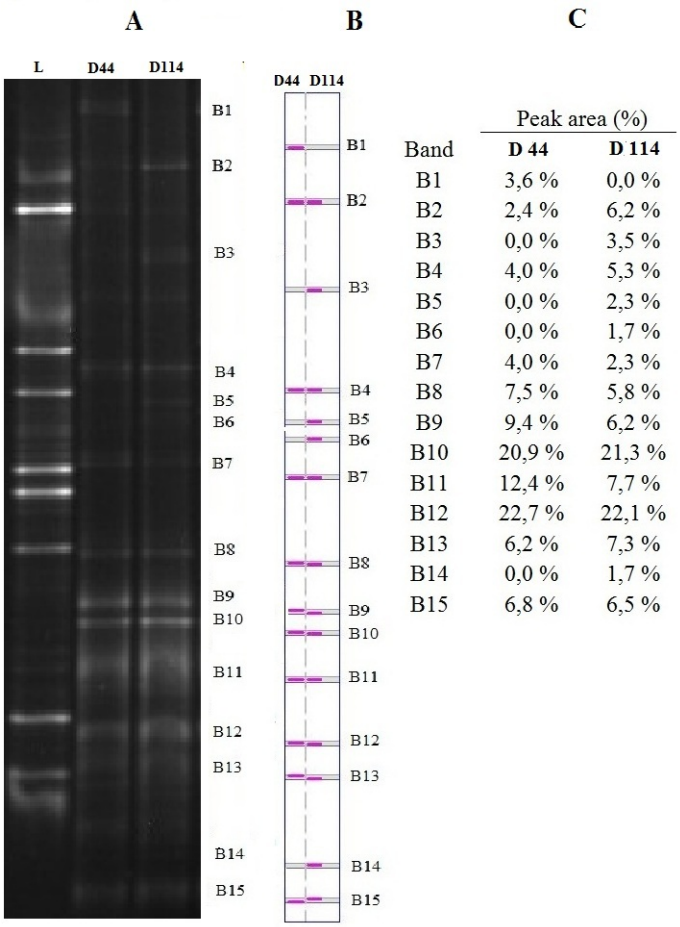

Band	Peak area (%) D 44	D 114
B1	3,6 %	0,0 %
B2	2,4 %	6,2 %
B3	0,0 %	3,5 %
B4	4,0 %	5,3 %
B5	0,0 %	2,3 %
B6	0,0 %	1,7 %
B7	4,0 %	2,3 %
B8	7,5 %	5,8 %
B9	9,4 %	6,2 %
B10	20,9 %	21,3 %
B11	12,4 %	7,7 %
B12	22,7 %	22,1 %
B13	6,2 %	7,3 %
B14	0,0 %	1,7 %
B15	6,8 %	6,5 %

Figure 3.8: ***A:*** A picture of the section in the DGGE gel with v3 16S rRNA fragments. The denaturing gradient was 35-50%. Only the section between approx. 43-50 % is included in the figure, because no bands were detected in the top part of the gel. The symbols **L**, **D44** and **D114** are representing the ladder/marker and the samples sampled at day 44 and 114, respectively. ***B:*** The corresponding band pattern from the Gel2k analysis.***C:*** Normalized peak area values of the bands determined by Gel2k.

Figure 3.8 shows that the microbial community to some extent changed from day 44 to day 114 in the continuous reactor. This observation is quantified by the Band richness (k) and the Shannon diversity index (H'). The Band richness was found (in PAST) to be highest for the day 114 community (k = 14) compared to the day 44 community (k = 11). Also the Shannon diversity index was higher for the day 114 community (H' = 2.33) compared to the day 44 community (H' = 2.16). The Bray-Curtis similarity between the two samples was found to be 0.76. As the Bray-Curtis similarity is ranging between 0 and 1, where 1 is representing complete similarity between two samples and 0 is complete dissimilarity (Bray and Curtis, 1957), the observed value of 0.76 is indicating a relative high level of similarity between the two samples from the reactor. This shows that the total composition of the microbial community at day 44 and 114 was reasonably similar, even though the Band richness and the Shannon diversity index increased by 27 % and 8 %, respectively.

The observed change of the microbial community from day 44 to 114 is illustrated by the bands denoted B1, B3, B5, B6 and B14. The band B1 was only detected in the day 44 community. This indicates that the corresponding species was not able to adapt to the salinity. The bands B3, B5, B6 and B14 were only detected in the day 114 community. This observation indicates that the corresponding species were able to grow when the salt was added to the system, thus being more competitive under saline conditions. For the rest of the bands present in both of the communities, represented by B2, B4, B7-B13 and B15, the corresponding species seemed to be able to acclimate to the salt. The corresponding species to the bands B2, B4 and B13 seemed to increase in total number because of their increased peak areas, thus being more competitive under the saline conditions.

3.3.1 Results from sequencing of the bands from the DGGE gel

The bands presented in Figure 3.8 except B14 and B15 were sent to GATC BIOTECH for sequencing. The bands B14 and B15 were not included due to bad separation in the lowest part of the gel (see Section 4.2). The results (received by email) were checked in the Ribosomal Database Project (RDP) with confidence threshold at 50 %. The percentages presented in Table 3.2 indicate the actual reliability with 95 % confidence (Wang et al., 2007). The bands B1, B3, B4 and B8 gave no results because the sequences were too short. The rest of the bands had 94-100 % reliability to the Bacteria domain. The results were in general relative inconclusive, as there were only the bands B2, B10, B12 and B13 that had more than 50 % reliability at the phylogenetic level *Order*. Table 3.2 presents the bands just described, in which there is only B10 that had a high level of reliability at the *Genus* level (96 %).

Table 3.2: The table presents the results with more than 50 % reliability obtained from search in the Ribosomal Data Project (confidence threshold at 50 %).

Band	Phylogenetic level	Phylogenetic level *name*	Reliability (%)
B2	Order	*Actinomycetales*	53
B10	Genus	*Ignavibacterium*	96
B12	Order	*Actinomycetales*	83
B13	Order	*Actinomycetales*	74

Table 3.2 shows that the order *Actinomycetales* were found in three of the bands sampled. This order has not been found to be related to anammox or nitrogen consumption in general. This is also the case for the genus *Ignavibacterium*. The results presented in this section are not in accordance with other reported results related to classification of anammox bacteria in anammox reactors, such as Kartal et al. (2006), Liu et al. (2009) and Yang et al. (2011) (all related to salinity) or Schmid et al. (2003), Penton et al. (2006) and Bae et al. (2010) (not related to salinity).

Chapter 4

General discussion and conclusions

4.1 Adaptation of the microbial community to salinity

During the experiment presented in this thesis, salinity (NaCl) was observed to be inhibiting the microbial community in the reactor, as the total nitrogen removal rate (TNRR) decreased each time the concentration of NaCl was increased, except for the last days of the experiment (day 144-147). When the NaCl was removed or the concentration of NaCl was decreased the TNRR increased again, indicating that the NaCl had a reversible inhibitory effect to the microbial community. Since the TNRR did not drop at the end of the experiment, it seems as the biomass was able to acclimate to the salinity level at 3.0 g NaCl/L.

The up flow in the reactor is reported to be a key selective factor to select for the granulation process, which makes the biomass more robust and to avoid wash out of the system (Jin et al., 2008). The problem of wash out in this particular experiment is believed to be low or absent, because there were no visible observations of washed out biomass in the sedimentation trap (presented in Figure 2.2). The possible effect of wash out of biomass due to the increased density of the medium when the NaCl was added was also low (presented in Section 1.5.1). This has likely not been a problem in the system because the concentration of NaCl was low during the experiment (maximum 3.0 g NaCl/L) compared to the concentration of NaCl in sea water.

The adaptation level to salinity in this experiment is low compared to others, presented in Table 1.2 on page 16. The lowest reported adaptation level was 7 g NaCl/L by Yi et al. (2011) and the highest was 30 g NaCl/L by Kartal et al. (2006), Liu et al. (2009), Yang et al. (2011) and Ma et al. (2012). In the previous reported experiments with continuous adaptation of anammox to salinity, 3 of 4 started the adaptation to NaCl by adding 5 g NaCl/L to the medium fed to their anammox reactor. The start concentration of 3 g NaCl/L was chosen in this experiment in case the microbial community was sensitive to new conditions, but still close to the reported experiments. Since 3 g NaCl/L seemed to inhibit the microbial community severely the first time it was added, the concentration was decreased and removed, and the next steps were much smaller compared to Kartal et al. (2006) (presented in Figure 1.6) and the other reported experiments. This strategy was the same as presented in Liu et al. (2009) when they experienced inhibition in the reactor. It is also similiar to Dapena-Mora et al. (2010) and Yang et al. (2011), but the total nitrogen loading rate was not decreased as they did.

Compared to several of the other experiments the adaptation in this experiment was started a short time after the start-up period. This means that the microbial community in this up flow reactor was less mature, and it had to put up with challenging conditions sooner than others. One specific example is Yang et al. (2011), which kept their anammox reactor without salt for 202 days before they reached stable performance within 90 days at 30 g NaCl/L. Other examples are Liu et al. (2009) and Dapena-Mora et al. (2010), who kept their anammox reactor without salt for 102 and 250 days, respectively. When they started the adaptation, they reached stable performance within 170 and 80 days, at 30 and 15 g NaCl/L, respectively.

The response to the salinity in the reactor was different in Period II and Period III (presented in Section 3.1). It might be that the initial microbial community (represented by Sample 1 in Figure 3.8) was not in possession of the required enzymes to tolerate the salt, *e.g.* the Na^+/K^+-ATPase mentioned in Section 1.5.1. Another explanation might be that the community was not given enough time to develop or activate the enzymatic capacity to tolerate the salinity. The second sample (Sample 2) presented in Section 3.3 was sampled from the reactor when the TNRR began to improve after a drop when the salinity was increased to 3 g NaCl/L. Because of the slow-growing anammox bacteria, Sample 2 is assumed to be representative for the microbial community some days after

the biomass was sampled as well, which is including the period where the TNRR was slowly improving. Because no sample of the microbial community was sampled at the end of the experiment, the community development is unknown at this point. It is a possibility that the new species present in Sample 2 compared to Sample 1 where triggered by the addition of salt to the system, thus improving the performance of the reactor in terms of nitrogen removal in Period III compared to Period II, as they would have needed time to grow. The last point discussed is at this point speculation, and further experiments will be required to be able to conclude whether this is the case or not.

The two major conclusions reported in the literature regarding adaptation to salinity and to new conditions is general are that there have either been a population shift in the community or an acclimation of the existing population (Kartal et al. (2006), Dapena-Mora et al. (2010)). Based on the results presented in this initial study it seems to be an acclimation of the existing population. This seems to be the case because the DGGE analysis showed that the composition of the microbial communities in the two sludge samples sampled from the reactor were similar.

Interestingly, both the Band richness and the Shannon diversity index (presented in Section 3.3) of the microbial community increased as a response to the salt. No such values have been found related to adaptation of anammox to salinity, as the focus on the community dynamics has been absent in the reported studies (presented in Section 1.5). The increase of the microbial diversity as a response to the salt contradicts other reported observations in nitrifying communities, where the microbial communities were less diverse as the response to the exposure to salt (Moussa et al. (2006), Wu et al. (2008) and Bassin et al. (2012)). The new bands detected in the DGGE gel for the D114 community (compared to the day 44 community) have not been classified, so the importance of the new corresponding species to the acclimation of the salt is unknown at this point.

4.2 Evaluation of the experimental methods

The experimental methods reported in this thesis regarding the microbial analysis are methods that have been optimized at the Department of Biotechnology, such as the amount and concentrations of the buffers and reagents used for the PCR experiments, and the procedure for the DGGE experiment. The primer pair that was utilized is an universal bacterial primer pair, which means that they will amplify as good as any present bacterial DNA present in the sample. A limitation of the PCR-DGGE combination is that is not possible to determine the most dominating species based on the most dominating bands in the DGGE gel pattern. This is due to PCR biases, caused by a potential better primer match with less dominating species (Inglis et al., 2012). This could lead to more PCR products of the less dominating species, and less PCR products of the most dominating species. In the gel pattern presented in Figure 3.8, the two most dominating bands (B10 and B12) in the D44 community were also the two most dominating bands in the D114 community. But this does not indicate that the two most dominating species in the D44 community were the most dominating species in the D114 community.

There was most likely some loss of information regarding the dynamics of the microbial community in the DGGE gel. The distance between the two lowest bands in the marker/DNA ladder to the left in Figure 3.8A (on page 55) should ideally have been longer. A possible explanation for this is some errors in the gradient in the gel. The result of this matter was that the separation of the bands in the lowest part of the gel seemed to be incomplete. This is the reason why no bands below B13 in Figure 3.8 were sampled for sequencing. If the DGGE experiment was repeated, there is a possibility that the number of bands would have changed due to better separation, thus resulting in a better identification of the bands in the lowest part of the gel. This could change the Band richness, the Shannon diversity index and the Bray-Curtis similarity.

The DGGE gel analysis is based on the composition of the DNA in the microbial community. Since there was no or little observations of washed out biomass in the sedimentation trap after the reactor, DNA from dead cells could be present in the reactor. This DNA could contribute to a wrong estimation of the actual, living community composition. This could especially be the case for the day 114 community, due to the addition of salt in the medium, which could cause cell decay due to the increase of the osmotic

pressure. The DGGE gel pattern does not distinguish between DNA from dead or living cells. The impacts of the contribution of the dead DNA on the analysis of the community dynamics is unknown, so this matter requires further experiments to be solved.

The results presented in Table 3.2 of the sequenced DNA are not related to anammox. The utilization of the universal primer pair might have contributed to this matter, because any present bacterial DNA would be amplified. The method used to sample the DNA from the DGGE gel may have contributed to deteriorate the quality of the sequences, as these were sampled under UV light, which is known to cause mutations in and to damage the DNA (Klug et al., 2009). If specific anammox primers had been used, there could have been some positive results related to anammox or nitrogen consumption in general. This would have been a time-consuming process in order to optimize the experimental methods. As the microbial analysis were conducted as an initial pilot study, the already established methods at the department were therefore utilized.

As earlier mentioned, the adaptation level in this experiment is low compared to other reported studies. Because of the sensitivity to the NaCl, the concentration was not increased any higher than 3 g NaCl/L. Only two samples of the biomass were sampled because of the low increase in salinity. Since the microbial community in the reactor only was sampled twice, this led to limitations of how much statistical analyses that could be carried out in order to analyze the dynamics in the reactor. If further statistical analyses are being implemented, these analyses could bring new information to the table regarding the dynamics at the community level during the adaptation to salinity.

4.3 Conclusions

Based on the results of the experiments covered in this study, the main conclusions are:

1. Acclimation of the microbial community to 3 g NaCl/L in the continuous reactor was reached.
2. Molecular and statistic analyses indicate that most of the bacterial species present in the original community were able to acclimate to the NaCl in the system.
3. Molecular and statistic analyses showed that the diversity of the microbial community in the continuous reactor increased after the NaCl was added to the system.
4. A small change in the microbial community was observed, because new bacterial species were observed and one bacterial species was absent in the microbial community after the NaCl was added to the system.

4.4 Future perspectives

Further work is required to reach the long-term goals of the pilot project described in Section 1.7, and the reactor will be operated further. There are several suggestions to improve the adaptation level. One suggestion is to split the biomass in two parallel reactors. One of the reactors could be operated as the one presented in this report as the reference, with NaCl as the selection factor. The other reactor could be added a mixture of NaCl and KCl to study if the potassium as an antagonistic effect to the microbial community as presented in Section 1.5.1 for other anaerobic microorganisms. This strategy is called the "salt in" strategy (Lay et al., 2010). Another option is to switch to sea water instead of the mineral medium used in this experiment , or a mixture of sea water and the mineral medium. If the biomass is found to be able to reach higher levels of adaptation, the proportion of sea water could be increased until complete sea water composition is reached, because adaptation to sea water/marine conditions is the real objective of the pilot project.

Since the operation of the reactor will be continued, it will be possible to take further samples of the microbial community. When the number of samples increases, it will be possible to do further and more thoroughly analyses of the community dynamics in the program PAST. The molecular methods should also be optimized and more specified to anammox bacteria. Both in terms of optimization of the PCR reagents and buffers and the gradient range of the DGGE analysis. Other molecular methods should also be considered, such as fluorescent *in situ* hybridization (FISH). For further analyses of the dynamics of the microbial community by DGGE, specific anammox primers should be tested. Overviews of possible primers and probes for DGGE and FISH are presented in *e.g.* Schmid et al. (2005) and Li and Gu (2011). The sludge samples presented in this study and their extracted DNA are available for further studies.

Bibliography

Abma, W., Schultz, C., Mulder, J., van der Star, W., Strous, M., Tokutomi, T., and van Loosdrecht, M. (2007). Full-scale granular sludge anammox process. *Water Science and Technology*, 55(8-9):27–33.

Acinas, S., Marcelino, L., Klepac-Ceraj, V., and Polz, M. (2004). Divergence and redundancy of 16s rrna sequences in genomes with multiple rrn operons. *Journal of Bacteriology*, 186(9):2629–2635.

Aktan, C., Yapsakli, K., and Mertoglu, B. (2012). Inhibitory effects of free ammonia on anammox bacteria. *Biodegradation*, 23(5):751–762.

Bae, H., Park, K.-S., Chung, Y.-C., and Jung, J.-Y. (2010). Distribution of anammox bacteria in domestic wwtps and their enrichments evaluated by real-time quantitative pcr. *Process Biochemistry*, 45(3):323–334.

Bakke, I., De Schryver, P., Boon, N., and Vadstein, O. (2011). Pcr-based community structure studies of bacteria associated with eukaryotic organisms: A simple pcr strategy to avoid co-amplification of eukaryotic dna. *Journal of Microbiological Methods*, 84(2):349–351.

Bassin, J., Kleerebezem, R., Muyzer, G., Rosado, A., Van Loosdrecht, M., and Dezotti, M. (2012). Effect of different salt adaptation strategies on the microbial diversity, activity, and settling of nitrifying sludge in sequencing batch reactors. *Applied Microbiology and Biotechnology*, 93(3):1281–1294.

Blackburne, R., Yuan, Z., and Keller, J. (2008). Partial nitrification to nitrite using low dissolved oxygen concentration as the main selection factor. *Biodegradation*, 19(2):303–312.

Bray, J. and Curtis, J. (1957). An ordination of the upland forest communities of southern wisconsin. *Ecological Monographs*, 27(4):325–349.

Broda, E. (1977). Two kinds of lithotrophs missing in nature. *Zeitschrift fur Allgemeine Mikrobiologie*, 17(6):491–493.

Dapena-Mora, A., Campos, J., Mosquera-Corral, A., Jetten, M., and Méndez, R. (2004). Stability of the anammox process in a gas-lift reactor and a sbr. *Journal of Biotechnology*, 110(2):159–170.

Dapena-Mora, A., Fernández, I., Campos, J., Mosquera-Corral, A., Méndez, R., and Jetten, M. (2007). Evaluation of activity and inhibition effects on anammox process by batch tests based on the nitrogen gas production. *Enzyme and Microbial Technology*, 40(4):859–865.

Dapena-Mora, A., Vázquez-Padín, J., Campos, J., Mosquera-Corral, A., Jetten, M., and Méndez, R. (2010). Monitoring the stability of an anammox reactor under high salinity conditions. *Biochemical Engineering Journal*, 51(3):167–171.

Date, Y., Isaka, K., Ikuta, H., Sumino, T., Kaneko, N., Yoshie, S., Tsuneda, S., and Inamori, Y. (2009). Microbial diversity of anammox bacteria enriched from different types of seed sludge in an anaerobic continuous-feeding cultivation reactor. *Journal of Bioscience and Bioengineering*, 107(3):281–286.

De Graaff, M., Temmink, H., Zeeman, G., van Loosdrecht, M., and Buisman, C. (2011). Autotrophic nitrogen removal from black water: Calcium addition as a requirement for settleability. *Water Research*, 45(1):63–74.

Doran, P. M. (1995). *Bioprocess Engineering Principles*. Academic Press, 525 B Street, Suite 1900, San Diego, CA 92101-4495, USA, 1 edition.

Drapcho, C. M., Nhuan, N. P., and Walker, T. H. (2008). *Biofuels Engineering Process Technology*. The McGraw-Hill Companies.

Fernández, I., Dosta, J., Fajardo, C., Campos, J., Mosquera-Corral, A., and Méndez, R. (2012). Short- and long-term effects of ammonium and nitrite on the anammox process. *Journal of Environmental Management*, 95(SUPPL.):170–174.

Ferris, M., Muyzer, G., and Ward, D. (1996). Denaturing gradient gel electrophoresis

profiles of 16s rrna-defined populations inhabiting a hot spring microbial mat community. *Applied and Environmental Microbiology*, 62(2):340–346.

Hall, J. E. and Guyton, A. C. (2006). *Textbook of medical physiology*. Elsevier Saunders, St. Louis, Mo.

Hames, B. D. (1998). *Molecular Genetic Analysis of Populations*. Oxford University Press, Great Clarendon Street, Oxford OX2 6DP, 2 edition.

Hammer, Ø., Harper, D., and Ryan, P. (2001). Past: Paleontological statistics software package for education and data analysis. *Palaeontologia Electronica*, 4(1):XIX–XX.

Hyde, D. (2009). *Introduction to Genetic Principles*. McGraw-Hill International Edition, 1221 Avenue of the Americas, New York, NY 1002.

Imajo, U., Tokutomi, T., and Furukawa, K. (2004). Granulation of anammox microorganisms in up-flow reactors. *Water Science and Technology*, 49(5-6):155–163.

Inglis, G., Thomas, M. C., Thomas, D. K., Kalmokoff, M. L., Brooks, S., and Selinger, L. (2012). Molecular methods to measure intestinal bacteria: A review. *Journal of AOAC International*, 95(1):5–23.

Isaka, K., Date, Y., Kimura, Y., Sumino, T., and Tsuneda, S. (2008). Nitrogen removal performance using anaerobic ammonium oxidation at low temperatures. *FEMS Microbiology Letters*, 282(1):32–38.

Jetten, M., Cirpus, I., Kartal, B., Van Niftrik, L., Van De Pas-Schoonen, K., Sliekers, O., Haaijer, S., Van Der Star, W., Schmid, M., Van De Vossenberg, J., Schmidt, I., Harhangi, H., Van Loosdrecht, M., Kuenen, J., Op Den Camp, H., and Strous, M. (2005). 1994-2004: 10 years of research on the anaerobic oxidation of ammonium. *Biochemical Society Transactions*, 33(1):119–123.

Jetten, M., Slickers, O., Kuypers, M., Dalsgaard, T., Van Niftrik, L., Cirpus, I., Van De Pas-Schoonen, K., Lavik, G., Thamdrup, B., Le Paslier, D., Op Den Camp, H., Hulth, S., Nielsen, L., Abma, W., Third, K., Engström, P., Kuenen, J., Jørgensen, B., Canfield, D., Sinninghe Damsté, J., Revsbech, N., Fuerst, J., Weissenbach, J., Wagner, M., Schmidt, I., Schmid, M., and Strous, M. (2003). Anaerobic ammonium oxidation

by marine and freshwater planctomycete-like bacteria. *Applied Microbiology and Biotechnology*, 63(2):107–114.

Jetten, M., Wagner, M., Fuerst, J., Van Loosdrecht, M., Kuenen, G., and Strous, M. (2001). Microbiology and application of the anaerobic ammonium oxidation ('anammox') process. *Current Opinion in Biotechnology*, 12(3):283–288.

Jin, R.-c., Hu, B.-l., Zheng, P., Qaisar, M., Hu, A.-h., and Islam, E. (2008). Quantitative comparison of stability of anammox process in different reactor configurations. *Bioresource Technology*, 99(6):1603–1609.

Jin, R.-C., Yang, G.-F., Yu, J.-J., and Zheng, P. (2012). The inhibition of the anammox process: A review. *Chemical Engineering Journal*, 197:67–79.

Jung, J., Kang, S., Chung, Y., and Ahn, D. (2007). Factors affecting the activity of anammox bacteria during start up in the continuous culture reactor. *Water Science and Technology*, 55(1-2):459–468.

Kanagawa, T. (2003). Bias and artifacts in multitemplate polymerase chain reactions (pcr). *Journal of Bioscience and Bioengineering*, 96(4):317–323.

Kartal, B., Koleva, M., Arsov, R., van der Star, W., Jetten, M., and Strous, M. (2006). Adaptation of a freshwater anammox population to high salinity wastewater. *Journal of Biotechnology*, 126(4):546–553.

Kartal, B., Kuenen, J., and Van Loosdrecht, M. (2010). Sewage treatment with anammox. *Science*, 328(5979):702–703.

Kartal, B., Kuypers, M., Lavik, G., Schalk, J., Op Den Camp, H., Jetten, M., and Strous, M. (2007). Anammox bacteria disguised as denitrifiers: Nitrate reduction to dinitrogen gas via nitrite and ammonium. *Environmental Microbiology*, 9(3):635–642.

Kartal, B., Maalcke, W., De Almeida, N., Cirpus, I., Gloerich, J., Geerts, W., Op Den Camp, H., Harhangi, H., Janssen-Megens, E., Francoijs, K.-J., Stunnenberg, H., Keltjens, J., Jetten, M., and Strous, M. (2011). Molecular mechanism of anaerobic ammonium oxidation. *Nature*, 479(7371):127–130.

Kartal, B., van Niftrik, L., Keltjens, J., Op den Camp, H., and Jetten, M. (2012).

Anammox-growth physiology, cell biology, and metabolism. *Advances in Microbial Physiology*, 60:211–262.

Kindaichi, T., Awata, T., Tanabe, K., Ozaki, N., and Ohashi, A. (2011). Enrichment of marine anammox bacteria in hiroshima bay sediments. *Water Science and Technology*, 63(5):964–969.

Klug, W. S., Cummings, M. R., Spencer, C. A., and Palladino, M. A. (2009). *Concepts of Genetics*. Pearson International Edition, San Francisco.

Kuenen, J. (2008). Anammox bacteria: From discovery to application. *Nature Reviews Microbiology*, 6(4):320–326.

Kuenen, J., Kartal, B., and Van Loosdrecht, M. (2011). Application of anammox for n-removal can turn sewage treatment plant into biofuel factory. *Biofuels*, 2(3):237–241.

Kumar, M. and Lin, J.-G. (2010). Co-existence of anammox and denitrification for simultaneous nitrogen and carbon removal-strategies and issues. *Journal of Hazardous Materials*, 178(1-3):1–9.

Lay, W., Liu, Y., and Fane, A. (2010). Impacts of salinity on the performance of high retention membrane bioreactors for water reclamation: A review. *Water Research*, 44(1):21–40.

Lewin, B. I. (2007). *Lewin's Cells*. Jones and Bartlett Publishers, 40 Tall Pine Drive, Sudbury, MA 01776, 2 edition.

Li, H., Zhou, S., Ma, W., Huang, G., and Xu, B. (2012). Fast start-up of anammox reactor: Operational strategy and some characteristics as indicators of reactor performance. *Desalination*, 286:436–441.

Li, M. and Gu, J.-D. (2011). Advances in methods for detection of anaerobic ammonium oxidizing (anammox) bacteria. *Applied Microbiology and Biotechnology*, 90(4):1241–1252.

Liu, C., Yamamoto, T., Nishiyama, T., Fujii, T., and Furukawa, K. (2009). Effect of salt concentration in anammox treatment using non woven biomass carrier. *Journal of Bioscience and Bioengineering*, 107(5):519–523.

Lotti, T., van der Star, W., Kleerebezem, R., Lubello, C., and van Loosdrecht, M. (2012). The effect of nitrite inhibition on the anammox process. *Water Research*, 46(8):2559–2569.

Ma, B., Peng, Y., Zhang, S., Wang, J., Gan, Y., Chang, J., Wang, S., Wang, S., and Zhu, G. (2013). Performance of anammox uasb reactor treating low strength wastewater under moderate and low temperatures. *Bioresource Technology*, 129:606–611.

Ma, C., Jin, R.-C., Yang, G.-F., Yu, J.-J., Xing, B.-S., and Zhang, Q.-Q. (2012). Impacts of transient salinity shock loads on anammox process performance. *Bioresource Technology*, 112:124–130.

Madigan, M. T., Martinko, J. M., Dunlap, P. V., and Clark, D. P. (2009). *Brock Biology of Microorganisms*. Pearson, San Francisco.

Moe, S. T. and Smidsrød, O. (2008). *Biopolymer Chemistry*. Tapir Academic Press.

Moussa, M., Sumanasekera, D., Ibrahim, S., Lubberding, H., Hooijmans, C., Gijzen, H., and Van Loosdrecht, M. (2006). Long term effects of salt on activity, population structure and floc characteristics in enriched bacterial cultures of nitrifiers. *Water Research*, 40(7):1377–1388.

Muyzer, G., De Waal, E., and Uitterlinden, A. (1993). Profiling of complex microbial populations by denaturing gradient gel electrophoresis analysis of polymerase chain reaction-amplified genes coding for 16s rrna. *Applied and Environmental Microbiology*, 59(3):695–700.

Muyzer, G. and Smalla, K. (1998). Application of denaturing gradient gel electrophoresis (dgge) and temperature gradient gel electrophoresis (tgge) in microbial ecology. *Antonie van Leeuwenhoek, International Journal of General and Molecular Microbiology*, 73(1):127–141.

Norland, S. (2004). Gel2k gel analysis software. *University of Bergen, Norway*.

Nozhevnikova, A., Simankova, M., and Litti, Y. (2012). Application of the microbial process of anaerobic ammonium oxidation (anammox) in biotechnological wastewater treatment. *Applied Biochemistry and Microbiology*, 48(8):667–684.

Peet, R. (1975). Relative diversity indices. *Ecology*, 56(2):496–498.

Penton, C., Devol, A., and Tiedje, J. (2006). Molecular evidence for the broad distribution of anaerobic ammonium-oxidizing bacteria in freshwater and marine sediments. *Applied and Environmental Microbiology*, 72(10):6829–6832.

Rønning, A. J. (2012). Enrichment of anaerobic ammonium oxidizing (anammox) bacteria in a continuous reactor. *Project work, NTNU*.

Ruiz, G., Jeison, D., and Chamy, R. (2003). Nitrification with high nitrite accumulation for the treatment of wastewater with high ammonia concentration. *Water Research*, 37(6):1371–1377.

Schalk, J., Oustad, H., Kuenen, J., and Jetten, M. (1998). The anaerobic oxidation of hydrazine: A novel reaction in microbial nitrogen metabolism. *FEMS Microbiology Letters*, 158(1):61–67.

Schmid, M., Maas, B., Dapena, A., Van De Pas-Schoonen, K., Van De Vossenberg, J., Kartal, B., Van Niftrik, L., Schmidt, I., Cirpus, I., Kuenen, J., Wagner, M., Sinninghe Damsté, J., Kuypers, M., Revsbech, N., Mendez, R., Jetten, M., and Strous, M. (2005). Biomarkers for in situ detection of anaerobic ammonium-oxidizing (anammox) bacteria. *Applied and Environmental Microbiology*, 71(4):1677–1684.

Schmid, M., Walsh, K., Webb, R., Rijpstra, W., Van De Pas-Schoonen, K., Verbruggen, M., Hill, T., Moffett, B., Fuerst, J., Schouten, S., Damsté, J., Harris, J., Shaw, P., Jetten, M., and Strous, M. (2003). Candidatus "scalindua brodae", sp. nov., candidatus "scalindua wagneri", sp. nov., two new species of anaerobic ammonium oxidizing bacteria. *Systematic and Applied Microbiology*, 26(4):529–538.

Sliekers, A., Third, K., Abma, W., Kuenen, J., and Jetten, M. (2003). Canon and anammox in a gas-lift reactor. *FEMS Microbiology Letters*, 218(2):339–344.

Strous, M., Fuerst, J., Kramer, E., Logemann, S., Muyzer, G., Van De Pas-Schoonen, K., Webb, R., Kuenen, J., and Jetten, M. (1999a). Missing lithotroph identified as new planctomycete. *Nature*, 400(6743):446–449.

Strous, M., Kuenen, J., and Jetten, M. (1999b). Key physiology of anaerobic ammonium oxidation. *Applied and Environmental Microbiology*, 65(7):3248–3250.

Strous, M., Pelletier, E., Mangenot, S., Rattei, T., Lehner, A., Taylor, M., Horn, M.,

Daims, H., Bartol-Mavel, D., Wincker, P., Barbe, V., Fonknechten, N., Vallenet, D., Segurens, B., Schenowitz-Truong, C., Médigue, C., Collingro, A., Snel, B., Dutilh, B., Op Den Camp, H., Van Der Drift, C., Cirpus, I., Van De Pas-Schoonen, K., Harhangi, H., Van Niftrik, L., Schmid, M., Keltjens, J., Van De Vossenberg, J., Kartal, B., Meier, H., Frishman, D., Huynen, M., Mewes, H.-W., Weissenbach, J., Jetten, M., Wagner, M., and Le Paslier, D. (2006). Deciphering the evolution and metabolism of an anammox bacterium from a community genome. *Nature*, 440(7085):790–794.

Strous, M., Van Gerven, E., Kuenen, J., and Jetten, M. (1997). Effects of aerobic and microaerobic conditions on anaerobic ammonium- oxidizing (anammox) sludge. *Applied and Environmental Microbiology*, 63(6):2446–2448.

Sun, W., Banihani, Q., Sierra-Alvarez, R., and Field, J. (2011). Stoichiometric and molecular evidence for the enrichment of anaerobic ammonium oxidizing bacteria from wastewater treatment plant sludge samples. *Chemosphere*, 84(9):1262–1269.

Suneethi, S. and Joseph, K. (2011). Anammox process start up and stabilization with an anaerobic seed in anaerobic membrane bioreactor (anmbr). *Bioresource Technology*, 102(19):8860–8867.

Taylor, J. R. (1997). *An Introduction To Error Analysis*. University Science Books.

Terada, A., Zhou, S., and Hosomi, M. (2011). Presence and detection of anaerobic ammonium-oxidizing (anammox) bacteria and appraisal of anammox process for high-strength nitrogenous wastewater treatment: A review. *Clean Technologies and Environmental Policy*, 13(6):759–781.

Trimmer, M., Nicholls, J., and Deflandre, B. (2003). Anaerobic ammonium oxidation measured in sediments along the thames estuary, united kingdom. *Applied and Environmental Microbiology*, 69(11):6447–6454.

Van de Graaf, A., Mulder, A., De Bruijn, P., Jetten, M., Robertson, L., and Kuenen, J. (1995). Anaerobic oxidation of ammonium is a biologically mediated process. *Applied and Environmental Microbiology*, 61(4):1246–1251.

Van Dongen, U., Jetten, M., and Van Loosdrecht, M. (2001). The sharon®-anammox®

process for treatment of ammonium rich wastewater. *Water Science and Technology*, 44(1):153–160. cited By (since 1996) 317.

van Rijn, J., Tal, Y., and Schreier, H. (2006). Denitrification in recirculating systems: Theory and applications. *Aquacultural Engineering*, 34(3):364–376.

Vogelsang, C. (2012). Norsk institutt for vannforskning.

Wang, Q., Garrity, G., Tiedje, J., and Cole, J. (2007). Naïve bayesian classifier for rapid assignment of rrna sequences into the new bacterial taxonomy. *Applied and Environmental Microbiology*, 73(16):5261–5267.

Ward, B. B., Arp, D. J., and Klotz, M. G. (2011). *Nitrification*. ASM Press, Washington.

Wu, G., Guan, Y., and Zhan, X. (2008). Effect of salinity on the activity, settling and microbial community of activated sludge in sequencing batch reactors treating synthetic saline wastewater. *Water Science and Technology*, 58(2):351–358.

Yang, J., Zhang, L., Hira, D., Fukuzaki, Y., and Furukawa, K. (2011). Anammox treatment of high-salinity wastewater at ambient temperature. *Bioresource Technology*, 102(3):2367–2372.

Ye, L., Peng, C.-y., Tang, B., Wang, S.-y., Zhao, K.-f., and Peng, Y.-z. (2009). Determination effect of influent salinity and inhibition time on partial nitrification in a sequencing batch reactor treating saline sewage. *Desalination*, 246(1-3):556–566.

Yi, Y., Yong, H., and Ping, D. (2011). Effect of salt on anammox process (conferance paper in the journal procadia environmental sciences). volume 10, pages 2036–2041.

Østgaard, K. (1995). *Miljøbioteknologi, Del I: Basis*. Institutt for bioteknologi, NTNU, 2 edition.

Appendices

Appendix A

Results from the continuous reactor

Appendix A presents the operational conditions, the measured concentrations in the inlet and the effluent of the reactor as well as calculated raw data for the figures presented in the report.

A.1 Reactor log

Table A.1 presents the reactor log. This includes the time, the temperature, the hydraulic retention time (HRT), the concentration of NaCl and the measured concentrations of $N-NO_2^-$, $N-NH_4^+$ and $N-NO_3^-$ in the inlet and the effluent of the continuous reactor. The table presents the raw data for Figure 3.1 on page 40 in the report.

Table A.1: The table presents the time, the temperature, the hydraulic retention time (HRT) and the salinity (g NaCl/L) in the reactor, as well as the measured concentrations of $N{-}NO_2^-$, $N{-}NH_4^+$ and $N{-}NO_3^-$ in the inlet and the effluent of the reactor.

Time (day)	Temperature (°C)	HRT (h)	Salinity (g NaCl/L)	$N-NO^-_{2,inlet}$ (mg N/L)	$N-NH^+_{4,inlet}$ (mg N/L)	$N-NO^-_{3,inlet}$ (mg N/L)	$N-NO^-_{2,effluent}$ (mg N/L)	$N-NH^+_{4,effluent}$ (mg N/L)	$N-NO^-_{3,effluent}$ (mg N/L)
0.7	30	30.0	0.0	20.6	20.0	0.0	11.3	14.2	2.8
1	30	30.0	0.0	20.6	20.0	0.0	10.5	11.7	2.8
2	30	30.0	0.0	20.6	20.0	0.0	8.4	9.8	2.4
3	30	30.0	0.0	20.6	20.0	0.0	6.8	7.3	1.8
5	30	30.0	0.0	20.6	20.0	0.0	9.4	3.9	2.5
6	30	30.0	0.0	22.8	23.7	0.0	6.6	0.2	4.7
7	30	30.0	0.0	22.8	23.7	0.0	5.7	3.1	2.6
8	30	30.0	0.0	22.8	23.7	0.0	6.6	3.6	3.7
9	30	30.0	0.0	25.8	27.2	0.0	5.5	5.6	5.4
10	30	30.0	0.0	25.8	27.2	0.0	4.2	6.1	9.0
11	30	30.0	0.0	25.8	27.2	0.0	3.3	8.6	12.6
12	30	30.0	0.0	27.6	28.7	0.0	2.6	7.7	12.4
13	30	30.0	0.0	27.6	28.7	0.0	1.7	7.7	9.4
14	30	30.0	0.0	27.6	28.7	0.0	2.5	9.5	10.4
15	30	30.0	0.0	26.8	28.4	0.0	1.3	5.5	15.1
16	30	30.0	0.0	26.8	28.4	0.0	2.8	10.1	6.1
18	30	30.0	0.0	26.8	28.4	0.0	2.2	11.3	10.3
19	30	30.0	0.0	30.7	30.4	0.0	2.4	11.6	10.1
20	30	30.0	0.0	30.7	30.4	0.0	2.2	9.1	7.1
21	30	30.0	0.0	30.7	30.4	0.0	2.6	9.3	9.4
22	30	30.0	0.0	33.9	32.1	0.0	2.0	9.5	9.1
23	30	30.0	0.0	33.9	32.1	0.0	2.2	9.3	6.6

Continued on next page

Table A.1 – *Continued from previous page*

Time (day)	Temperature (°C)	HRT (h)	Salinity (g NaCl/L)	$N-NO^{-}_{2,inlet}$ (mg N/L)	$N-NH^{+}_{4,inlet}$ (mg N/L)	$N-NO^{-}_{3,inlet}$ (mg N/L)	$N-NO^{-}_{2,effluent}$ (mg N/L)	$N-NH^{+}_{4,effluent}$ (mg N/L)	$N-NO^{-}_{3,effluent}$ (mg N/L)
24	30	30.0	0.0	33.9	32.1	0.0	1.9	8.5	10.0
26	30	30.0	0.0	32.2	25.6	0.0	2.4	4.0	9.0
27	30	30.0	0.0	32.2	25.6	0.0	0.9	3.8	6.7
29	30	30.0	0.0	31.7	27.6	0.0	0.5	5.6	4.7
30	30	30.0	0.0	31.7	27.6	0.0	1.4	5.1	6.4
33	30	27.0	0.0	33.8	26.0	0.0	1.4	3.9	8.3
34	30	21.0	0.0	33.8	26.0	0.0	0.9	3.6	14.8
36	30	21.0	0.0	35.8	30.9	0.0	2.0	4.6	8.9
38	30	21.0	0.0	35.8	30.9	0.0	1.7	0.4	6.5
40	30	21.0	0.0	37.8	29.1	0.0	2.1	4.0	5.6
42	30	18.0	0.0	38.0	29.5	0.0	2.3	4.9	6.3
44	30	18.0	0.0	38.0	29.5	0.0	1.4	1.2	6.3
46	30	18.0	0.0	38.3	29.5	0.0	2.0	2.7	3.6
47	30	18.0	0.0	38.3	29.5	0.0	1.0	0.5	3.5
48	30	18.0	3.0	38.0	32.5	0.0	5.8	10.4	3.2
49	30	18.0	3.0	38.0	32.5	0.0	8.7	8.9	4.6
50	30	18.0	3.0	38.0	32.5	0.0	9.9	4.2	5.5
51	30	18.0	3.0	38.9	31.5	0.0	13.1	8.6	8.6
53	30	18.0	3.0	38.9	31.5	0.0	16.5	6.6	7.6
54	30	18.0	3.0	38.2	31.5	0.0	18.1	13.2	7.0
55	30	18.0	3.0	38.2	31.5	0.0	21.3	13.6	7.8
56	30	18.0	3.0	38.2	31.5	0.0	23.9	11.8	10.0
57	30	18.0	1.5	38.0	31.4	0.0	24.3	9.9	11.5
58	30	18.0	1.5	38.0	31.4	0.0	23.2	9.0	11.3

Continued on next page

Table A.1 – *Continued from previous page*

Time (day)	Temperature (°C)	HRT (h)	Salinity (g NaCl/L)	$N-NO^{-}_{2,inlet}$ (mg N/L)	$N-NH^{+}_{4,inlet}$ (mg N/L)	$N-NO^{-}_{3,inlet}$ (mg N/L)	$N-NO^{-}_{2,effluent}$ (mg N/L)	$N-NH^{+}_{4,effluent}$ (mg N/L)	$N-NO^{-}_{3,effluent}$ (mg N/L)
59	30	18.0	1.5	38.0	31.4	0.0	20.1	4.0	12.4
61	30	18.0	0.0	38.3	31.0	0.0	19.5	7.0	7.6
62	30	18.0	0.0	38.3	31.0	0.0	13.4	2.1	8.8
63	30	18.0	0.0	39.0	31.0	0.0	11.9	4.4	3.8
64	30	18.0	0.0	39.0	31.0	0.0	10.6	2.4	4.6
65	30	18.0	0.0	39.0	31.0	0.0	5.1	0.4	10.4
66	30	18.0	0.0	39.7	32.8	0.0	4.7	1.8	5.9
68	30	18.0	0.0	39.7	32.8	0.0	0.4	0.2	6.4
69	30	18.0	0.8	37.7	31.0	0.0	3.7	2.5	5.7
70	30	18.0	0.8	37.7	31.0	0.0	4.3	2.3	3.6
71	30	18.0	0.8	37.7	31.0	0.0	2.7	0.5	4.5
73	30	18.0	0.8	36.9	31.1	0.0	3.3	2.4	4.7
74	30	18.0	0.8	36.9	31.1	0.0	2.0	0.1	7.1
75	30	18.0	1.7	37.5	30.9	0.0	9.2	9.8	7.0
76	30	18.0	1.7	37.5	30.9	0.0	17.5	10.4	6.9
77	30	18.0	1.7	37.5	30.9	0.0	14.0	7.3	10.2
78	30	18.0	1.7	37.5	30.9	0.0	13.0	2.5	10.4
79	30	18.0	1.0	38.5	31.5	0.0	5.3	0.8	11.0
81	30	18.0	1.0	38.5	31.5	0.0	3.5	1.5	11.0
82	30	18.0	1.0	38.5	31.5	0.0	6.4	2.1	9.1
83	30	18.0	1.0	38.5	31.5	0.0	20.0	0.3	16.0
84	30	18.0	1.0	38.7	30.3	0.0	1.5	8.8	1.7
85	30	18.0	1.0	38.7	30.3	0.0	1.2	17.0	4.7
86	30	18.0	0.0	37.6	30.8	0.0	5.6	13.4	6.9

Continued on next page

Table A.1 – *Continued from previous page*

Time (day)	Temperature (°C)	HRT (h)	Salinity (g NaCl/L)	$N-NO^{-}_{2,inlet}$ (mg N/L)	$N-NH^{+}_{4,inlet}$ (mg N/L)	$N-NO^{-}_{3,inlet}$ (mg N/L)	$N-NO^{-}_{2,effluent}$ (mg N/L)	$N-NH^{+}_{4,effluent}$ (mg N/L)	$N-NO^{-}_{3,effluent}$ (mg N/L)
87	30	18.0	0.0	37.6	30.8	0.0	6.9	4.2	10.6
88	30	18.0	0.0	37.6	30.8	0.0	21.1	2.0	7.6
89	30	18.0	0.0	39.2	31.2	0.0	3.3	7.2	8.5
90	30	18.0	0.0	39.2	31.2	0.0	2.1	6.3	10.7
91	30	18.0	0.0	39.0	32.7	0.0	4.4	7.8	9.5
92	30	18.0	0.0	39.0	32.7	0.0	4.8	6.2	8.7
93	30	18.0	0.0	40.2	32.1	0.0	4.9	4.9	11.3
94	30	18.0	0.0	40.2	32.1	0.0	0.6	0.6	8.5
95	30	18.0	1.0	39.9	31.2	0.0	1.0	1.7	7.5
96	30	18.0	1.0	39.9	31.2	0.0	0.2	0.8	6.1
97	30	18.0	1.0	38.5	31.0	0.0	0.7	2.8	6.4
98	30	18.0	1.0	38.5	31.0	0.0	0.5	1.4	4.6
99	30	18.0	1.0	38.7	31.0	0.0	1.0	3.9	6.0
100	30	18.0	1.0	38.7	31.0	0.0	1.8	3.8	6.9
101	30	18.0	1.5	40.6	31.8	0.0	4.8	4.9	7.7
102	30	18.0	1.5	40.6	31.8	0.0	4.1	4.8	8.0
103	30	18.0	1.5	40.6	31.8	0.0	5.1	4.9	9.1
104	30	18.0	2.0	40.7	32.0	0.0	6.3	4.6	10.7
105	30	18.0	2.0	40.7	32.0	0.0	3.7	4.5	7.4
106	30	18.0	2.0	38.9	32.3	0.0	2.8	4.7	6.8
107	30	18.0	2.0	38.9	32.3	0.0	1.6	6.6	7.5
108	30	18.0	2.0	40.3	31.5	0.0	6.0	8.3	8.1
109	30	18.0	2.0	40.3	31.5	0.0	7.3	8.5	9.4
110	30	18.0	3.0	38.3	32.1	0.0	9.5	12.3	7.9

Continued on next page

Table A.1 – *Continued from previous page*

Time (day)	Temperature (°C)	HRT (h)	Salinity (g NaCl/L)	$N-NO^{-}_{2,inlet}$ (mg N/L)	$N-NH^{+}_{4,inlet}$ (mg N/L)	$N-NO^{-}_{3,inlet}$ (mg N/L)	$N-NO^{-}_{2,effluent}$ (mg N/L)	$N-NH^{+}_{4,effluent}$ (mg N/L)	$N-NO^{-}_{3,effluent}$ (mg N/L)
111	30	18.0	3.0	38.3	32.1	0.0	13.5	10.6	8.2
112	30	18.0	3.0	40.0	32.3	0.0	10.0	15.7	8.9
113	30	18.0	3.0	40.0	32.3	0.0	10.9	12.2	9.4
114	30	18.0	3.0	40.7	32.3	0.0	11.4	7.8	8.7
115	30	18.0	3.0	40.7	32.3	0.0	11.4	14.0	7.1
116	30	18.0	3.0	40.8	31.9	0.0	9.3	11.5	7.5
117	30	18.0	3.0	40.8	31.9	0.0	7.0	10.5	7.7
118	30	18.0	3.0	38.0	32.7	0.0	9.0	10.8	8.4
119	30	18.0	3.0	38.0	32.7	0.0	8.2	12.3	6.1
120	30	18.0	3.0	39.5	31.6	0.0	7.3	10.7	6.5
122	30	18.0	3.0	39.5	31.6	0.0	6.2	10.4	5.1
123	30	18.0	3.0	39.5	32.7	0.0	6.2	9.5	6.1
124	30	18.0	3.0	39.5	32.7	0.0	6.3	7.8	8.9
125	30	18.0	3.0	39.5	32.7	0.0	6.6	2.1	10.5
126	30	18.0	3.0	40.2	32.6	0.0	3.3	1.4	6.3
127	30	18.0	3.0	40.2	32.6	0.0	7.5	0.7	8.2
128	30	18.0	3.0	40.2	32.6	0.0	13.2	1.5	15.8
129	30	18.0	3.0	39.7	31.1	0.0	14.0	1.8	9.9
130	30	18.0	3.0	39.7	31.1	0.0	18.0	0.5	10.7
131	30	18.0	3.0	41.0	32.1	0.0	18.9	1.5	8.2
132	30	18.0	3.0	41.0	32.1	0.0	28.2	0.7	12.4
133	30	18.0	1.5	42.5	34.6	0.0	10.4	1.6	8.2
134	30	18.0	1.5	42.5	34.6	0.0	19.9	0.3	8,4
135	30	18.0	1.5	42.5	34.6	0.0	5.0	8.7	7.1

Continued on next page

Table A.1 – *Continued from previous page*

Time (day)	Temperature (°C)	HRT (h)	Salinity (g NaCl/L)	$N-NO^{-}_{2,inlet}$ (mg N/L)	$N-NH^{+}_{4,inlet}$ (mg N/L)	$N-NO^{-}_{3,inlet}$ (mg N/L)	$N-NO^{-}_{2,effluent}$ (mg N/L)	$N-NH^{+}_{4,effluent}$ (mg N/L)	$N-NO^{-}_{3,effluent}$ (mg N/L)
136	30	18.0	1.5	39.8	31.8	0.0	3.3	11.0	3.8
137	30	18.0	1.5	39.8	31.8	0.0	4.0	11.0	4.9
139	30	18.0	1.5	39.8	31.8	0.0	3.1	7.4	6.1
140	30	18.0	1.5	38.7	30.6	0.0	2.1	11.4	4.5
141	30	18.0	1.5	38.7	30.6	0.0	3.8	12.9	5.6
142	30	18.0	1.5	38.7	30.6	0.0	1.8	9.3	6.8
143	30	18.0	1.5	39.9	31.3	0.0	2.4	8.5	5.4
144	30	18.0	3.0	39.9	31.3	0.0	4.0	8.9	6.3
145	30	18.0	3.0	39.9	31.3	0.0	4.1	7.7	7.0
146	30	18.0	3.0	37.3	31.3	0.0	3.9	7.9	9.2
147	30	18.0	3.0	37.3	31.3	0.0	2.5	6.0	7.3

A.2 Total performance in the reactor

Table A.2 presents the time, the salinity, the removal rates of nitrite, ammonium and total nitrogen, the production rate of nitrate, the loading rate of total nitrogen,the consumption ratio of nitrite and ammonium, the production ratio of nitrate over ammonium and the loss of nitrogen in the reactor. The values given in the table are the raw data for Figure 3.2, Figure 3.3, 3.4 and 3.5 in the report. The values are calculated by the use of Equation 2.1-2.8 presented in Section 2.2 in the report, and the values used are presented in Table A.1 in Appendix A.1. Examples of the calculations are given in Appendix A.3.

Table A.2: The table shows the total performance in the continuous reactor; the time, the salinity, the nitrite removal rate (NRR), the ammonium removal rate (ARR), the nitrate production rate (NPR), the total nitrogen loading rate (TNLR), the total nitrogen removal rate (TNRR), the consumption ratio of nitrite and ammonium, the production ratio of nitrate and ammonium and the loss of nitrogen in the reactor.

Time (day)	Salinity (g NaCl/L)	NRR (mg $N-NO_2^-$/L d)	ARR (mg $N-NH_4^+$/L d)	NPR (mg $N-NO_3^-$/L d)	TNLR (mg N/L d)	TNRR (mg N/L d)	Consumption ratio (mg $N-NO_2^-$/ mg $N-NH_4^+$)	Production ratio (mg $N-NO_3^-$/ mg $N-NH_4^+$)	Loss of N (mg N/ mg N)
0.7	0.0	7.4	4.6	2.3	32.5	12.1	1.60	0.49	0.81
1	0.0	8.1	6.6	2.2	32.5	14.7	1.22	0.33	0.85
2	0.0	9.8	8.2	1.9	32.5	17.9	1.19	0.24	0.89
3	0.0	11.0	10.2	1.5	32.5	21.2	1.08	0.14	0.93
5	0.0	9.0	12.9	2.0	32.5	21.9	0.69	0.15	0.91
6	0.0	13.0	18.8	3.7	37.2	31.7	0.69	0.20	0.88
7	0.0	13.7	16.4	2.1	37.2	30.1	0.83	0.13	0.93
8	0.0	13.0	16.1	3.0	37.2	29.1	0.80	0.18	0.90
9	0.0	16.2	17.3	4.3	42.4	33.6	0.94	0.25	0.87
10	0.0	17.3	16.8	7.2	42.4	34.1	1.03	0.43	0.79
11	0.0	18.0	14.9	10.1	42.4	32.9	1.21	0.68	0.69
12	0.0	20.0	16.8	9.9	45.0	36.8	1.19	0.59	0.73
13	0.0	20.7	16.8	7.5	45.0	37.6	1.23	0.45	0.80
14	0.0	20.1	15.4	8.3	45.0	35.5	1.31	0.54	0.77
15	0.0	20.4	18.3	12.1	44.2	38.7	1.11	0.66	0.69
16	0.0	19.2	14.6	4.8	44.2	33.8	1.31	0.33	0.86
18	0.0	19.7	13.7	8.2	44.2	33.4	1.44	0.60	0.75
19	0.0	22.6	15.0	8.1	48.9	37.7	1.51	0.54	0.79
20	0.0	22.8	17.0	5.7	48.9	39.8	1.34	0.33	0.86

Continued on next page

Table A.2 – *Continued from previous page*

Time (day)	Salinity (g NaCl/L)	NRR (mg N−NO_2^-/L d)	ARR (mg N−NH_4^+/L d)	NPR (mg N−NO_3^-/L d)	TNLR (mg N/L d)	TNRR (mg N/L d)	Consumption ratio (mg N−NO_2^-/ mg N−NH_4^+)	Production ratio (mg N−NO_3^-/ mg N−NH_4^+)	Loss of N (mg N/ mg N)
21	0.0	22.5	16.8	7.5	48.9	39.3	1.33	0.45	0.81
22	0.0	25.5	18.1	7.3	52.8	43.6	1.41	0.40	0.83
23	0.0	25.4	18.3	5.3	52.8	43.6	1.39	0.29	0.88
24	0.0	25.6	18.9	8.0	52.8	44.5	1.35	0.42	0.82
26	0.0	23.8	17.3	7.2	46.2	41.1	1.38	0.42	0.83
27	0.0	25.0	17.5	5.4	46.2	42.5	1.43	0.31	0.87
29	0.0	25.0	17.6	3.8	47.4	42.6	1.42	0.21	0.91
30	0.0	24.2	18.0	5.1	47.4	42.3	1.34	0.28	0.88
33	0.0	28.8	19.7	7.4	53.2	48.5	1.47	0.37	0.85
34	0.0	37.6	25.7	16.9	68.3	63.3	1.47	0.66	0.73
36	0.0	38.6	30.0	10.2	76.2	68.6	1.29	0.34	0.85
38	0.0	39.0	34.9	7.4	76.2	73.8	1.12	0.21	0.90
40	0.0	40.8	28.7	6.4	76.5	69.5	1.42	0.22	0.91
42	0.0	47.6	32.8	8.4	90.0	80.4	1.45	0.26	0.90
44	0.0	48.8	37.7	8.4	90.0	86.5	1.29	0.22	0.90
46	0.0	48.4	35.7	4.8	90.4	84.1	1.35	0.13	0.94
47	0.0	49.7	38.7	4.7	90.4	88.4	1.29	0.12	0.95
48	3.0	42.9	29.5	4.3	94.0	72.4	1.46	0.14	0.94
49	3.0	39.1	31.5	6.1	94.0	70.6	1.24	0.19	0.91
50	3.0	37.5	37.7	7.3	94.0	75.2	0.99	0.19	0.90
51	3.0	34.4	30.6	11.5	93.9	65.0	1.13	0.38	0.82
53	3.0	29.9	33.2	10.1	93.9	63.1	0.90	0.30	0.84
54	3.0	26.8	24.4	9.3	92.9	51.2	1.10	0.38	0.82

Continued on next page

Table A.2 – *Continued from previous page*

Time (day)	Salinity (g NaCl/L)	NRR (mg N−NO_2^-/L d)	ARR (mg N−NH_4^+/L d)	NPR (mg N−NO_3^-/L d)	TNLR (mg N/L d)	TNRR (mg N/L d)	Consumption ratio (mg N−NO_2^-/ mg N−NH_4^+)	Production ratio (mg N−NO_3^-/ mg N−NH_4^+)	Loss of N (mg N/ mg N)
55	3.0	22.5	23.9	10.4	92.9	46.4	0.94	0.43	0.78
56	3.0	19.1	26.3	13.4	92.9	45.3	0.73	0.51	0.71
57	1.5	18.3	28.7	15.4	92.5	46.9	0.64	0.54	0.67
58	1.5	19.7	29.9	15.0	92.5	49.6	0.66	0.50	0.70
59	1.5	23.9	36.5	16.5	92.5	60.4	0.65	0.45	0.73
61	0.0	25.1	32.0	10.2	92.4	57.1	0.78	0.32	0.82
62	0.0	33.2	38.6	11.8	92.4	71.8	0.86	0.31	0.84
63	0.0	36.1	35.5	5.1	93.3	71.6	1.02	0.14	0.93
64	0.0	37.9	38.1	6.1	93.3	76.0	0.99	0.16	0.92
65	0.0	45.2	40.8	13.9	93.3	86.0	1.11	0.34	0.84
66	0.0	46.7	41.3	7.8	96.7	88.0	1.13	0.19	0.91
68	0.0	52.4	43.5	8.6	96.7	96.0	1.21	0.20	0.91
69	0.8	45.3	38.0	7.6	91.6	83.2	1.19	0.20	0.91
70	0.8	44.5	38.3	4.8	91.6	82.8	1.16	0.13	0.94
71	0.8	46.7	40.6	6.0	91.6	87.3	1.15	0.15	0.93
73	0.8	44.8	38.3	6.3	90.7	83.1	1.17	0.16	0.92
74	0.8	46.6	41.3	9.4	90.7	87.9	1.13	0.23	0.89
75	1.7	37.7	28.1	9.3	91.2	65.9	1.34	0.33	0.86
76	1.7	26.7	27.3	9.2	91.2	54.0	0.98	0.34	0.83
77	1.7	31.3	31.5	13.6	91.2	62.8	0.99	0.43	0.78
78	1.7	32.7	37.9	13.9	91.2	70.5	0.86	0.37	0.80
79	1.0	44.3	41.0	14.7	93.3	85.3	1.08	0.36	0.83
81	1.0	46.7	40.0	14.7	93.3	86.7	1.17	0.37	0.83

Continued on next page

Table A.2 – *Continued from previous page*

Time (day)	Salinity (g NaCl/L)	NRR (mg N−NO_2^-/L d)	ARR (mg N−NH_4^+/L d)	NPR (mg N−NO_3^-/L d)	TNLR (mg N/L d)	TNRR (mg N/L d)	Consumption ratio (mg N−NO_2^-/ mg N−NH_4^+)	Production ratio (mg N−NO_3^-/ mg N−NH_4^+)	Loss of N (mg N/ mg N)
82	1.0	42.8	39.2	12.2	93.3	82.0	1.09	0.31	0.85
83	1.0	24.7	41.6	21.3	93.3	66.3	0.59	0.51	0.68
84	1.0	49.6	28.7	2.3	92.0	78.3	1.73	0.08	0.97
85	1.0	50.0	17.8	6.3	92.0	67.8	2.81	0.35	0.91
86	0.0	42.7	23.2	9.2	91.2	65.9	1.84	0.40	0.86
87	0.0	40.9	35.5	14.1	91.2	76.4	1.15	0.40	0.82
88	0.0	22.0	38.4	10.1	91.2	60.4	0.57	0.26	0.83
89	0.0	47.9	32.0	11.3	93.9	79.9	1.50	0.35	0.86
90	0.0	49.5	33.2	14.3	93.9	82.7	1.49	0.43	0.83
91	0.0	46.1	33.2	12.7	95.6	79.4	1.39	0.38	0.84
92	0.0	45.6	35.3	11.6	95.6	80.9	1.29	0.33	0.86
93	0.0	47.1	36.3	15.1	96.4	83.3	1.30	0.42	0.82
94	0.0	52.8	42.0	11.3	96.4	94.8	1.26	0.27	0.88
95	1.0	51.9	39.4	10.0	94.8	91.3	1.32	0.25	0.89
96	1.0	52.9	40.5	8.1	94.8	93.4	1.31	0.20	0.91
97	1.0	50.4	37.6	8.5	92.7	88.0	1.34	0.23	0.90
98	1.0	50.7	39.5	6.1	92.7	90.2	1.28	0.15	0.93
99	1.0	50.3	36.1	8.0	92.9	86.4	1.39	0.22	0.91
100	1.0	49.2	36.3	9.2	92.9	85.5	1.36	0.25	0.89
101	1.5	47.7	35.9	10.2	96.5	83.6	1.33	0.28	0.88
102	1.5	48.7	36.0	10.7	96.5	84.7	1.35	0.30	0.87
103	1.5	47.3	35.9	12.1	96.5	83.2	1.32	0.34	0.85
104	2.0	45.9	36.5	14.3	96.9	82.3	1.26	0.39	0.83

Continued on next page

Table A.2 – *Continued from previous page*

Time (day)	Salinity (g NaCl/L)	NRR (mg N$-NO_2^-$/L d)	ARR (mg N$-NH_4^+$/L d)	NPR (mg N$-NO_3^-$/L d)	TNLR (mg N/L d)	TNRR (mg N/L d)	Consumption ratio (mg N$-NO_2^-$/ mg N$-NH_4^+$)	Production ratio (mg N$-NO_3^-$/ mg N$-NH_4^+$)	Loss of N (mg N/ mg N)
105	2.0	49.3	36.7	9.9	96.9	86.0	1.34	0.27	0.89
106	2.0	48.1	36.7	9.1	94.9	84.9	1.31	0.25	0.89
107	2.0	49.7	34.3	10.0	94.9	84.1	1.45	0.29	0.88
108	2.0	45.7	31.0	10.8	95.7	76.7	1.48	0.35	0.86
109	2.0	44.0	30.6	12.5	95.7	74.6	1.44	0.41	0.83
110	3.0	38.4	26.5	10.5	93.9	64.9	1.45	0.40	0.84
111	3.0	33.1	28.6	10.9	93.9	61.7	1.15	0.38	0.82
112	3.0	40.0	22.1	11.9	96.4	62.1	1.81	0.54	0.81
113	3.0	38.8	26.7	12.5	96.4	65.5	1.45	0.47	0.81
114	3.0	39.1	32.7	11.6	97.3	71.7	1.20	0.35	0.84
115	3.0	39.1	24.3	9.5	97.3	63.4	1.60	0.39	0.85
116	3.0	42.0	27.2	10.0	96.9	69.2	1.55	0.37	0.86
117	3.0	45.1	28.5	10.3	96.9	73.5	1.58	0.36	0.86
118	3.0	38.7	29.1	11.2	94.3	67.8	1.33	0.38	0.83
119	3.0	39.7	27.2	8.1	94.3	67.0	1.46	0.30	0.88
120	3.0	42.9	27.9	8.7	94.9	70.9	1.54	0.31	0.88
122	3.0	44.4	28.4	6.8	94.9	72.8	1.57	0.24	0.91
123	3.0	44.4	30.9	8.1	96.3	75.3	1.44	0.26	0.89
124	3.0	44.3	33.2	11.9	96.3	77.5	1.33	0.36	0.85
125	3.0	43.9	40.9	14.0	96.3	84.7	1.07	0.34	0.83
126	3.0	49.2	41.6	8.4	97.1	90.8	1.18	0.20	0.91
127	3.0	43.6	42.5	10.9	97.1	86.1	1.03	0.26	0.87
128	3.0	36 .0	41.5	21.1	97.1	77.5	0.87	0.51	0.73

Continued on next page

Table A.2 – *Continued from previous page*

Time (day)	Salinity (g NaCl/L)	NRR (mg N−NO_2^-/L d)	ARR (mg N−NH_4^+/L d)	NPR (mg N−NO_3^-/L d)	TNLR (mg N/L d)	TNRR (mg N/L d)	Consumption ratio (mg N−NO_2^-/ mg N−NH_4^+)	Production ratio (mg N−NO_3^-/ mg N−NH_4^+)	Loss of N (mg N/ mg N)
129	3.0	34.3	39.1	13.1	94.4	73.4	0.88	0.34	0.82
130	3.0	28.9	40.8	14.3	94.4	69.7	0.71	0.35	0.80
131	3.0	29.5	40.8	10.9	97.5	70.3	0.72	0.27	0.84
132	3.0	17.1	41.9	16.5	97.5	58.9	0.41	0.39	0.72
133	1.5	42.8	44.0	10.9	102.8	86.6	0.97	0.25	0.87
134	1.5	30.1	45.7	11.2	102.8	75.9	0.66	0.25	0.85
135	1.5	50.0	34.5	9.5	102.8	84.5	1.45	0.27	0.89
136	1.5	48.7	27.7	5.1	95.9	76.4	1.75	0.18	0.93
137	1.5	47.7	27.7	6.5	95.5	75.5	1.72	0.23	0.91
139	1.5	48.9	32.5	8.1	95.5	81.4	1.51	0.25	0.90
140	1.5	48.8	25.6	6.0	92.4	74.4	1.91	0.23	0.92
141	1.5	46.5	23.6	7.5	92.4	70.1	1.97	0.32	0.89
142	1.5	49.2	28.4	9.1	92.4	77.6	1.73	0.32	0.88
143	1.5	50.0	30.4	7.2	94.9	80.4	1.64	0.24	0.91
144	3.0	47.9	29.9	8.4	94.9	77.7	1.60	0.28	0.89
145	3.0	47.7	31.5	9.3	94.9	79.2	1.52	0.30	0.88
146	3.0	44.5	31.2	12.3	91.5	75.7	1.43	0.39	0.84
147	3.0	46.4	33.7	9.7	91.5	80.1	1.38	0.29	0.88

A.3 Examples of calculations

This appendix presents examples of the calculations by the use of the equations presented in Section 2.2 in the report. The numbers used in the calculations are taken from day 100, where the measured concentrations were as following (see Appendix A.1):
Inlet $N{-}NO_2^-$: 38.7 mg/L
Inlet $N{-}NH_4^+$: 31.0 mg/L
Effluent $N{-}NO_2^-$: 1.8 mg/L
Effluent $N{-}NH_4^+$: 3.8 mg/L
Effluent $N{-}NO_3^-$: 6.9 mg/L
The HRT was 18 hours.

- The ammonium removal rate (ARR) (Eq. 2.1) at day 100 was:

$$ARR\ (mg\,N{-}NH_4^+/L\,d) = \frac{31.0\,mg/L - 3.8\,mg/L}{18\,h} \cdot \frac{24h}{day} = 36.3\,mg\,N{-}NH_4^+/L\,d$$

- The nitrite removal rate (NRR) (Eq. 2.2) at day 100 was:

$$NRR\ (mg\,N{-}NO_2^-/L\,d) = \frac{38.7\,mg/L - 1.8\,mg/L}{18\,h} \cdot \frac{24h}{day} = 49.2\,mg\,N{-}NO_2^-/L\,d$$

- The total nitrogen removal rate (TNRR) (Eq. 2.3) at day 100 was:

$$TNRR\ (mg\,N/L\,d) = 36.3\,mgN/L\,d + 49.2\,mgN/L\,d = 85.5\,mgN/L\,d$$

- The total nitrogen loading rate (TNLR) (Eq. 2.4) at day 100 was:

$$TNLR\ (mg\,N/L\,d) = \frac{38.7\,mgN/L + 31.0\,mgN/L}{18\,h} \cdot \frac{24h}{day} = 92.9\,mgN/L\,d$$

- The nitrate production ratio (NPR) (Eq. 2.5) at day 100 was:

$$NPR\ (mg\,N/L\,d) = \frac{6.9\,mg/L}{18\,h} \cdot \frac{24h}{day} = 9.2\,mg\,N{-}NO_3^-/L\,d$$

- The consumption ratio of nitrite and ammonium (Eq. 2.6) at day 100 was:

$$Consumption\ ratio\ \left(mg\ \mathrm{N{-}NO_{2\ consumed}^{-}}/mg\ \mathrm{N{-}NH_{4\ consumed}^{+}}\right) = \frac{49.2\,mgN/L\,d}{36.3\,mgN/L\,d} = 1.36$$

- The production ratio of nitrate with respect to the consumption of ammonium (Eq. 2.7) at day 100 was:

$$Production\ ratio\ \left(mg\ \mathrm{N{-}NO_{3\ produced}^{-}}/mg\ \mathrm{N{-}NH_{4\ consumed}^{+}}\right) = \frac{9.2\,mgN/L\,d}{36.3\,mgN/L\,d} = 0.25$$

- The loss of nitrogen (Eq. 2.8) at day 100 was:

$$Loss\ of\ N\ (mg\ N/mg\ N) = \frac{(38.7+31.0)\,mgN/L-(1.8+3.8+6.9)\,mgN/L}{(38.7+31.0)\,mgN/L-(1.8+3.8)\,mgN/L} = 0.89$$

Appendix B

Effect of salinity, calculations

This appendix presents the calculations of the correlation coefficients (r) between salinity and the total nitrogen removal rate (TNRR). The correlation coefficients are also presented in Figure 3.6 and 3.7 on page 52 and 53 in the report. The calculated numbers presented are calculated by the use integrated summarizing functions in Microsoft Excel. The equation for the correlation coefficient is presented in Equation (B.1) (Taylor, 1997). In the equation, x = salinity and y = TNRR.

$$r = \frac{\sum(x_i - \bar{x})(y_i - \bar{y})}{\sqrt{\sum(x_i - \bar{x})^2 \times \sum(y_i - \bar{y})^2}} \tag{B.1}$$

For simplicity, Eq. (B.1) is rearranged to Eq. (B.2).

$$r = \frac{A}{\sqrt{B \times C}} \tag{B.2}$$

B.1 Calculations for Figure 3.6

The points includes in these calculations are from day 42 to day 147.
The average salinity, $\bar{x}$ = 1.7.
The average TNRR, $\bar{y}$ = 75.5
The term A = -474.
The term B = 126.
The term C = 12053.
This makes in total the $|r|$ = 0.38.

B.2 Calculations for Figure 3.7

The points included in these calculations are day 42-47, 50-51, 53-56, 59, 63-66, 68, 71-74, 77-78, 81-85, 88-94, 97-100, 103, 106-109, 112-132, 135-143 and 146-147.
The average salinity, $\bar{x}$ = 1.7.
The average TNRR, $\bar{y}$ = 76.0.
The term A = -460.
The term B = 101.
The term C = 7972.
This makes in total the $|r|$ = 0.51.

Appendix C

Effect of NO_2^- on measurements of NO_3^-

An experiment to check the effect of present nitrite in the nitrate cuvette tests was conducted. The experiment was done by keeping the concentration of nitrate (NO_3^-) constant (10 mg $N-NO_3^-$), and increasing the concentration of nitrite (NO_2^-). Nitrate was added as $NaNO_3$ and nitrite was added as $NaNO_2$. Table C.1 presents the measured concentrations of both $N-NO_2^-$ and $N-NO_3^-$. These measured concentrations are the raw data for Figure C.1. The experiment was conducted by adding 6,08 g of $NaNO_3$ to 1 L of distilled water. This mixture was split into 10x100 mL, and $NaNO_2$ was added to each sample as presented in Table C.1. The samples was diluted to get within the linear range of the Dr. Lange tests (LCK 339 (nitrate) and LCK 341 (nitrite)). Figure C.1 presents the correlation between the concentrations of nitrite and the measured levels of nitrate. It has been assumed that these results are valid for any concentration of nitrate, even though only one concentrations (10 mg $N-NO_3^-$/L) has been tested.

Table C.1: Measured concentrations of $N-NO_2^-$ and $N-NO_3^-$ to check the effect of nitrite on the nirate Dr. Lange tests.

Sample number	Nitrate concentration (mg $N-NO_3^-$/L)	Nitrite concentration (mg $N-NO_2^-$/L)
0	9.7	0.0
1	9.9	1.0
2	10.0	2.2
3	11.0	4.3
4	11.3	5.9
5	11.7	8.0
6	12.2	9.7
7	11.2	14.9
8	13.8	20.5
9	15.9	30.1
10	18.5	44.3

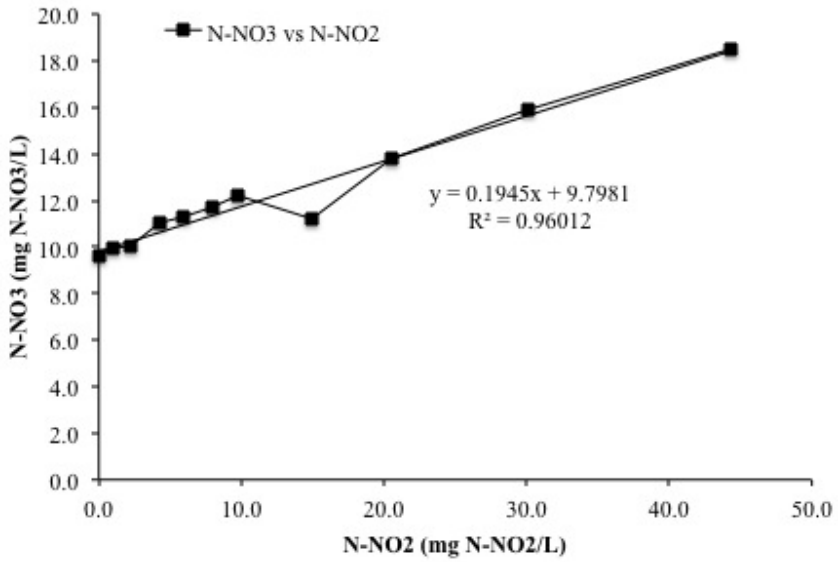

Figure C.1: The figure presents the correlation between concentration of nitrite and measured concentration of nitrate. The equation given in the figure has been used to adjust effluent concentrations of nitrate when the concentrations of nitrite were above 15 mg $N-NO_2^-$/L.

Appendix D

Verification of PCR products

Figure D.1 shows the result of the PCR products from the extracted DNA sampled from reactor on an agarose gel. The different symbols in the figure are used to identify the different samples, which are: L=Ladder, 1=Sample of reactor at day 44, 2=Sample of reactor at day 114, 3=Storage biomass 1, 4=Storage biomass 2, C=control. Only the PCR products from the samples 1 and 2 were used in further analysis presented in Section 3.3 in the report.

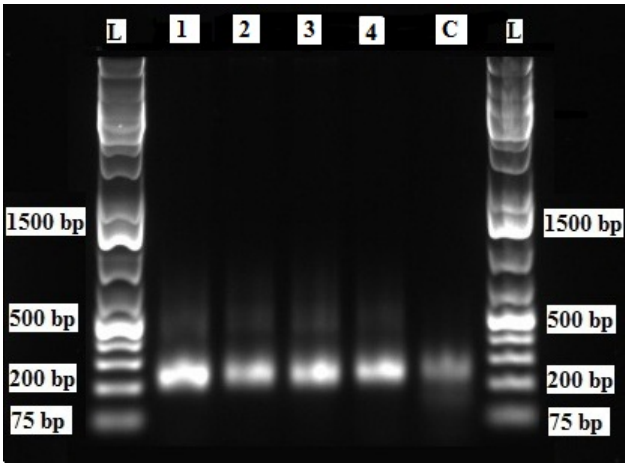

Figure D.1: Picture of the agarose gel after PCR with extracted DNA from the reactor. The different symbols in the figure are used to identify the different samples, which are: L=Ladder, 1=Sample of reactor at day 44, 2=Sample of reactor at day 114, 3=Storage biomass 1, 4=Storage biomass 2, C=control.

As can be seen in the figure, The PCR products are on the same line through the whole gel at 200 bp, which indicates that the PCR was successful. Figure D.2 shows the result of the PCR products from the DNA bands sampled from the DGGE gel presented. The bands that were sampled were the bands denoted B1-B13 in Figure 3.8 on page 55 in the report. The numbers in the top of the gel are identifying each DNA bands that were taken from the DGGE gel. The letter L is the ladder and the letter C is the control.

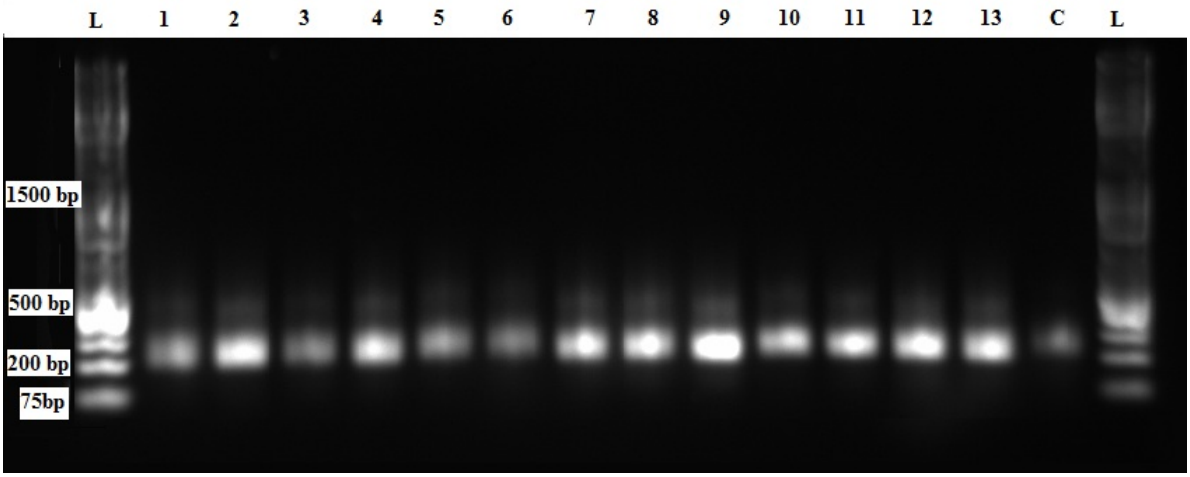

Figure D.2: Picture of agargel after PCR with purified DNA from the DGGE gel.

The PCR products are on the same line through the whole gel at 200 bp, which indicates that the PCR was successful. Even though the gel is not perfect, it stills shows that the PCR products are of the desired length (200 bp). 5 μL of each PCR product was mixed with 5μL of the primer 338F-M13R and they were all sent to GATC BIOTECH (Germany) for sequencing.

Appendix E

DGGE protocol

This appendix is presenting the protocol for the preparation of the DGGE gel, including chemicals and the preparation of the different solutions.

Mounting of glass plates

1. Wash the two glass plates, the spacer and the comb using Deconex soap and hot tap water. Finally rinse well with water to remove any traces of soap. Polish one side of each glass plate using 96% ethanol and Kimwipe paper.
2. Assemble the glass plates and spacer, and place it all in the gel box. Assure that the spacer is aligned to the lower edge of the glass plates. Tighten the screws.
3. Loosen the two uppermost screws, mount the comb, and then tighten the screws again.

Preparation of DGGE solutions

1. Determine the acrylamide percent and the denature gradient of the gel. (For recipes og solutions, see below.)

2. Make acrylamide solutions with the desired denaturing percentage in two 50 ml tubes. (Total volume in each tube will be 24 mL; see table below for volumes of 0% and 80% denaturing solutions.)

3. The 0% denat. acrylamide solution can be added to the 50 mL tubes without filtration. The 80% denat. acrylamide solution needs to be filtered before upon addition. (In order to remove urea crystals).

4. Prepare a 50 mL tube with 8 mL 0% denat. acrylamide solution. (Stacking gel for the top part of the gel.)

5. When ready to pour the gel, add $16\mu L$ tetramethylethylenediamine (TEMED) to the 24 mL gel solutions, and $10\mu L$ TEMED to the 8 mL stacking solution.

6. Prior to pouring the gel, add $87\mu L$ APS (10% ammonium per-sulphate) in both 24 mL gel solutions. (For the stacking gel, add $40\mu L$ APS, but not until the stacking gel is ready for pouring.)

Casting the gel

1. Rinse the gradient mixer and the tubes by pumping mq-water through the system.

2. Turn off the pump, close the valve between the chambers off the gradient mixer, and put the gradient mixer on stirring.

3. Pour the gel solution with low denat. percentage in the left chamber. Quickly open and close the valve to remove any air bubbles in the channel between the chambers. Use a pipette to remove any small amounts of gel solution in the right chamber.

4. Pour the gel solution with high denat. percentage in the right chamber.

5. Start the pump and wait a few seconds until the solution from the right chamber has migrated 7-8 cm out in the tube. Then open the valve between the chambers. Assure stirring in both chambers.

6. Place the syringe between the glass plates. (Assure no water from the washing step is left in the tube.)

7. When the gel reaches approximately 1 cm below the comb, stop the comb, remove the syringe, and empty any leftovers from the mixing chamber and tubes. Rinse the system with a small amount of mq-water.

8. When the mixing chambers are empty from water, close the valve and stop the pump. Add APS to the stacking gel solution, mix, and pour into the right chamber of the mixer.

9. Start the pump. When the glass plates are completely filled with the stacking gel, turn of the pump, and press the comb down and in to the gel. Tighten the screws.

10. Leave the gel for polymerization for at least two hours.

11. Pump mq-water through the system to avoid gel polymerization in the tubes.

Preparations and addition of samples

1. Make 20 L of 0.5X TAE buffer (200 mL 50X TAE and 20 L of mq-water) and add approximately 17 L to the buffer tank. (The buffer may be used for three runs.) Turn on the instrument to heat the buffer to 60°C.

2. Carefully remove the comb from the gel. Loosen all screws, and carefully press down the spacer. Tighten the screws at the sides of the glass plates. (The screws on the bottom should be loose throughout the electrophoresis.)

3. Place the gel system in the buffer tank. Avoid air bubbles beneath the gel.

4. Attach the electrical wires and recirculation tube and turn on the recirculation. Rinse the wells using a syringe with buffer. Turn the power on (100 V; should result in approximately 27 - 35 mA) and let run while preparing the samples.

5. Add 3 μL loading dye to 5 μL PCR sample. When all samples are ready for loading, turn off the recirculation and push the "low voltage" button. Apply the samples to the wells. Avoid using the 2-3 outermost wells due to "smiling" effects.

Running the gel

1. Turn on the "high voltage" button, set the voltage to 100 V. Run the gel for 5-10 minutes without buffer recirculation.
2. Turn on the recirculation and run gel for 17-18 hours.

Staining and visualization

1. Turn of the instrument; lift the gel system out.
2. Loosen the screws, and lift out the gel. Carefully separate the glass plates.
3. Transfer the gel to a plastic foil sheet and place it in a suitable lidded box.
4. Prepare the staining solution by adding 30 mL mq-water, $3\mu L$ SYBR Gold, 600 μL 50X TAE buffer in a 50 mL tube.
5. Distribute the staining solution evenly on the gel. Put the lid on the box, and leave for 1-2 hours.
6. Carefully take out the gel and rinse with mq-water. Carefully let the water run of the gel, use a paper towel at the edges of the gel to remove excess water.
7. Wash the UV plate of the "gel dock" with distilled water and ethanol. Use Kimwipe papers to remove any dust or other particles on the UV plate. Distribute some mq-water on the plate (This allows for easy movement of the gel on the plate).
8. Carefully transfer the gel from the plastic foil to the UV plate (by turning the plastic foil "upside down"). Before removing the foil, position the gel on the plate.
9. Photograph the gel at different exposures, and save the pictures in the original format, and *e.g.* pdf or other formats.

Eluation of bands for sequencing

1. Print out a picture of the gel, and number the bands that are to be sequenced.
2. Add 20 μL sterile mq-water to eppendorf tubes, and number the tubes according to the number of bands.
3. Pull out the UV plate, and pull down the UV screen. Cover the wrists to avoid UV radiation. Use blue 1 mL pipette tips to stick out material from the bands. Take care to avoid touching other bands. Use a pipette to blow out the material in the eppendorf tube with water.
4. Place the tubes in the fridge over night.
5. Use $1\mu L$ of the eluate as template in a $25\mu L$ PCR reaction.

Chemical recipes

For all the solutions mention under, add distilled water to obtain the final volume.

50X TAE buffer

The 50 X TAE buffer is prepared according to Table F.1. Prior of use, autoclave the buffer.

Table E.1: 50 X TAE Buffer (20 L).

Compound	*Amount*
Tris base	242 g
Glacial acetic acid	57.1 mL
0.5 M EDTA (pH 8.0)	100 mL

Deionized formamide

Deionize 200 mL formamide by adding 7.5 g DOWEX RESIN AG 501X8, and stir for one hour at room temperature.

Acrylamid solution (0% denaturing)

8% acrylamide in 0.5 X TAE buffer (per 250 ml):

1. 50 mL of 40% acrylamide solution (BioRadLab Inc)
2. 2.5 mL of 50 X TAE buffer

Store solution at 4°C, protected from light.

Acrylamid solution (80% denaturing)

8% acrylamide, 5.6 M urea, 32% formamide, in 0.5 X TAE buffer (per 250 ml):

1. 50 mL of 40% acrylamide solution (BioRadLab Inc.)
2. 2.5 mL of 50 X TAE buffer
3. 84 g of urea
4. 80 mL of deionized formamide

Store solution at 4°C, protected from light. Must be sterile filtered before pouring the gel.

0% stacking gel

Prepared by taking 8 mL of the 0% acrylamide solution and adding $40\mu L$ 10% APS and $10\mu L$ TEMED.

10% ammonium per-sulphate (APS)

1. Dissolve 10 g of ammonium per-sulphate in 100 mL dH_2O.
2. Sterile filter the solution.
3. Divide solution in 250μL fractions in eppendorf tubes and store in freezer.
4. Used eppendorf tubes are discharged after use.

Composition of low and high denaturing solutions

Table E.2 shows the composition of low and high denature solutions. 0%- and 80% stock refers to the amount of the 0% and 80% acrylamid solutions needed.

Table E.2: Composition of low and high denature solutions. 0%- and 80% stock refers to the amount of the 0% and 80% acrylamid solutions needed

Denaturing %	0% stock	80% stock	TEMED + 10% APS	Total volume
15	19.5	4.5	16 + 87	24
25	16.5	7.5	17 + 87	24
30	15	9	18 + 87	24
35	13.5	10.5	19 + 87	24
40	12	12	20 + 87	24
45	10.5	13.5	21 + 87	24
50	9	15	22 + 87	24
55	7.5	16.5	23 + 87	24
60	6	18	24 + 87	24
75	1.5	22.5	25 + 87	24